Strengthening of Reinforced Concrete Beams Having Circular Openings Using Near Surface Mounting Steel Bars

A Thesis

Submitted to the Council of the Erbil Technical Engineering College at Erbil Polytechnic University in Partial Fulfillment of the Requirements for the Degree of Master of Science in Structural Engineering

By

Hoshang Hayder Anwer

B.Sc. in Technical Civil Engineering (2015)

Supervised by

Assist. Prof. Dr. Bahman Omar Taha

Erbil, Kurdistan

February 2024

بِسۡمِ ٱللَّهِ ٱلرَّحۡمَٰنِ ٱلرَّحِيمِ

اقْرَأْ بِاسْمِ رَبِّكَ الَّذِي خَلَقَ ﴿١﴾ خَلَقَ الْإِنْسَانَ مِنْ عَلَقٍ
﴿٢﴾ اقْرَأْ وَرَبُّكَ الْأَكْرَمُ ﴿٣﴾ الَّذِي عَلَّمَ بِالْقَلَمِ ﴿٤﴾ عَلَّمَ
الْإِنْسَانَ مَا لَمْ يَعْلَمْ ﴿٥﴾

صدق الله العظيم

سورة العلق:(١-٥)

In the name of Allah, the Most Gracious, the Most Merciful

Read: In the Name of your Lord, who created (1) Created man from a clinging clot (2) Read: And your Lord is the Most Generous (3) He Who taught by the pen (4) Taught man what he never knew (5)

DECLARATION

I declare that the Master Thesis entitled: ***Strengthening of Reinforced Concrete Beams Having Circular Openings Using Near Surface Mounting Steel Bars***," my original work, and hereby I certify that unless stated, all work contained within this thesis is my independent research and has not been submitted for the award of any other degree at any institution, except where due acknowledgment is made in the text.

Signature: Hoshang

Student Name: Hoshang Hayder Anwer

Date: 20 / 2 / 2024

SUPERVISOR CERTIFICATE

This thesis has been written under my supervision and has been submitted for the award of the degree of Master in Structural Engineering with my approval as supervisor.

Signature

Name: Assist. Prof. Dr. Bahman Omar Taha

Date: 20 / 2 / 2024

I confirm that all requirements have been fulfilled.

Signature:

Name: Assist. Prof. Dr. Bahman Omar Taha

Head of the Department of Technical Civil Engineering department

Date: 20 / 2 / 2024

I confirm that all requirements have been fulfilled.

Postgraduate Office

Signature:

Name: Assist. Lect. Mr. Bayad Abdulqader Ahmed

Date: 20 / 2 / 2024

EXAMINATION COMMITTEE CERTIFICATION

We certify that we have read this thesis: ***Strengthening of Reinforced Concrete Beams Having Circular Openings Using Near Surface Mounting Steel Bars***," and as an examining committee examined the student (Hoshang Hayder Anwer) in its content and what related to it. We approve that it meets the standards of a thesis for the degree of Master of structural engineering.

Signature:

Name: Assist. Prof. Dr. Najmadeen M. Saeed

Member

Date: 21 / 2 / 2024

Signature:

Name: Assist. Prof. Dr. Rahel Kh. Ibrahim

Member

Date: 21 / 2 / 2024

Signature:

Name: Assist. Prof. Dr. Bahman Omar Taha

Supervisor

Date: 21 / 2 / 2024

Signature:

Name: Prof. Dr. Mereen Hassan Fahmi

Chairman

Date: 20 / 2 / 2024

Signature:

Name: Prof. Dr. Ayad Zaki Saber Agha

Dean of Erbil Technical Engineering College

Date: 20 / 2 / 2024

LINGUISTIC REVIEW

I confirm that I have reviewed the thesis titled " Strengthening of Reinforced Concrete Beams Having Circular Openings Using Near Surface Mounting Steel Bars" from the English linguistic point of view, and I can confirm that it is free of grammatical and spelling errors.

LEGAL TRANSLATOR
IRAQ ERBIL
Ibrahim Saeed Awla
License No. 41 / 2020
Judicial Council
Sworn Translator

Signature:

Name of Reviewer: Ibrahim Saeed Awla

Date: 29/11/2023

TO

MY PARENTS

MY WIFE

MY BROTHER

MY SON MEER

Hoshang

ACKNOWLEDGEMENTS

In the name of Allah, the most Merciful, and Gracious

First and foremost, gratitude is expressed to Allah, the Lord of the World, for His abundant blessings. Subsequently, heartfelt appreciation is extended to specific individuals whose assistance and support were invaluable throughout the course of this research project.

Special acknowledgment is reserved for my lovely parents, my beloved wife, my supervisor (Assist. Prof. Dr. Bahman Omar Taha), (Dr. Kamaran S. Ismail), (Mr. Halmat Awla), (Assist. Prof. Dr. Andam Mustafa) and my colleague (Eng. Muhammed Rasool). Additionally, sincere thanks are extended to all those who played a role in the accomplishment of this research endeavor.

Hoshang Hayder

February 2024

ABSTRACT

Reinforced concrete (RC) beams characterized by circular openings present inherent structural challenges, resulting in a compromise of their load-bearing capacity and overall structural integrity. This thesis endeavors to confront and resolve this issue through the implementation of an innovative approach involving Near Surface Mounting (NSM) steel bars. Circular openings, integral to architectural designs, frequently engender a diminution in the strength of beams. This study investigated the effectiveness of utilizing near-surface mounted (NSM) steel bars to restore the shear strength of deep beams and the presence of openings in slender beams. The experimental work involved testing fourteen simply supported reinforced concrete beams. These beams were divided into two groups, each consisting of beams with different shear span-to-depth ratios (a/h = 1.5 and 3.65). Two specimens served as control samples, while the remaining beams had openings located at various positions. The openings were categorized as large or small, with opening height ratios (h_o/h) of 0.4 and 0.2, respectively. In the second group, six specimens were strengthened using near-surface mounted (NSM) steel bars arranged in three different stirrup configurations: (square, diamond, and parallelogram). All the beams had a cross-section of 100 mm × 200 mm and a total length of 2000 mm. The variables examined in the tests included the sizes and locations of the openings, the diameter of the bars, and the arrangement of the strengthening bars around the openings. The test results revealed that the presence of openings in the beams led to a reduction in the ultimate load. For specimens with large circular openings in the deep beam's shear zone, large circular openings in the slender beam subjected to shear, large circular openings subjected to shear and flexural loads, and small openings in the slender beam subjected to shear and flexural loads, the ultimate load decreased by approximately 45%, 18.7%, 14.6%, and

19.5%, respectively. Additionally, the test results showed that specimens strengthened with diamond stirrup bars exhibited an improvement in the ultimate load of up to 33.1%. Meanwhile, specimens strengthened with square and parallelogram stirrup bars demonstrated improvements of up to 21.5% and 26.5%, respectively. Changing the bar diameter had a slight effect on increasing the ultimate load, specifically for the parallelogram and square schemes, resulting in an increase of approximately 10% and 7%, respectively.

List of contents

1 CHAPTER ONE 1

1.1 BACKGROUND 1
1.2 STRENGTHENING OF R.C BEAMS HAVING THE OPENING: 4
1.2.1 Strengthening RC Beams by NSM Technic: 4
1.3 FAILURE TYPES OF NEAR SURFACE MOUNTED METHOD: 5
1.4 THE AIMS OF THE RESEARCH: 6
1.5 THESIS LAYOUT: 7

2 CHAPTER TWO 8

2.1 INTRODUCTION: 8
2.2 PREVIOUS STUDY ON RC BEAMS WITH OPENINGS: 8
2.3 STUDIES ON RC BEAMS WITH CIRCULAR OPENINGS: 9
2.3.1 Studies on RC Beams with Small Circular Openings: 9
2.3.2 Studies on RC Beams with Large Circular Openings: 17
2.4 STUDIES ON STRENGTHENING OF THE RC BEAMS USING NSM TECHNIC: 22
2.5 SUMMARY: 31

3 CHAPTER THREE 33

3.1 INTRODUCTION 33
3.2 TEST PROGRAM: 33
3.2.1 Identification of Beams 33
3.2.2 Description of Beams 35
3.2.2.1 Group One Description 35
3.2.2.2 Group Two Description 37
3.3 MATERIAL PROPERTIES 40
3.3.1 Cement 40
3.3.2 Fine Aggregate 41
3.3.3 Coarse Aggregate 42
3.3.4 Superplasticizer (CHRYSO) 43
3.3.5 Concrete job mix 44
3.3.6 Mixing Water 44
3.3.7 Mix Design 44
3.3.8 Steel rebars test 45
3.3.9 Epoxy paste 46
3.4 BEAM MOLD 47
3.5 CAGE AND PLACEMENT 48
3.6 CASTING 49
3.7 DRILLING RC BEAMS BY CORE MACHINE 51
3.8 NSM STEEL BAR INSTALLATION PROCEDURE 52
3.9 INSTRUMENTATION 55
3.9.1 Load Measurements 55
3.9.2 Deflection Measurements 57
3.9.3 Concrete Strain Measurements 57
3.10 TESTING PROCEDURE 58
3.11 MECHANICAL PROPERTIES OF CONCRETE: 59
3.11.1 Compressive Strength of Concrete (fc^-) 59
3.11.2 Splitting Tensile Strength (fc_t) 60
3.11.3 Flexure Strength (fr) 61

4 CHAPTER FOUR 62

4.1 INTRODUCTION 62
4.2 MECHANICAL PROPERTIES OF NORMAL STRENGTH CONCRETE (NSC): 62
4.2.1 Compressive Strength (fcu) 63
4.2.2 Tensile Splitting Strength (fc_t) 63

4.2.3 Flexure Strength (fr) 63
4.3 THE BEHAVIOR OF TESTED BEAMS: 64
4.3.1 Specimen Behavior in Group One 65
4.3.2 Specimen Behavior in Group Two 66
4.4 LOAD-DEFLECTION RELATIONSHIP 68
4.4.1 Group One un-strengthened Specimens: 68
4.4.2 Group Two Strengthened Specimens – Scheme Square Steel Bar: 71
4.4.3 Group Two Strengthened Specimens – Scheme Diamond Steel Bar: 72
4.4.4 Group Two Strengthened Specimens – Scheme parallelogram Steel Bar: 73
4.5 CRACK PATTERN AND FAILURE MODE: 75
4.5.1 Un-strengthened Specimens - Group One 75
4.5.2 Strengthened Specimens - Group Two 78
4.6 STRAIN MEASUREMENTS: 81
4.6.1 Concrete strain 81
4.7 ULTIMATE LOADS AND FAILURE MODE 83

5 CHAPTER FIVE 86

5.1 INTRODUCTION 86
5.2 FINITE ELEMENT METHOD 86
5.2.1 ABAQUS Software 87
5.2.1.1 Abaqus/explicit 89
5.3 MATERIALS: 90
5.3.1 Concrete 90
5.3.2 Steel rebars 95
5.4 ELEMENT TYPES 97
5.5 ELEMENT INTERACTIONS: 97
5.5.1 Interaction between Concrete and Internal Reinforcement 98
5.5.2 Interaction between Concrete and support loading plates 98
5.6 BOUNDARY CONDITIONS AND LOADING 99
5.7 MESHING 99
5.8 RESULTS AND DISCUSSION: 101
5.8.1 Load and Deflection 101
5.8.2 Comparison of Failure Load Between ABAQUS Simulation and Experimental Results 104
5.8.3 Crack Pattern 105

6 CHAPTER SIX 111

CONCLUSIONS AND RECOMMENDATIONS 111
6.1 CONCLUSIONS 111
6.1.1 Experimental work 111
6.1.2 Numerical Study 112
6.2 RECOMMENDATION 113

REFERENCE 114

List of Figures

Fig. No.	Titles	Page No.
1-1	R.C. Beam with openings.	2
1-2	Typical service ducting and pipe configuration by Prentzas (1968).	3
1-3	Small openings are defined based on their dimensions.	3
1-4	Large Openings are defined based on Structural Response.	3
2-1	Pipes for water supply systems, and sewage through beam webs.	9
2-2	Description of Small Openings.	10
2-3	The definition of small and large openings in beams, as well as the approximate validity of Bernoulli's hypothesis of plane strain distribution.	10
2-4	Shear failure of a beam with no shear reinforcing around small openings.	11
2-5	Reinforcement schemes applied to beams that have small openings were studied by Salam in (1977).	12
2-6	Beam B4 failed in shear at the throat section, as reported by Salam in (1977).	12
2-7	The patterns of cracking observed in beams tested by Mansur et al. (1999).	13
2-8	The patterns of cracks observed in beams by Tan (2003).	14
2-9	Rc Beams with Small Circular Opening in Shear Zones by Shubbar et al., (2017).	16
2-10	Description of large openings based on structural reaction.	17
2-11	Flexural failure of RC beams with large opening.	18
2-12	A sample of RC beams with circular openings.	19
2-13	RC deep beam with circular openings.	20
2-14	The failure in the shear zone was observed in the un-strengthened beams with large openings.	21
2-15	Strengthening of RC beam with CFRP.	22
2-16	T-Beam cross-section and representation of NSM rodes in the tension zone.	23
2-17	Strengthening schemes.	29
3-1	Details of the tested beam in (Group One).	37
3-2	Details of the tested beam in (Group Two).	39
3-3	Grading curve for fine aggregate (Sand).	42
3-4	Grading curve for fine aggregate (Gravel)	43

3-5	The machine is used for testing the tensile strength of steel bars.	45
3-6	Epoxy paste (Polypoxy-NF)	47
3-7	Beam molds.	47
3-8	Reinforcement Beam Cages in Groups One and Two.	48
3-9	Reinforcement beam cage inside the formwork	49
3-10	Casting concrete.	50
3-11	Removing formwork and curing the samples.	50
3-12	Marking the position of openings.	52
3-13	A sample of the core.	52
3-14	Cutting and grooving process.	54
3-15	Cleaning and epoxy process.	54
3-16	Testing Machine Details.	56
3-17	Load Cell.	56
3-18	Dial gauge used for deflection measurement.	57
3-19	Location of concrete strain gauge.	57
3-20	Loading arrangement with measuring instrumentation	59
3-21	Compressive Strength Machine.	60
3-22	Compressive Machine for Splitting Tensile Strength Test.	60
3-23	Compression machine for flexure strength (fr).	61
4-1	First crack load and load carrying capacity of tested beams.	68
4-2	Load deflection curves for group one	70
4-3	Load-deflection response of control and large opening specimens in group one.	70
4-4	Load-deflection response of control and small opening specimens.	71
4-5	Load-deflection behavior of the square strengthening scheme and DBLS specimens.	72
4-6	Load-deflection behavior of the diamond strengthening scheme and DBLS specimens.	73
4-7	Load-deflection behavior of the parallelogram strengthening scheme and DBLS specimens.	74
4-8	Load-deflection behavior of the parallelogram strengthening scheme and DBLS specimens.	74
4-9	Crack patterns and failure mode for group one specimens.	77
4-10	Crack patterns and failure mode for group two specimens.	81
4-11	Load-compression strain relationship for specimens in group one.	82
4-12	Load-compression strain relationship for specimens in group two.	82

5-1	Modeling Plastic Damage of Reinforced Concrete in Finite-Element Applications.	91
5-2	Compressive and tensile stress-strain relationship by Euro code.	91
5-3	Compression behavior of concrete.	93
5-4	Tensile behavior of concrete.	95
5-5	Steel reinforcements tensile behavior.	96
5-6	Components within the Finite Element Method as described in the ABAQUS Documentation from 2010.	97
5-7	Interaction of the models.	100
5-8	Loading and boundary conditions.	100
5-9	The meshing of RC models.	100
5-10	Group one Numerical and Experimental load-deflection curves.	102
5-11	Group two Numerical and Experimental load-deflection curves.	104
5-12	Crack patterns of Numerical and Experimental group one specimen.	107
5-13	Crack patterns of Numerical and Experimental group two specimens.	109

List of Tables

Table No.	Titles	Page No.
2-1	Test result.	18
3-1	Details of the sample.	34
3-2	Physical properties of the cement.	40
3-3	Chemical properties of the cement.	40
3-4	Grading of fine aggregate (Sand).	41
3-5	Grading of coarse aggregate (Gravel).	42
3-6	CHRYSO Superplasticizer properties.	43
3-7	Concrete job mix properties.	44
3-8	Concrete Mixture proportions.	44
3-9	Steel rebars test.	45
3-10	Technical specification of Epoxy paste.	46
4-1	Compressive Strength of Cubes.	63
4-2	Splitting tensile flexure strength result.	64
4-3	Flexure strength result.	64
4-4	Summary of test results.	67
4-5	Ultimate loads and Failure mode results.	85
5-1	Concrete properties.	90
5-2	Parameters of plastic damage.	93
5-3	Steel rebar material properties.	96
5-4	Experimental and ABAQUS failure load results.	105

List of Notations

Symbol	Meaning
%	Percentage
a/h	Shear span-to-depth ratios
a	Shear span
a	Distance from the centroid of the opening to the support, mm
b	Beam width
D	diameter of openings
d	Effective depth
E_c	Modulus of Elasticity of Concrete
E_s	Modulus of elasticity of steel
F_{cu}	Compressive Strength of Concrete (cube)
F_y	Steel yield stress
fct	Splitting Tensile Strength
fr	Flexure Strength
ho/h	Opening height ratios
Ø	Diameter of reinforcement bar (mm)
L	Length of the beam, mm
P_{cr}	Cracking Load
Pmax	Ultimate Load
P_u	Ultimate Load
w/c	Water to cement ratio
ν	Poisson’s ratio
fc'	Compressive Strength of Concrete (cylinder)
Δcr	Midspan Deflection at the first cracking stage
Δpeak	Mid span Deflection at the Peak Load.

List of Abbreviations

ACI	American Concrete Institution
ASTM	American Society for Testing and Materials
ABAQUS/CAE	A backronym with a root in Computer-Aided Engineering
C/C	Center to Center
CFRP	Carbon-fiber-reinforced polymers
EBR	Externally bonded reinforcement
DCB	Deep control beam
DBLS	Deep beam with (large opening in the shear zone)
DBLSS8	Deep beam with (large opening in shear zone and strengthened by square stirrup rebar Ø8)
DBLSS10	Deep beam with (large opening in shear zone and strengthened by square stirrup rebar Ø10)
DBLSD8	Deep beam with (large opening in shear zone and strengthened by diamond stirrup rebar Ø8)
DBLSD10	Deep beam with (large opening in shear zone and strengthened by diamond stirrup rebar Ø10)
DBLSP8	Deep beam with (large opening in shear zone and strengthened by parallelogram stirrup rebar Ø8)
DBLSP10	Deep beam with (large opening in shear zone and strengthened by parallelogram stirrup rebar Ø10)
EB	External bonding
FRP	Fiber Reinforced Polymer
FEM	Finite Element Method
IQ. S	Iraqi specification
kN	Kilo Newton
MPa	Mega Pascal

Mid.	Middle
NSM	Near Surface Mounted
RC	Reinforced concrete
SCB	Slender control beam
SBLS	Slender beam with (large opening in the shear zone)
SBLF	Slender beam with (large opening in flexure zone)
SBLSF	Slender beam with (large opening in shear and flexure zones)
SBSF	Slender beam with (small opening in the flexure zone)
SBSSF	Slender beam with (a small opening in shear and flexure zones)

CHAPTER ONE

INTRODUCTION

CHAPTER ONE

INTRODUCTION

1.1 Background

In practical terms, transverse openings in Reinforced Concrete beams are a facility that allows a service line, such as a network of pipes and ducts (which is required to accommodate essential services such as water supply, sewage, air-conditioning, electricity, telephone, and network device), to pass through the building as shown in Fig. (1-1) Providing web holes allow the designer to reduce the height of the structure, particularly in a high-rise building, resulting in an affordable pricing design. To eliminate the ceiling problem generated by suspending such services pipes and ducts, it has recently been the usual practice to provide holes through the floor beams for the passage of utility pipes and ducts Mansur and Tan, (1999). Transverse openings convert simple beam behavior into more complicated behavior by causing a sudden change in the dimension of the beam's cross-section. Furthermore, because the opening represents a point of weakness, the failure zone always passes through it.

Ultimate strength, shear strength, crack width, and stiffness may all suffer as a result. The existence of an opening in the web of a reinforced concrete beam causes a variety of difficulties in beam behavior, including decreased beam stiffness, excessive cracking, excessive deflection, and decreased beam strength Amiri et al., (2011), as well as a significant distribution of forces and internal moments in a continuous beam. As a consequence, the impact of openings on the strength and behavior of reinforced concrete beams must be examined, and the design of these beams requires special consideration.

Fig. 1-1 R.C. Beam with openings.

This research examines slender and deep reinforced concrete beams, both with and without openings. Deep beams in reinforced concrete play a crucial role in various structures such as high-rise buildings, offshore constructions, long-span structures (acting as transferring girders), footings, and water reservoirs. Despite deep beams typically failing in shear at their ultimate limit state, accurately defining their shear capacities is crucial. According to recent codes like ACI-318 (2019), a beam is considered deep when the span-to-overall member depth ratio (L/h) is 4 or less. Alternatively, it is classified as deep if the shear span-to-overall component depth ratio (a/h) is 2 or less, and the span-to-depth ratio (L/d) is 4 or less, or if the shear span-to-depth ratio (a/d) is 2 or less. The strength of a deep beam is often governed by shear, rather than flexure, provided that normal amounts of longitudinal reinforcement are used.

RC beams with web openings by size and placement, with openings categorized as small or large and varying in shape. Fig. (1-2) shows a typical service pipe layout in high-rise buildings. Circular and rectangular openings are preferred, as noted by Prentzas (1968), with researchers using terms like "small" or "large" to describe their size.

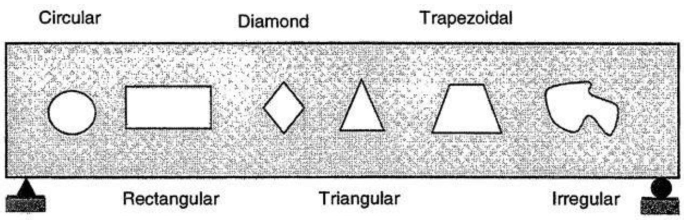

Fig. 1-2 Typical service ducting and pipe configuration by Prentzas (1968).

Somes and Corley (1974) define a small opening as having a depth (d) or diameter (D) less than or equal to 0.25 times the beam's depth (h) and a length not exceeding its depth, as shown in Fig. (1-3). However, they contend that categorizing an opening as small or large is primarily determined by the beam's structural response. Large openings in beams, like small ones, require additional vertical and horizontal struts. Schäfer and Schlaich (1993) argue that Bernoulli's plane strain distribution is inaccurate for large openings, as shown in Figs. (1-4). According to Somes and Corley (1974), an opening is considered large when its depth (d) or diameter (D) exceeds 0.25 times the beam's depth (h), and its length (l) surpasses its depth (d). Such large openings weaken the beam's strength and induce beam-like behavior.

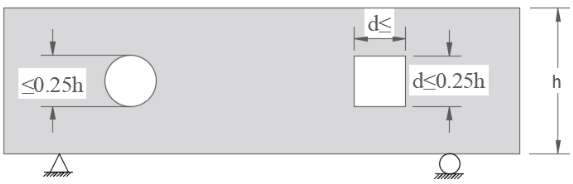

Fig. 1-3 Small openings are defined based on their dimensions.

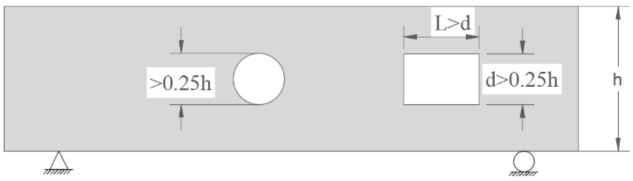

Fig. 1-4 Large Openings are defined based on Structural Response.

1.2 Strengthening of R.C Beams having the Opening:

Various methods, including externally bonded laminates (EB), (NSM) bars/strips, mechanical anchoring, or grooving with or without adhesives, are used to reinforce concrete beams De Lorenzis et al., (2001). EB FRP strengthening can involve multiple layer arrangements like side bonding, U-wrapping, or complete wrapping. NSM strips are inserted into grooves on beam tension faces, covered with concrete layers or adhesive materials. Properly anchoring fiber ends is crucial to maximize FRP effectiveness in strengthening and minimize the risk of debonding Hawileh et al., (2016).

1.2.1 Strengthening RC Beams by NSM Technic:

The NSM strengthening technology offers reliable solutions for repairing concrete structures Hassanien, (2015), with NSM steel rebars enhancing the flexural and shear strength of defective concrete elements De Lorenzis et al., (2001). Concrete structures often require strengthening or rehabilitation due to various factors, such as increased service load, environmental effects, construction errors, and mechanical damage. While external reinforcement materials are commonly used, NSM reinforcing bars are susceptible to mechanical damage, vandalism, and fire due to their proximity to the concrete surface Hassanien, (2015). Repairing or rehabilitating reinforced concrete structures is often necessary due to material deterioration, corrosion, fire hazards, earthquakes, and structural function changes Diab et al., (2020). The NSM technology originated in Finland in 1940, initially used to reinforce a bridge deck slap Kamonna and Alkhateeb, (2020). Near Surface Mounted (NSM) techniques involve cutting grooves in concrete covers and inserting rebar with a specialized groove filler (epoxy or cement mortar), which has proven successful. While the NSM strengthening process was considered new in the early

1950s Asplund, (1949), steel bars embedded in cement mortar were the primary concept initially. Later, shotcrete was used to cover the exterior bars, but this approach didn't provide strong bonding, and sometimes casting concrete around the strengthened members wasn't feasible. In the early 1960s, the epoxy industry advanced NSM technology by introducing structural fillers and using resins as groove fillers.

1.3 Failure Types of Near Surface Mounted Method:

(NSM) method reinforces concrete structures by placing steel bars within a groove cut into the concrete surface. It is widely recognized as a dependable and effective technique for strengthening concrete structures. Nevertheless, like any construction method, there are potential failure modes that may occur. Some of the common modes of failure associated with the NSM method are as follows:

1) **Concrete cover separation:**

   The NSM method includes cutting a groove in the concrete surface, reducing the concrete cover thickness. Insufficient concrete cover may result in the separation of the cover, exposing the reinforcement and leading to corrosion.

2) **Bond failure:** The NSM method depends on the bond between the steel reinforcement bars and the adjacent concrete to transmit stresses. Insufficient bonding between the steel and concrete may lead to bond failure, causing a decrease in the structure's load-carrying capacity.
3) **Corrosion:** The steel reinforcement bars corrosion can occur due to the exposure of the bars to the environment or due to the penetration of moisture into the concrete. Corrosion can weaken the reinforcement bars, ultimately causing the failure of the NSM strengthening system.

4) **Shear failure:** The NSM strengthening system is designed to increase the shear strength of the concrete structure. If the shear forces exceed the capacity of the strengthened section, then shear failure can occur.

1.4 The Aims of the Research:

This study aims to explore the influence of openings on the behavior of reinforced concrete beams and assess the feasibility of strengthening these structural elements using Near Surface Mounted (NSM) steel bars. The specific objectives are as follows: The research project investigates the effectiveness of using Near Surface Mounted (NSM) steel rebars as a strengthening technique for Reinforced Concrete (RC) beams with openings.

1) The study aims to investigate the effects of changes in the size and location of openings on the shear capacity of Reinforced Concrete (RC) beams, as well as variations in the shear span ratio (a/d).
2) The research project aims to evaluate the effectiveness of the NSM technique with different schemes around openings.
3) The use of NSM steel rebars is a promising technique for strengthening RC beams with openings, as it can increase the load-carrying capacity and stiffness of the beam without significantly altering its overall geometry.
4) The study involves a numerical analysis of the tested specimens using the ABAQUS program. The aim is to compare the numerical results with the experimental results to confirm the accuracy of the finite element simulation pattern used for such structural members. Additionally, the study will present a numerical parametric analysis.
5) The ultimate goal of the research project is to develop design guidelines for using NSM steel rebars as a strengthening technique and provide a better understanding of the behavior of RC beams with openings.

1.5 Thesis layout:

The thesis has been partitioned into six sections;

Chapter One: This section provides a summary of the research problem, study objectives, research questions or hypotheses, and the employed methodology.

Chapter Two: This section provides a comprehensive review of the relevant literature on the topic, highlighting the main findings and identifying any gaps in the existing research.

Chapter Three: This section offers details about the testing materials utilized in this thesis, and information about the control specimens.

Chapter Four: This section presents the main findings of the study, often using tables, graphs, and other visual aids to illustrate the results.

Chapter Five: This chapter unveils the outcomes of the finite element analysis of RC beams conducted with ABAQUS software and compare the findings with experimental data.

Chapter Six: This section gives an overview of the conclusions derived from the research and provides recommendations for future studies.

CHAPTER TWO

LITERATURE REVIEW

CHAPTER TWO

LITERATURE REVIEW

2.1 Introduction:

In this chapter, prior theoretical and experimental studies on the behavior of RC beams are described, both with and without openings, especially circular openings of various sizes and locations. Additionally, the strengthening of RC Beams with openings using (NSM) techniques will be explored through various methods.

2.2 Previous Study on RC Beams with Openings:

Numerous investigations have explored the performance of reinforced concrete beams featuring openings of diverse shapes and dimensions, spanning simply supported beams, continuous two- and three-span beams, and T-beams. Various models and equations have been formulated using the collected data to anticipate the structural capacity of RC beams, considering factors such as flexural, shear, and/or torsional behavior Chin et al., (2015). Typically, introducing openings in the web of a reinforced concrete beam reduces its stiffness, leading to increased cracking, deflection, and a strength decrease. Therefore, reinforced concrete beams with openings require assessment for strength, or the area around the opening must be appropriately designed to restore the lost strength Mansur, (1983).

Various experimental methods and computational techniques have been developed to offer adequate reinforcement around openings in RC members Chin et al., (2015), and an upgraded version of such a method was published Mansur, (2006). Even during the predesign and construction phases, all of these studies took the position and size of the entrance into account.

2.3 Studies on RC Beams with Circular Openings:

In practice, beam circular opening is extremely common to offer a conventional path for pipes and ducts for water supply systems, sewage, and electrical cables as shown in Fig. (2-1). The presence of an opening in an RC beam reduces its stiffness, leading to heightened deflection under service load and the occurrence of fractures. The opening might be circular, rectangular, triangular, or even irregular in form and size. In reality, though, circular and rectangular openings are the most prevalent (Mansur, 1999).

Fig. 2-1 Pipes for water supply systems, and sewage through Beam webs by Özkılıç et al., (2022).

2.3.1 <u>Studies on RC Beams with Small Circular Openings:</u>

Circular and square openings are considered small if their depth (d) or diameter (D) is 0.25 times the entire depth of the beam or less, as indicated by Somes and Corley (1974) as shown in Fig. (2-2).

In a strut-and-tie model navigating openings in a beam, it is presumed that no extra struts or ties are needed in the bottom or top chords. This implies an almost linear strain distribution in the opening's cross-section, illustrated in Fig. 2-3a, according to the work of Schlaich and Schafer in 1991. Fig (2-3. a) Schlaich and Schafer, (1991).

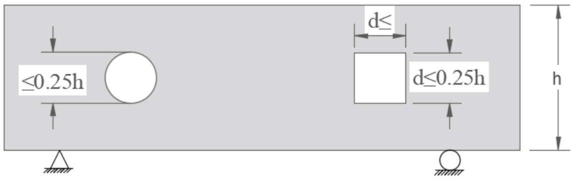

Fig. 2-2 Description of Small Openings.

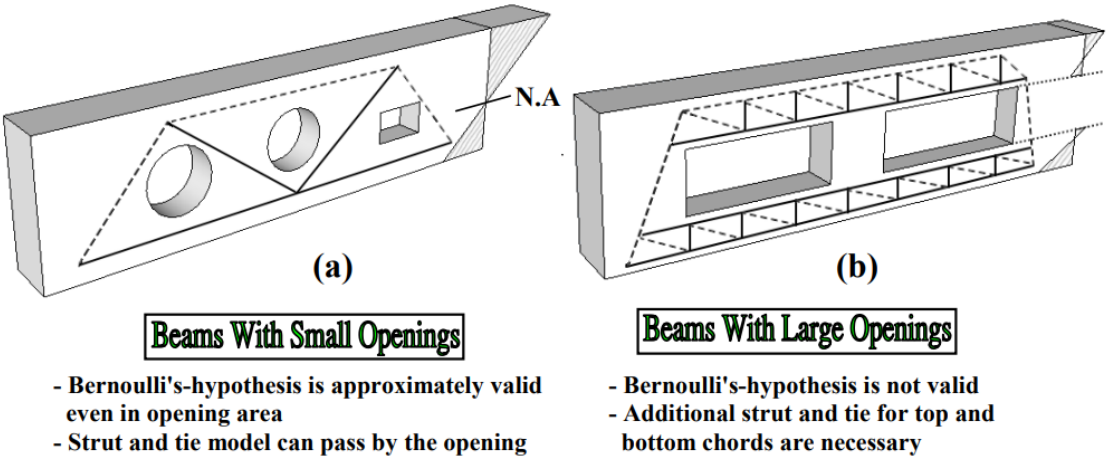

Fig. 2-3 The definition of small and large openings in beams, as well as the approximate validity of Bernoulli's hypothesis of plane strain distribution.

Somes and Corley, (1974), studied transverse reinforced T-beams with square and circular small openings in the web. They found that a small opening near the support does not affect strength Fig. (2-4). As the opening moves away from the support, its strength gradually decreases until stabilizes. The investigation showed that the vertical location of the opening has minimal influence. However, enlarging the opening leads to a nearly linear strength reduction. Adding stirrups on both sides of the opening can restore the beam's strength. Nonetheless, there appears to be a threshold opening size below which there is no shear strength reduction. This dimension is approximately 20 percent of the beam depth for square openings and 30 percent for circular openings.

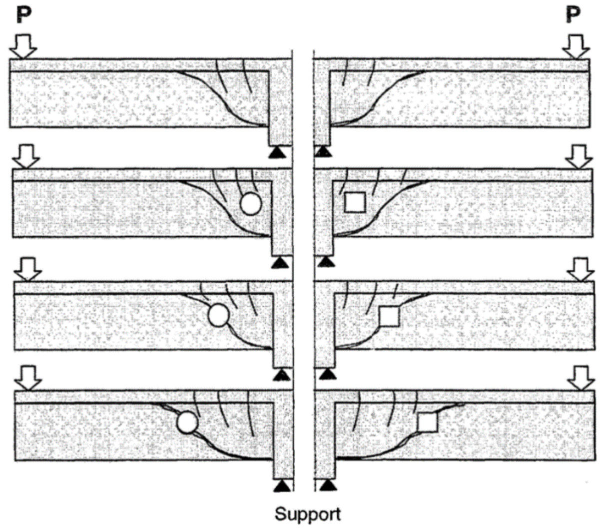

Fig. 2-4 Shear failure of a beam with no shear reinforcing around small openings by Somes and Corley (1974).

Salam (1977), investigated rectangular cross-section perforated beams subjected to two symmetrical point loads. The goal was to devise an effective reinforcement scheme to restore their strength to that of a solid beam. Fig. (2-5) illustrates the reinforcement schemes and beam details used in the study. Salam concluded that, in addition to longitudinal reinforcement and full-depth stirrups, short stirrups were essential above and below the opening to address the weakness introduced by openings. Salam also observed that providing sufficient reinforcement to prevent failure along a diagonal crack passing through the center of the opening, spanning the entire depth, failed the minimum section. In such cases, the beam is divided into two separate segments, leading to ultimate failure. The cracking pattern of Beam B4, failing in this manner, is depicted in Fig. (2–6).

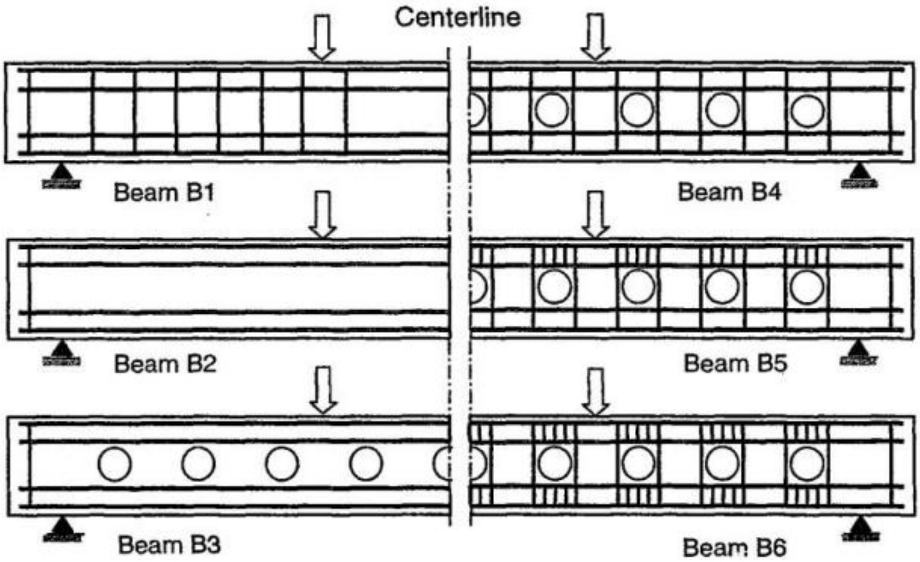

Fig. 2-5 Reinforcement schemes applied to beams that have small openings were studied by Salam in 1977.

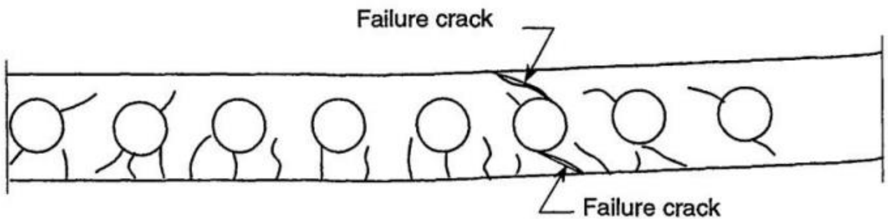

Fig. 2-6 Beam B4 failed in shear at the throat section, as reported by Salam in 1977.

Mansur and Tan, (1999)**,** conducted an investigation involving the fabrication and testing of nine beams with circular, small openings through the web. The purpose was to simulate the drilling of holes in an existing beam for service ducts or to assess in-place concrete strength. The study examined the size and location of the openings, subjecting the beams to failure tests, as illustrated in Fig. (2–7).

The findings indicated that a sizable opening located near the concentrated load region of an existing beam can significantly jeopardize the safety and serviceability of the structure. Filling the opening with non-shrink grout, a common practice for openings resulting from removing concrete cores to assess in-place concrete strength in old buildings, proves insufficient in restoring the beam's original strength and stiffness. However, the risk can be mitigated by restricting the opening size or drilling without cutting any stirrup. Regardless, the designer must conduct a thorough analysis and assessment. Unless the original design incorporates a larger-than-usual factor of safety or appropriate measures to reinforce the beam are implemented, creating an opening in an existing beam is not recommended.

While the study had a limited number of tests, it disclosed that introducing openings in existing beams can result in weaknesses, including cracking, deflection, and reduced ultimate strength. Strengthening the opening region using methods like externally bonded Fiber Reinforced Polymer (FRP) plates can eliminate these weaknesses. The text underscores the significance of meticulous analysis and assessment by the designer when creating openings in existing beams and emphasizes the necessity for appropriate measures to reinforce the beam, preserving its structural integrity.

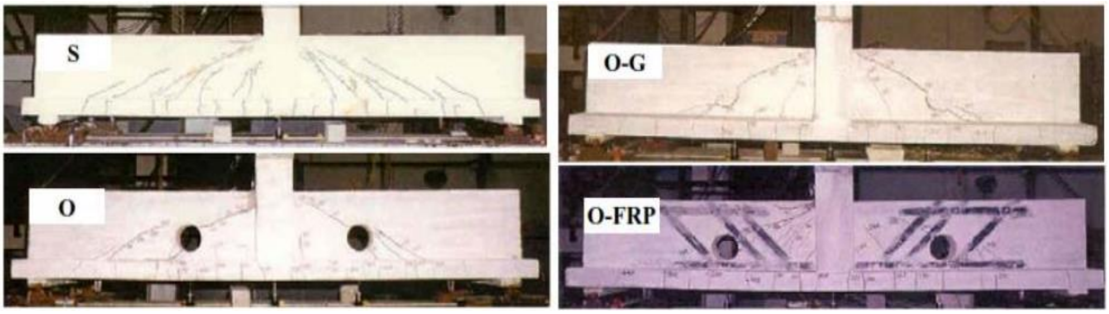

Fig. 2-7 The patterns of cracking observed in beams tested by Mansur et al. (1999).

Tan, (2003), conducted a study evaluating the applicability of the ACI Code approach to shear design for T-beams with circular web openings. The research included the design and testing of seven T-beams featuring circular web small openings, subjected to moderate to high shear force. The testing involved placing the beams in an inverted position to replicate conditions in the negative moment region of a continuous beam, as depicted in Fig. (2-8).

The test outcomes demonstrated that introducing reinforcement around the opening is effective in controlling cracks and preserving ultimate strength. The inclusion of diagonal bars was observed to decrease high stress in the compression chord and prevent premature crushing of the concrete. However, the existence of transverse openings altered the beam's behavior from simple to complex, leading to stress concentration and early cracking around the opening. This change may significantly impact the ultimate strength of the beam. Hence, it is essential to incorporate special reinforcement around the opening to control crack width and avert potential premature failure of the beam.

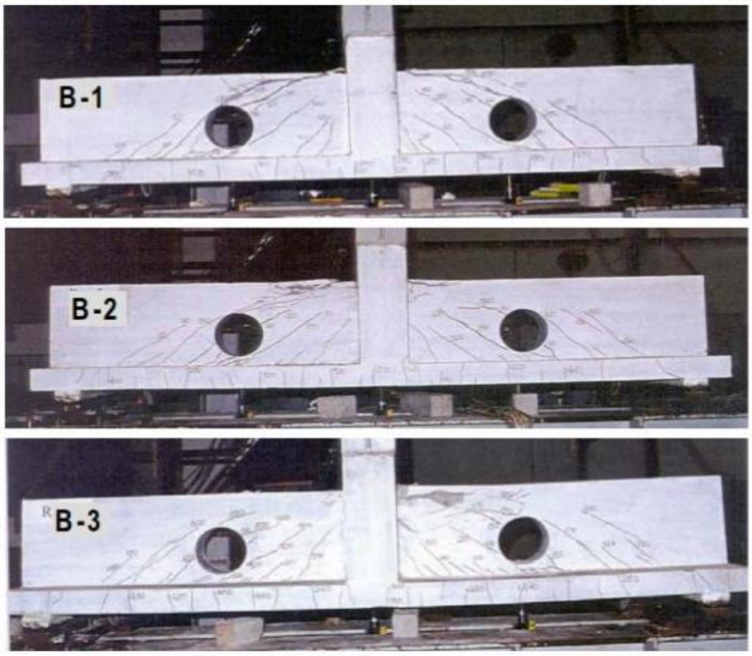

Fig. 2-8 The patterns of cracks observed in beams by Tan, (2003).

Khalil et al., (2004), conducted an experimental study on 16 deep beams made of high and normal-strength concrete, with and without openings. The study considered various parameters, including concrete grade, location, size, shape of the opening, reinforcement arrangement, and (a/d) ratio. The results showed that high-strength RC deep beams with openings were significantly influenced by the grade of concrete, reinforcement arrangement around the opening, and the presence and position of openings.

However, concrete strength did not affect the final failure mode of deep beams, as all specimens ultimately failed in shear. Additional reinforcement around the web opening had no significant effect on failure loads but resulted in less deflection than deep beams without additional reinforcement around the opening. The deflection was not affected in the case of deep beams with openings at the tension side of the beam. On the other hand, openings in the web at the compression zone of the beam resulted in an overall loss of stiffness, leading to about 31% higher deflection.

Shifting the horizontal position of the web opening at the mid-depth of the beam led to increased deflection when the openings intersected the load path, with no impact on deflection observed due to variations in the shape of the opening.

Amiri and Alibygie, (2004), investigated the effects of small circular openings on flexural and shear zones of reinforced concrete (RC) beams were investigated. Beams with different diameters and concrete strengths were tested, and it was found that diagonal shear reinforcement was effective in controlling cracks and limiting their width. To boost the ultimate shear strength of the beams, it was recommended to incorporate diagonal reinforcement and add stirrups at both the top and bottom of the opening. Additionally, the study revealed that when the diameter of the opening surpasses one-third of the beam depth, it diminishes the serviceability of the beam. The nearest position relative to support is the most critical location of opening to achieve ultimate strength.

Shubbar et al., (2017), researched to examine the RC beam's behavior with varying sizes and positions of openings, then simulated the samples by ABAQUS FEM. Seven RC beams with diameters of 120cm,15cm, and 15cm under three-point loads were evaluated. Group A comprises three RC beams featuring circular openings in the shear zone with diameters of 4 cm, 5 cm, and 6.5 cm. In contrast, Group B consists of three RC beams with circular openings in the flexural zone, featuring diameters of 40 mm, 55 mm, and 65 mm. The research reveals that increasing the diameter of the openings leads to a higher maximum deflection and a reduction in ultimate failure stress compared to a beam without openings. Openings in the flexural zone result in a maximum deflection increase ranging from 1.5% to 19.7% and a decrease in ultimate failure load by 6% to 13% compared to the beam without openings. On the other hand, openings in the shear zone cause an improvement in maximum deflection ranging from 4% to 22% and a decrease in ultimate failure load ranging from 26% to 36% compared to the control beam, as illustrated in Fig. (2-9). The optimal location for placing circular openings in this investigation was identified to be in the flexural zone of the beam with a diameter smaller than 30% of the beam depth.

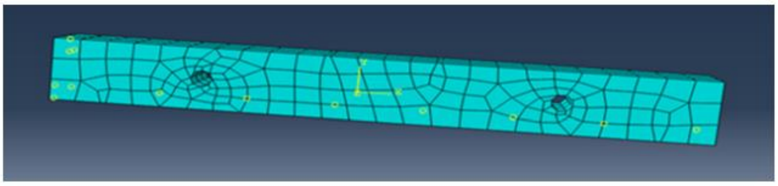

Fig. 2-9 Rc Beams with Small Circular Opening in Shear Zones by Shubbar et al., (2017).

2.3.2 Studies on RC Beams with Large Circular Openings:

According to Schlaich and Schafer, (1991), a large opening in a beam is characterized by the need for extra vertical and horizontal struts in the chords above and below it. This distinguishes it from a beam with small openings.

Bernoulli's hypothesis of a plane strain distribution does not hold for the entire cross-section of a beam with a large opening, as depicted in Fig. 2-3b. An opening is classified as large when its depth (d) or diameter (D) exceeds 0.25 times the depth of the beam (h), and its length (ℓ) is greater than its depth (d). The inclusion of such openings diminishes the strength of the beam and leads to beam-type behavior resembling that shown in Fig. (2-10), according to Somes and Corley (1974).

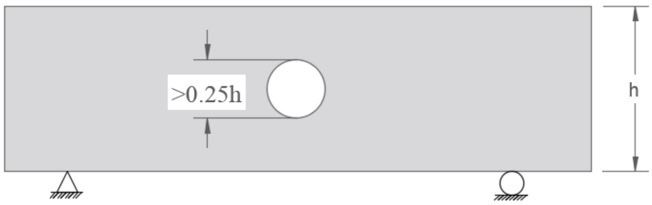

Fig. 2-10 Description of large openings based on structural reaction.

The researcher S C Chin, Shafiq, and Nuruddin (2011) explored the application of Carbon Fiber Reinforced Polymer (CFRP) laminates for strengthening R/C beams featuring large circular and square openings in the flexural zone. The circular and square openings had area-to-effective depth ratios of 0.82 and 0.75, respectively, categorizing them as large openings. The specimens, measuring 2000 mm in length with a rectangular cross-section of 120 x 300 mm, were subjected to 4-point loading to assess ultimate load, deflection, and failure mode. The test results indicated that a large opening in the flexural zone diminishes beam capacity and stiffness while escalating cracking and deflection.

Table (2-1) outlines the ultimate load and failure mode of the examined beams. According to the table, beam "C-con-f" achieved a maximum load of 96.57 kN, while beam "S-con-f" (square opening in flexural) reached a maximum load of 78.14 kN. The capacity reduction in beam "C-con-f" (circular opening in flexural) and beam "S-con-f," as depicted in Fig. (2-11), was 17% and 32%, respectively, compared to the solid control beam without an opening. Large square openings exhibit a greater reduction in flexural strength than large circular openings. In terms of deflection, an RC beam with a large circular opening experiences approximately 30% more deflection than the control beam, while a beam with a square opening result in 10% less deflection than the control beam.

Table 2-1 Test result.

Beam Specimens	Ultimate Load, P_u (kN)	Failure Mode
Control beam, CB	115.67	Shear
C-con-f	96.57	Flexure at opening
S-con-f	78.14	Flexure at opening
C-CFRP-f	164.4	Shear at opening
S-CFRP-s	86.07	Flexure at opening

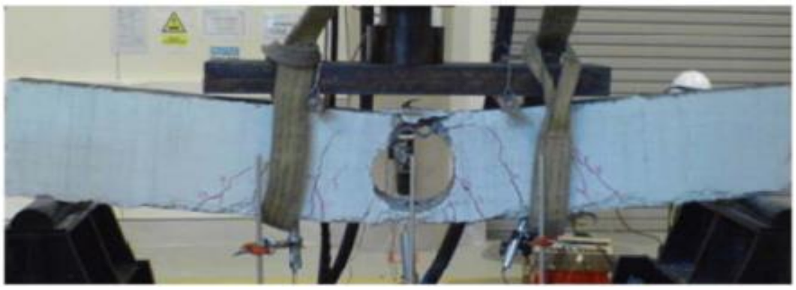

Fig. 2-11 Flexural failure of RC beams with large opening by S C Chin, Shafiq, and Nuruddin (2011).

the researcher Amiri, Masoudnia, and Pabarja (2011) examined simply supported concrete beams featuring circular openings of varying sizes to investigate the impact of circular opening size on beam behavior.

For the verification phase, two samples were taken, and various models of simply supported reinforced concrete rectangular section beams with circular and square openings were subjected to monotonically increasing loads with two concentrated loads. The load-deflection behavior of the beams was modeled and compared to that of a solid concrete beam. All beams shared the same cross-section of 100mm by 250mm and were 2000mm in length, as depicted in Fig. (2-12). Circular openings had diameters of 150mm, 130mm, 120mm, 110mm, 100mm, 80mm, and 60mm, along with an equivalent square hole with a 133mm diameter. The findings indicated that introducing circular openings with diameters less than 0.48D (D being the depth of the beam web) did not impact the ultimate load capacity of RC rectangular section beams. However, introducing a circular opening with a diameter exceeding 0.48D led to a reduction in the ultimate load capacity of the RC rectangular section beams by at least 26%.

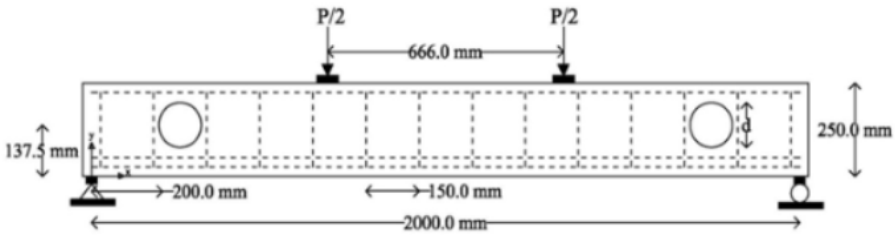

Fig. 2-12 A sample of RC beams with circular openings by Amiri, Masoudnia, and Pabarja (2011).

The investigation by Siew Choo Chin et al. (2015) focused on the performance of an RC deep beam featuring a large circular opening in the composite shear zone, subsequently reinforced using CFRP. The study analyzed the ultimate load, deflection, and failure mode to assess the structural behavior of the beam. The beam had a cross-section of 120mm by 600mm and a length of 2400mm, with openings positioned 300mm from the beam's edge on both supports. These openings had a diameter of

0.45 h, categorized as a large opening, and the shear span ratio was 0.83 or 50cm between the loading and support, as illustrated in Fig. 2-13.

The beam featuring a large circular opening in the shear zone exhibited a strength loss ratio of 51% compared to the control beam. The control beam experienced a deflection of 12.79mm, whereas the beam with a large circular opening in both shear spans had an 8mm deflection.

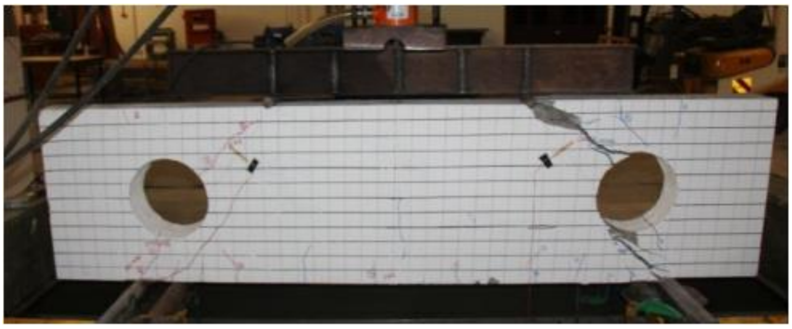

Fig. 2-13 RC deep beam with circular openings by Siew Choo Chin et al. (2015).

The study by Morsya and Barima (2019) delved into the behavior of reinforced concrete (R.C.) beams with openings, both reinforced and unreinforced. A total of 24 specimens underwent testing in two series to investigate how openings affect the beams' behavior, considering factors such as the shape, aspect ratio, and orientation of the opening. The research also explored the impact of various strengthening methods for the openings, encompassing both internal and external reinforcement. All specimens were subjected to three-point loading with a 1500mm effective span and were designed to experience flexural failure rather than shear failure. The findings indicated that circular openings exhibited the least reduction in load capacity compared to rectangular and square openings of equivalent area.

Fig. (2-14) illustrates that a beam with a circular opening in the flexure zone, devoid of any reinforcement, displayed its initial crack at a load of 3.0 tons. All observed cracks were concentrated in the flexure zone.

The beam ultimately failed at a load of 10.0 tons, experiencing only a 10% reduction in load capacity. Strengthening the openings with externally bonded carbon fiber-reinforced polymer (CFRP) proved to enhance both the strength and ductility of the beams when compared to alternative strengthening methods.

Fig. 2-14 The failure in the shear zone was observed in the un-strengthened beams with large openings by Morsya and Barima (2019).

The paper by Hamid et al. (2022) explores the flexural behavior of reinforced concrete beams featuring circular openings at mid-beam span, strengthened using externally bonded textile-reinforced concrete (TRC) sheets, carbon fiber-reinforced polymer (CFRP) sheets, and carbon fiber-reinforced polymer (CFRP) plates. The study conducted tests on five beams, including one solid control beam, one beam with an un-strengthened circular opening, and three beams strengthened with a circular opening. The circular opening, with a diameter of 80 mm and a ratio of 0.32, is depicted in Fig. 2-15, and all beam specimens shared the same dimensions. Results indicate that the incorporation of circular openings marginally decreased the ultimate load of the beam by approximately 6.2%, along with a reduction in stiffness. Nevertheless, the application of strengthening in beams with circular openings significantly increased the beam capacity by 17.5% to 22.6% compared to unstrengthened RC beams with an opening.

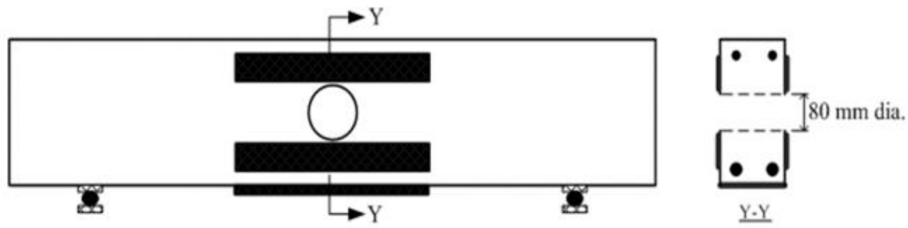

Fig. 2-15 Strengthening for RC beam with CFRP Hamid et al. (2022).

2.4 Studies on Strengthening of the RC Beams Using NSM Technic:

The Near Surface Mounted (NSM) technique involves reinforcing reinforced concrete (RC) beams by affixing reinforcing bars or strips to the beam's surface using an adhesive. This method is employed to augment the load-carrying capacity, enhance stiffness, and improve the ductility of RC beams. Research has been undertaken to assess the efficacy of the NSM technique in reinforcing RC beams. These investigations generally encompass experimental studies and numerical simulations covering the following aspects:

Blaschko and Zilch (1999), conducted a study that compared the use of NSM and glue on the surface for the rehabilitation of four specimens, each with a cross-section of 150 x 350 mm and a length of 300 mm. Two specimens had a height of 350 mm, while the other two had a height of 150 mm and were treated as slabs with a rotated cross-section. The study found that NSM had a greater impact than the external bonded (EBR) technique and provided greater ductility for both beam and slab specimens.

De Lorenzis, Nanni, and La Tegola (2000), conducted a study on the flexural reinforcement of T-beams using the NSM technique, focusing on the bond characteristics of this method. The study involved testing four specimens with cross-sections of 381x101.6 mm for the flange and 304.8x152.4 mm for the web as shown in Fig. (2-16), and a length of 4.57

m. One beam acted as a control without any reinforcement, while the other three specimens featured grooves, and various diameter CFRP bars were incorporated using epoxy as a filler. The findings indicated that deformed and sand-coated rebars exhibited superior bond strength compared to smooth-surfaced ones. Additionally, the tested NSM beams demonstrated an increase of about 25.7% to 44.3% compared to the control beams.

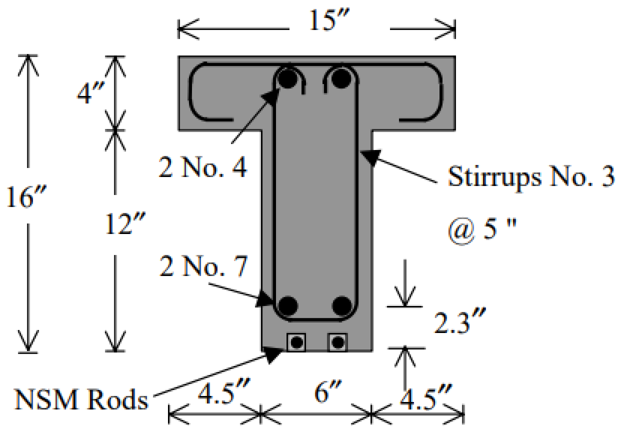

Fig 2-16 T-Beam cross-section and representation of NSM in the tension zone by De Lorenzis, Nanni, and La Tegola (2000).

De Lorenzis, Miller, and Nanni (2001), the study assessed the efficacy of near-surface mounted (NSM) fiber-reinforced polymer (FRP) bars for reinforcing reinforced concrete (RC) beams in shear. Eight full-scale beams were subjected to testing, comprising six strengthened beams and two control beams. Variables included interior steel shear reinforcement, end anchorage of the bars, strengthening configuration, and the distance between the bars. Results demonstrated a significant enhancement in shear strength due to NSM FRP bars, with effectiveness varying based on the test variables. Even in the presence of shear reinforcement, NSM bars contributed significantly to improving beam strength. The study revealed that NSM FRP bars could increase beam strength by up to 106% compared to control beams lacking steel stirrups and by 35% compared to un-strengthened beams with minimal shear reinforcement.

De Lorenzis and Nanni (2002), experimented the study to assess the bond characteristics between NSM rods and concrete. The experiment involved 22 specimens featuring an inverted T-section without any steel reinforcement, designed to maximize the tension area. A two-point load was applied across a clear span of 1066.8 mm. The NSM bars were installed at the bottom with full. The study explored various factors, including the nominal diameter of the FRP bars (9.5 and 13 mm), the bonded length (ranging from 6 to 24 times the bar diameter), the type of FRP rods employed (CFRP and GFRP), the surface configuration of the bars (deformed and sandblasted), and the size of the groove-bedded sides, and the bond length varied for the other bars. The study explored various factors, including the nominal diameter of the FRP bars (9.5 and 13 mm), the bonded length (ranging from 6 to 24 times the bar diameter), the type of FRP rods employed (CFRP and GFRP), the surface configuration of the bars (deformed and sandblasted), and the size of the groove.

Teng et al. (2006)**,** focused on the flexural performance of reinforced concrete beams enhanced with NSM CFRP strips, with a specific emphasis on investigating the debonding failure mechanism associated with the embedment length of the strips. The research employed extensive strain gauges on the NSM CFRP strips to monitor their bonding behavior. Detailed examinations included failure modes, load-deflection curves, local bond stresses at the CFRP-epoxy interface, and strain distributions in the CFRP strips. Comparative analyses were conducted with estimations from an analytical model where necessary. The results indicated a significant improvement in the ultimate load and, to a lesser extent, post-cracking stiffness for all embedment lengths except the shortest one.

Debonding failure was observed in all specimens, except for the case strengthened with the longest embedment length of CFRP strips.

Novidis and Pantazopoulou, (2008), conducted a test on approximately 45 specimens to investigate the bond characteristics of NSM, with dimensions of (240×240×210 mm), embedded with different steel and CFRP bars. The study delved into crucial parameters such as groove dimensions, embedment length, surface roughness, and material of the bar in the context of NSM reinforcement. A modified pull-out test was employed to address shortcomings in traditional manufacturer tests. The findings revealed that, with a given groove dimension, bond strength increased as the embedded length extended until reaching a critical length equivalent to five times the NSM bar diameter. Moreover, for the same bond development length, the bond load capacity rose with an increase in groove depth. Additionally, the research highlighted an augmented bond capacity with a rise in NSM bar material stiffness, manifested in higher bond strength for smooth and deformed steel bars compared to their smooth and sand-blasted CFRP counterparts.

Al-Mahmoud et al. (2009), analyzed the flexural performance of reinforced concrete components reinforced with NSM CFRP rods. Eight specimens, measuring 3 meters in total length and having dimensions of 150 x 280 mm, underwent a four-point bending test. The study explored various parameters including concrete compressive strength (C30 and C60), NSM bar details (1φ12 mm vs. 2φ6 mm), filling material (epoxy resin or mortar), and the length of CFRP bar coverage (2100 mm, 2700 mm, and 3000 mm). Findings revealed that higher concrete strength, using a single (φ12 mm) bar rather than two (φ6 mm), employing epoxy resin, and extending the running length of NSM bars resulted in increased stiffness.

Pimanmas, (2010), focused on enhancing RC beams with openings using NSM-CFRP rods. Test specimens featured square or circular openings positioned at the shear span's center. CFRP rods were externally applied within grooves, either forming a closed square around the opening or placed diagonally next to it, extending throughout the beam's depth. The comparative analysis involved specimens with CFRP reinforcement and those containing prefabricated internal steel bars around the opening. While CFRP reinforcement improved the beam's strength, it did not fully replicate the failure mode of solid beams. However, placing CFRP rods diagonally beside the opening resulted in a load capacity similar to that of a solid beam, with the bottom diagonal CFRP rod exhibiting superior shear resistance to the top rod. Analytical analysis indicated that inclined rods were more effective when positioned perpendicular to cracks than vertically placed ones. Placing the strengthening system away from the opening did not enhance the beam's strength, especially when the opening was sizable, leading to a reduced strut area in the concrete and diminishing the significance of CFRP rods in carrying tension stresses. Additionally, the length of CFRP rods was observed to impact the beam's performance.

Deepa and Surumi, (2012), explored the efficacy of near-surface-mounted (NSM) glass fiber-reinforced polymer (GFRP) materials in shear-strengthening applications for deep beams. Twelve specimens, measuring 1400 mm in length with a cross-section of 175 mm x 250 mm, were cast and subjected to four-point bending with a/d = 1.84, and a concrete compressive strength of 34.88 MPa. The beams were divided into two groups, with five beams in group one and seven beams in group two. Results indicated that NSM outperformed external bonding in shear strengthening, and the utilization of laminates yielded higher shear capacity compared to GFRP bars. Concentrating NSM in the shear span led to increased member capacity but reduced ductility when compared to the use of rebars across the entire section.

Mansour, (2019) , investigated the efficacy of employing near-surface-mounted carbon fiber-reinforced polymer (NSM-CFRP) reinforcement to recover the shear strength of deep concrete beams with significant disruptions caused by a web opening. Employing a strut-and-tie model (STM), three distinct strengthening solutions were developed around the regions affected by the discontinuity. A total of eight deep beam specimens were constructed and subjected to laboratory testing. The results indicated that the introduction of a web opening resulted in a 40% reduction in shear strength. However, the NSM-CFRP strengthening solutions effectively restored the original shear strength, with only two cases exhibiting a restoration of 93% and 94% of the capacity. The STM provided reliable and consistent predictions for the nominal strength of the tested specimens, while the finite element (FE) models' predictions were sensitive to the mesh size and the concrete constitutive law adopted in the analysis.

Mansour, M.S., (2019), examined the performance of deep-reinforced concrete beams reinforced with near-surface mounted carbon fiber-reinforced polymer (NSM-CFRP) in the presence of structural discontinuities, illustrated in Fig. (2-17). The main outcomes are outlined as follows:

1. Incorporating a square opening with a height-to-depth ratio of 0.2 within the shear spans of deep beams led to a 40% decrease in load capacity.

2. The NSM-CFRP strengthening methods devised in the research effectively reinstated the initial load capacity for the majority of specimens.

Nonetheless, two beams achieved only 93% and 94% of their original capacity.

3. The failure modes differed based on the configuration. The solid specimen experienced failure due to shear compression, while the un-strengthened specimen with an opening failed in diagonal tension. The NSM-CFRP reinforcement changed the failure mode to diagonal splitting or strut crushing.

4. The study assessed the efficacy of various strut-and-tie models (STM). Both STM I and STM II, featuring a single inclined tie in each shear span, demonstrated superior performance compared to STM III, which had two inclined ties. Increasing the quantity of NSM-CFRP reinforcement led to strength improvements of 23% and 10% for STM I and STM III, respectively. Doubling the CFRP for STM II did not yield additional strength gains, possibly because the mode of failure was primarily influenced by the diagonal splitting of the bottom chord.

5. The STM predictions aligned with the guidelines outlined in the ACI 318-14 code and were both realistic and accurate, showing an average predicted-to-measured strength ratio of 1.01. Nonetheless, disparities were noted between the failure modes predicted by STM and the actual experimental failure modes observed during testing.

6. The STM predictions, following the guidelines of the CSA S806 code, tended to be conservative, except for the solid deep beam, where the predicted strength exceeded the experimental result by 31%. The average predicted-to-measured strength ratio stood at 0.71.

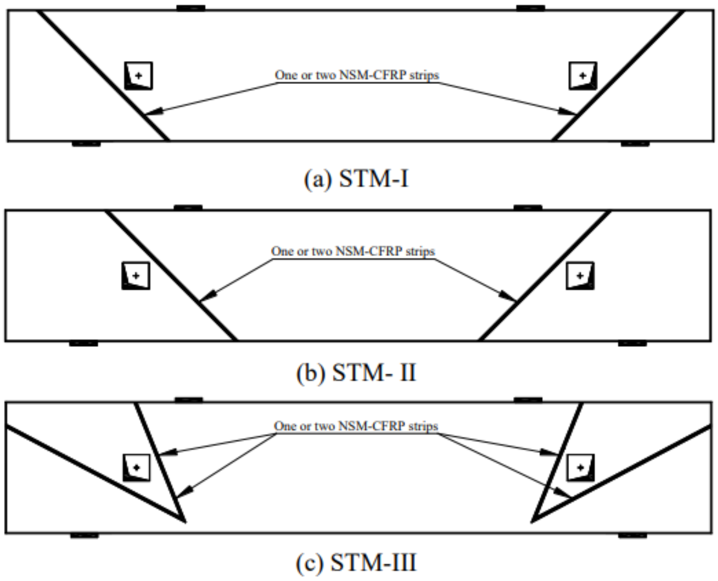

Fig. 2-17 Strengthening schemes by Mansour, M.S., (2019).

Kammona and Alkhateeb, (2020), this study conducted both experimental and numerical analyses on simply supported reinforced concrete deep beams with openings. The primary focus was on examining their behavior when strengthened using near-surface mounted (NSM) steel bars. The study considered various parameters such as opening size, location, steel bar diameter, and strengthening configurations. Thirteen specimens were tested, including four without any strengthening (one without openings and three with symmetrically located openings), and nine specimens strengthened with NSM steel bars in different configurations around the openings.

The test results showed that the presence of openings along the load path reduced the ultimate load by approximately 56% and 70% for square openings of 150mm and rectangular openings of 250 mm x 150 mm, respectively. Locating the openings at a 75mm distance from the load path led to an approximately 49% reduction in the ultimate load.

Reinforcing the openings with vertical steel bars resulted in an improvement of approximately 12% and 14% in the ultimate load for beams with square openings positioned along and away from the load path, respectively. Introducing both vertical and horizontal steel bars, each with a 12mm diameter, around the openings increased the ultimate load by roughly 36% and 40% for square and rectangular openings measuring 250 mm x 150 mm, respectively. However, a beam with square openings away from the load path exhibited only a slight increase in the ultimate load, around 5%, attributed to the interruption of the load path by the vertical steel bars.

Reinforcing the openings with inclined steel bars enhanced the beam capacity by approximately 9.4% and 34% for specimens with square openings near the loading point and openings measuring 250 mm x 150 mm, respectively. However, reinforcing square openings along the load path with inclined steel bars did not contribute to any improvement in the ultimate load due to issues related to crack propagation and separation of concrete cover.

The numerical analysis conducted using the finite element method demonstrated good agreement with the experimental findings. The parametric study revealed that circular openings resulted in a reduction of the failure load by about 42%, while square openings of equivalent size led to a reduction of approximately 56%. The utilization of inclined and horizontal strengthening bars around the openings significantly increased the ultimate load by about 117% and restored approximately 98% of the beam's strength.

2.5 Summary:

Based on the overview of the research discussed in this chapter, the following observations can be made:

1) The near-surface mounted (NSM) steel rebar method has demonstrated positive outcomes in increasing the strength and load-carrying capacity of RC beams with openings of various sizes. The effectiveness of NSM steel rebars in strengthening RC beams depends on factors such as the size and location of the openings, as well as the configuration and diameter of the steel rebars.
2) In the case of RC beams featuring substantial openings, it is crucial to strategically position NSM steel rebars to offer sufficient reinforcement around the opening and ensure effective load distribution.
3) The sizes of the openings play a crucial role in determining the effectiveness of the strengthened beams. Larger openings might necessitate additional reinforcement strategies to efficiently restore the beam's capacity.
4) Ensuring optimal strengthening outcomes relies on careful design and installation of NSM steel rebars, taking into account factors like bonding, cover thickness, and anchorage.
5) The experimental and numerical studies reviewed in this chapter demonstrate that strengthening RC beams with NSM steel rebars can significantly improve their load-carrying capacity and structural performance.
6) Prior research on deep beam strengthening has predominantly emphasized the use of CFRP bars in the NSM technique as the primary strengthening material, rather than steel bars. It's noteworthy that steel bars are more cost-effective and exhibit

superior bond strength compared to CFRP bars, making them less prone to debonding failures. Hence, there is a need to advance the knowledge and application of steel bars as strengthening materials instead of CFRP bars.

7) Further research and testing are still needed to explore the long-term behavior, durability, and overall effectiveness of the NSM technique for strengthening RC beams with large and small openings.

In summary, employing NSM steel rebars presents a practical and effective solution for improving the strength and performance of RC beams with various opening sizes, demonstrating potential applications in the field of structural engineering and construction practices.

CHAPTER THREE

EXPERIMENTAL WORK

CHAPTER THREE
EXPERIMENTAL WORK

3.1 Introduction

In this chapter experimental work, 14 RC beams with openings in different sizes and locations and strengthens the large opening in the shear zone in the different configurations, in addition to the material characteristics, and preparation samples have been described.

3.2 Test Program:

The experimental program included the casting and testing of 14 reinforced concrete beams with openings in shear and flexural zones, then strengthening large openings in the shear zone by NSM technique.

3.2.1 Identification of Beams

The experimental study involved the testing of 14 reinforced concrete (RC) beams. Among these, six beams were reinforced with near-surface mounted (NSM) steel bars around openings in the shear region, featuring various configurations. The beams were categorized into two groups based on their (a/d) ratios. All specimens shared identical dimensions, with a simply supported configuration and consistent flexural and transverse reinforcement (2φ12mm and φ8@85mm) respectively. The examined beams were further classified into two groups, as outlined in Table (3-1), possessing the same cross-section and length: 2000 mm long, 100 mm wide, and 200 mm high. The prototypes of the specimens measured (300*600*6000)mm.

Table 3-1 Details of the sample.

Group no.	Beam name	Shear span ratio a/d	Opening position	Opening size D (mm)	NSM stirrup Ø	NSM Details	Samples
Group One	SCB	3.61	N/A	N/A	N/A	N/A	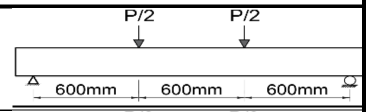
	SBLS	3.61	Shear zone	Large opening D=80mm	N/A	N/A	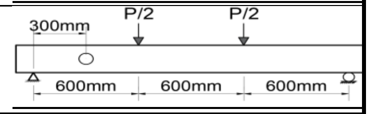
	SBLF	3.61	Flexural zone	Large opening D=80mm	N/A	N/A	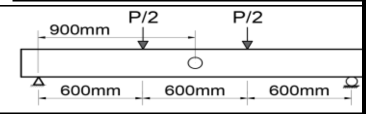
	SBLSF	3.61	Shear and Flexural zone	Large opening D=80mm	N/A	N/A	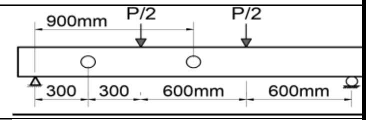
	SBSF	3.61	Flexural zone	Small opening D=40mm	N/A	N/A	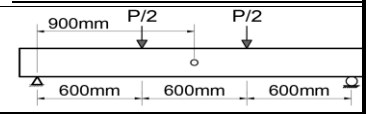
	SBSSF	3.61	Shear and Flexural zone	Small opening D=40mm	N/A	N/A	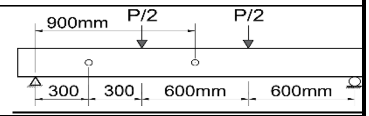
Group Two	DCB	1.5	N/A	N/A	N/A	N/A	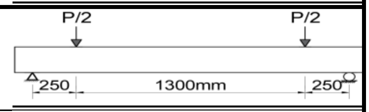
	DBLS	1.5	Shear zone	Large opening D=80mm	N/A	N/A	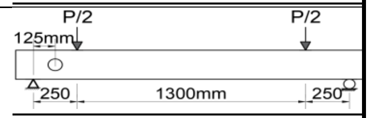
	DBLSS 8	1.5	Shear zone	Large opening D=80mm	Ø8 mm	Square stirrup strengthening	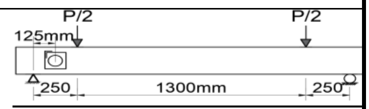
	DBLSS 10	1.5	Shear zone	Large opening D=80mm	Ø10 mm	Square stirrup strengthening	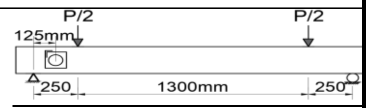
	DBLSD 8	1.5	Shear zone	Large opening D=80mm	Ø8 mm	Diamond stirrup strengthening	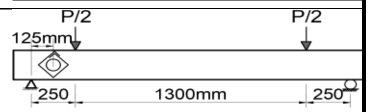
	DBLSD 10	1.5	Shear zone	Large opening D=80mm	Ø10 mm	Diamond stirrup strengthening	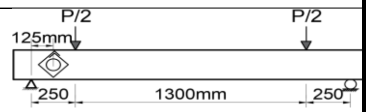
	DBLSP 8	1.5	Shear zone	Large opening D=80mm	Ø8 mm	Parallelogram stirrup strengthening	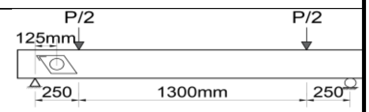
	DBLSP 10	1.5	Shear zone	Large opening D=80mm	Ø10 mm	Parallelogram stirrup strengthening	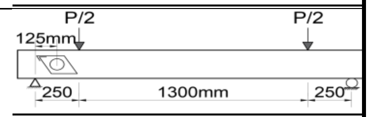

3.2.2 Description of Beams

The experimented beams are divided into two separate categories based on their (a/d) ratios, position, and size of openings. Each group has a control beam (which is un-strengthen and unopened) and group two strengthened specimens made of NSM steel bar using various shapes around openings, as shown in (Fig. 3-2). The selected shear span to effective depth ratio were (3.61 and 1.5). All openings were kept vertically aligned so that they were centered at the beam depth.

3.2.2.1 Group One Description

This group consists of six samples, five of the tested beams had openings (large and small, D=80mm, D=40mm respectively) which are located in shear, flexural, and (shear and flexure) zones except for the control beam. All specimens were rectangular with 100*200 mm in cross-section and had clear covers of 20 mm. Flexural and transverse reinforcement (2φ12mm and φ8@85mm) respectively with shear span ratios (a/d) 3.61. The beams underwent loading at two points, and precautions were taken to prevent local failure at the load points and supports by using steel plates. The configurations of the beams, along with their geometric and reinforcement specifics for group one, are depicted in Fig. (3-1).

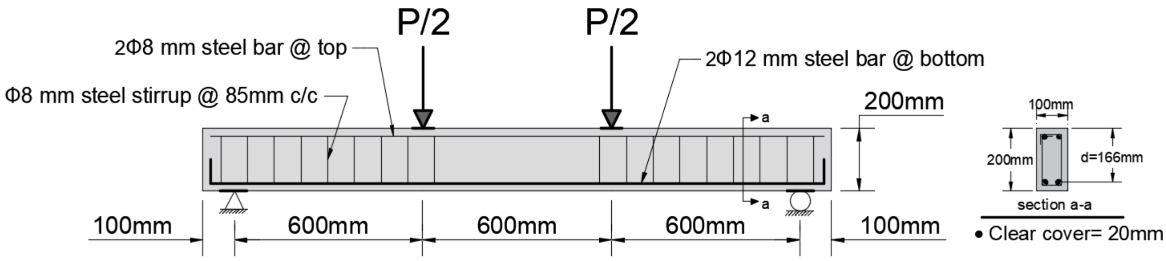

a) SCB

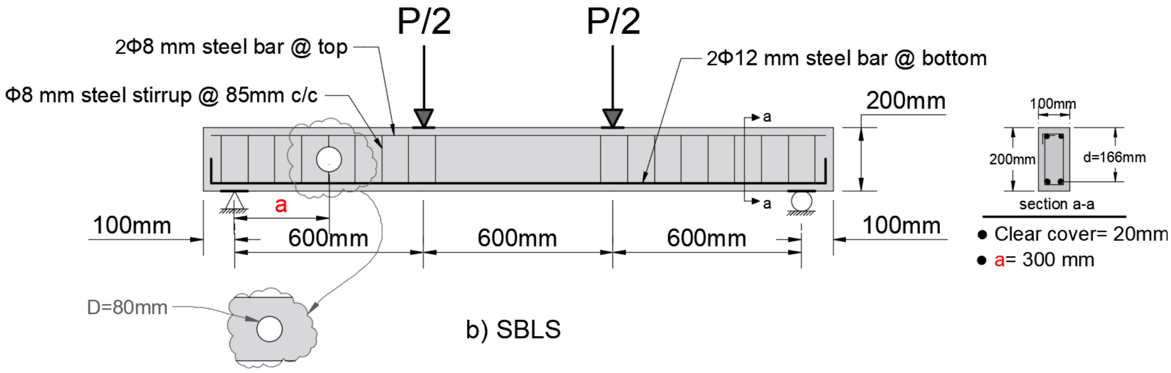

b) SBLS

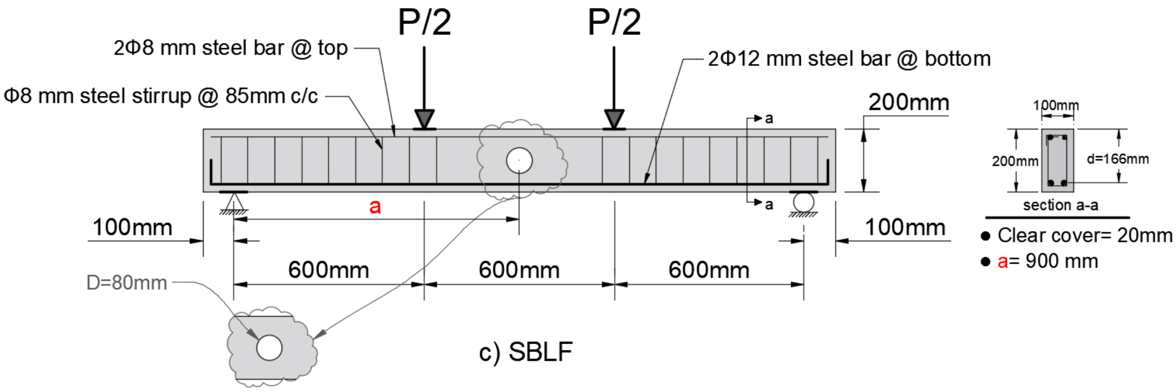

c) SBLF

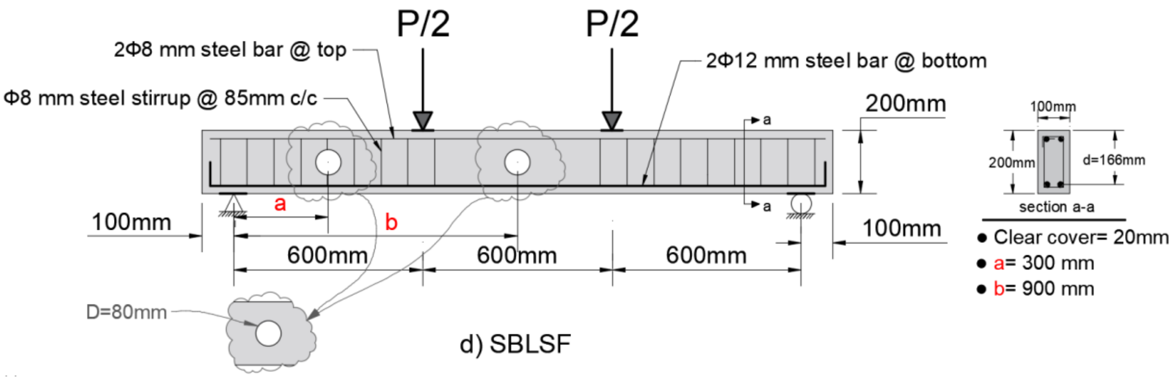

d) SBLSF

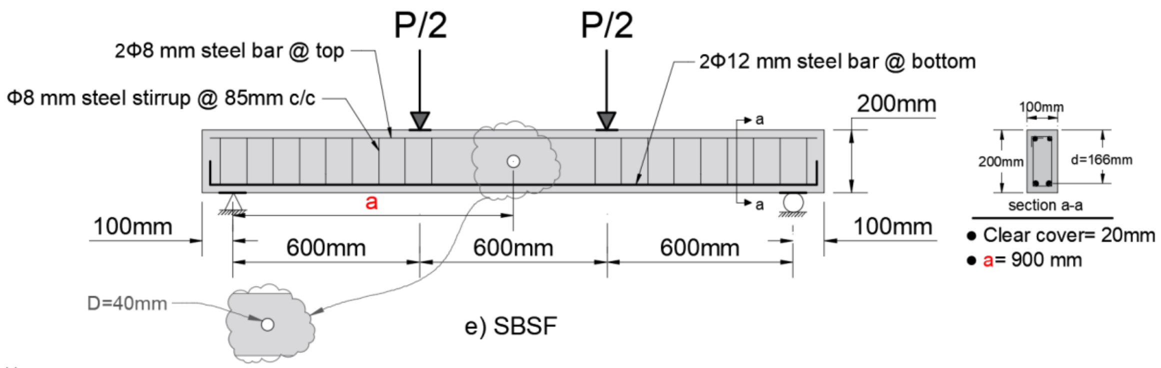

e) SBSF

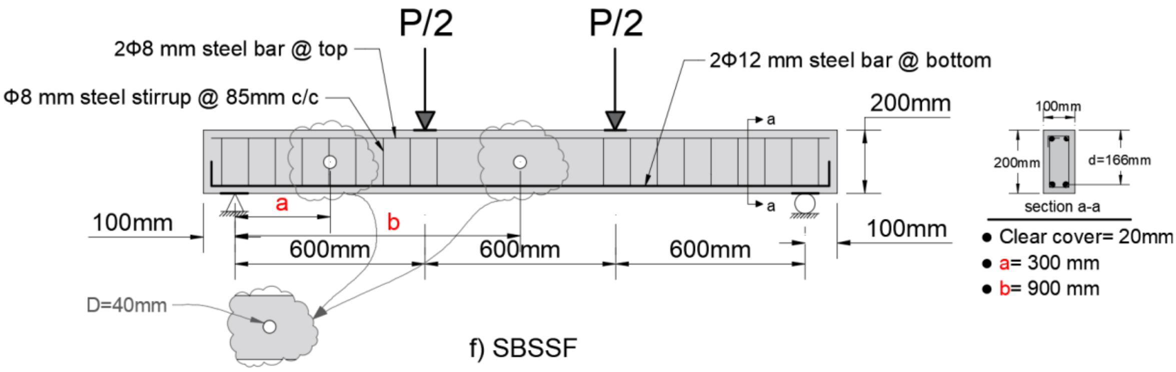

Fig 3-1 Details of the tested beam in (Group One).

3.2.2.2 Group Two Description

This group consists of eight samples, seven of the beam samples had openings (large D=80mm) which are located in shear zones except for the control beam. All specimens were rectangular with 100*200 mm in cross-section and had clear covers of 20 mm. One of the test specimens remained un-strengthened, while the remaining six beams were reinforced with diverse arrangements of near-surface mounted (NSM) stirrup steel bars around openings, featuring varying diameters of steel bars (φ 8mm and φ 10mm).

Flexural and transverse reinforcement (2φ12mm and φ8@85mm) respectively. with shear span ratios(a/d) 1.5. The beams underwent loading at two points, and measures were taken to prevent local failure at the load points and supports by employing steel plates. The configurations of the beams, along with their geometric and reinforcement details for group two, are illustrated in Fig. (3-2).

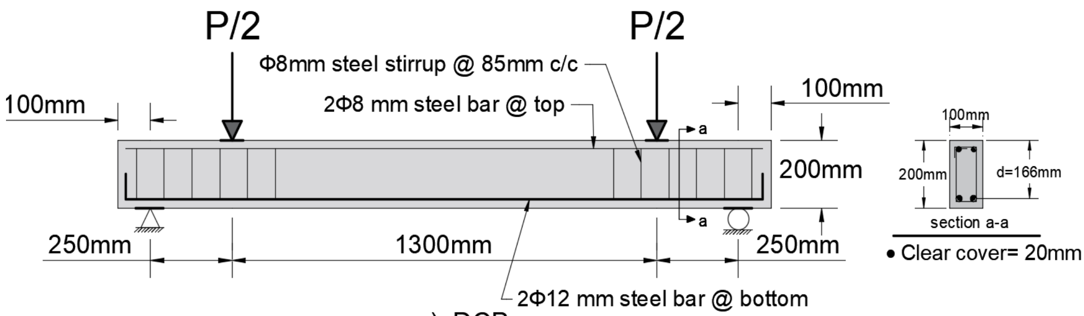

a) DCB

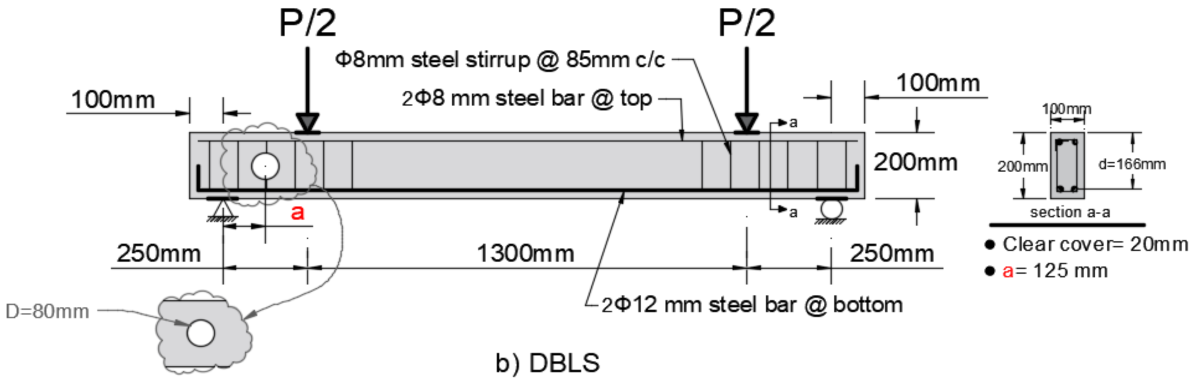

b) DBLS

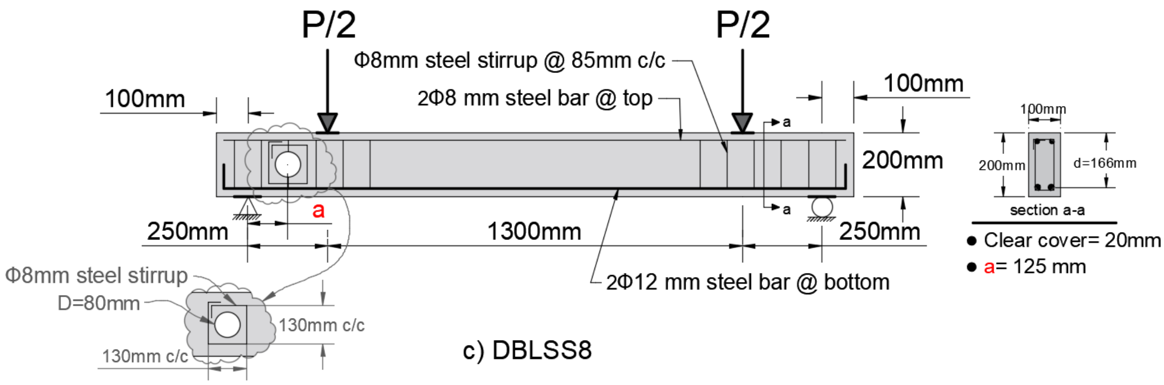

c) DBLSS8

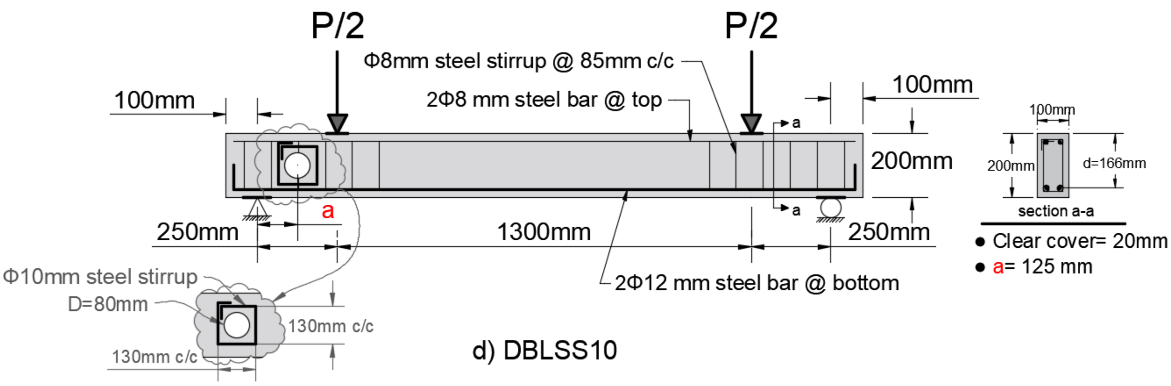

d) DBLSS10

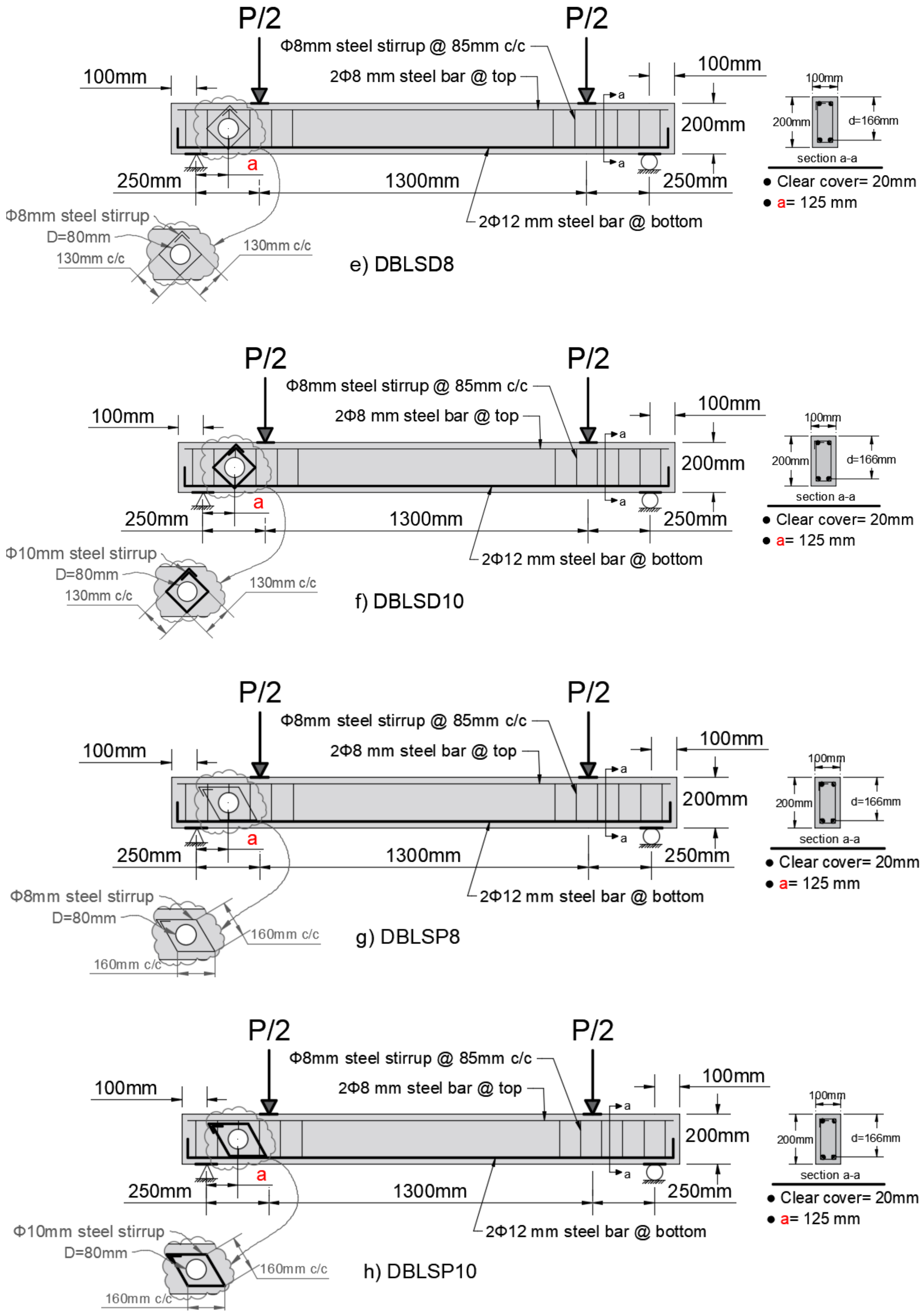

Fig. 3-2 Details of the tested beam in (Group two)

3.3 Material properties

The concrete mix components were provided by Iberia Ready Mix Concrete Company. The used materials throughout the study are briefly described below, and they were tested by the Directory of Construction Laboratory-Hawler.

3.3.1 Cement

Throughout this investigation, ordinary Portland cement from the KAR factory was used in all mixes. Tables 3-2 and 3-3 display the physical and chemical properties, respectively. The cement successfully met the requirements of the (IQ. S/5/1984) test.

Table 3-2: Physical properties of the cement.

Physical Test		Unit	Results*	Specific limits
Setting time Vicat needle	initial set	min	60	> 45
	Final set	min	105	< 600
Compressive strength	3-day age	MPa	28.4	> 14.7
	7-day age	MPa	36.7	> 22.5
fineness		m^2/kg	325	> 230
soundness expansion		mm	1.7	< 10

* Tested by Directory of Construction Laboratory-Hawler.

Table 3-3: Chemical properties of the cement.

Chemical tests	Test Required	Unit	Results*	Specification limits	IQS-5-84
	Loss in Ignition	%	2.47	4% Max.	
	Insoluble material	%	0.47	1.5% Max.	
	SiO_2	%	21		
	CaO	%	63.11		
	Al_2O_3	%	3.03		
	Fe_2O_3	%	3.99		
	MgO	%	1.97	5% Max.	
	SO_3	%	2.31	2.8% Max	

(Table 3-3) Continue …

	Test Required	Unit	Results*	Specification limits	
Chemical tests	C_3A	%	1.28		IQS-5-84
	L.S.F	%	0.94	(0.66-1.02)	
	C_3S	%	64.67		
	C_2S	%	11.63		
	C_4AF	%	12.14		

*Tested by Directory of Construction Laboratory-Hawler.

3.3.2 Fine Aggregate

Well-graded and clean fine aggregate (sand) has been used from the local natural river. The gradation curve of fine aggregate has been done according to the ASTM limits (C33) as shown in (Fig. 3-3) and the sieve analysis results are listed in Table (3-4).

Table 3-4: Grading of fine aggregate (Sand).

Sieve size (mm)	% Passing	ASTM limits (C33)	
		Lower	Upper
9.5	100	100	100
4.75	96.7	95	100
2.36	82.5	80	100
1.18	58.5	50	85
0.6	35	25	60
0.3	14.2	10	30
0.15	4.5	2	10
Bulk specific gravity (SSD*)	2.7		

*Saturated surface dry

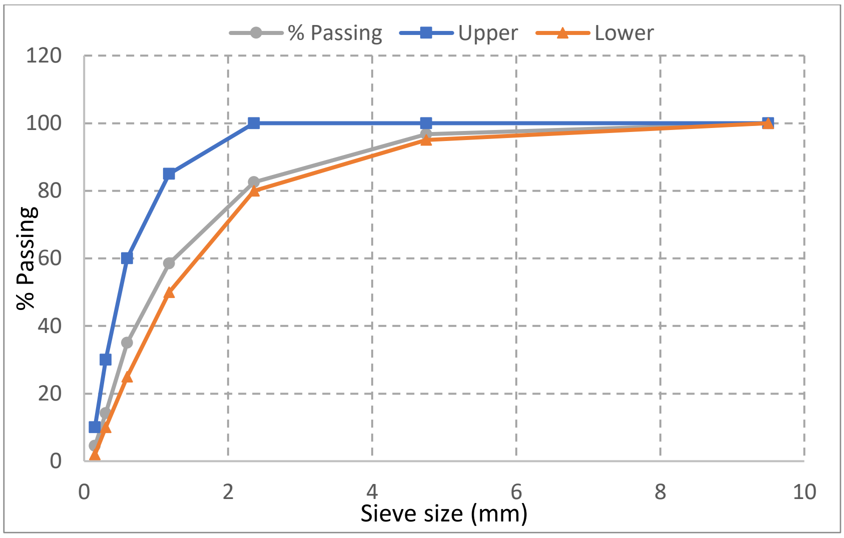

Fig. 3-3 Grading curve for fine aggregate (Sand)

3.3.3 Coarse Aggregate

The used coarse aggregate in this concrete was crushed river gravel. The gravel ranged in size from 1.18 to 12.5mm. The coarse aggregate gradation curve was generated using ASTM limits (C33), as shown in Fig. (3-4), and the sieve analysis findings are presented in Table (3-5).

Table 3-5: Grading of coarse aggregate (Gravel)

Sieve size (mm)	% Passing	ASTM limits (C33)	
		Lower	Upper
12.5	100	100	100
9.5	98.2	85	100
4.75	18.4	10	30
2.36	2.22	0	10
1.18	0.1	0	5
Bulk specific gravity (SSD*)	2.69		

*Saturated surface dry

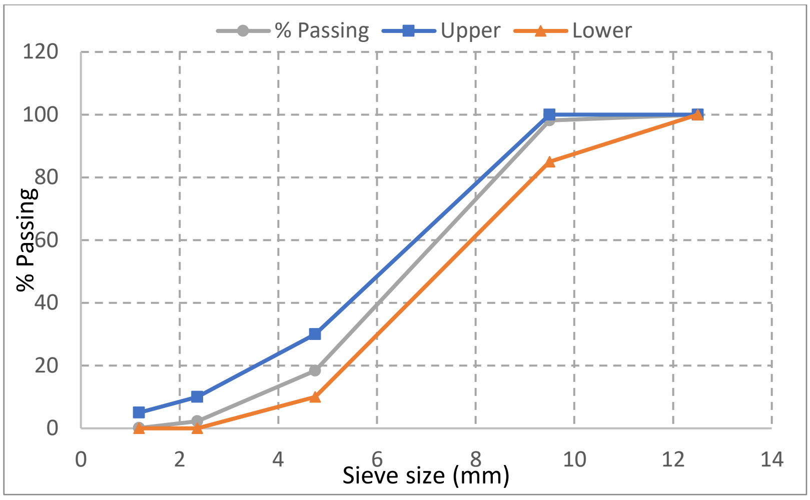

Fig. 3-4 Grading curve for coarse aggregate (Gravel).

3.3.4 Superplasticizer (CHRYSO)

CHRYSO superplasticizer offers solutions to extend the workability of concrete while minimizing the impact on early strengths. CHRYSO created very high-range water-reducing superplasticizers to improve the strength and finish of fresh concrete. The most important properties of a superplasticizer are resistance to carbonation, increased durability, reduced shrinkage and creep, and lower permeability. Table (3-6) illustrates the properties of the Superplasticizer that were used.

Table 3-6: CHRYSO Superplasticizer properties.

Items	Properties*
Product Nature	liquid
Color	Brown
Lifetime	18 months
CI- Ions content	$\leq 0.100\%$
Equivalent Content NA_2O	$\leq 3.50\%$
Specific gravity (20°C) in kg/dm3	1.125 ± 0.015
Dosage	0.2 to 0.8 kg for 100 kg of cement.
pH(20°C)	6.00 ± 1.00
Freezing Point	-3°C
Dry Extract (SYNAD - IFSTTAR)	23.40%: 1.20

*Tested by Directory of Construction Laboratory-Hawler.

3.3.5 Concrete job mix

Concrete job mix formula to manufacture concrete mix properties as shown in Table (3-7) below.

Table 3-7: Concrete job mix properties

Maximum size of aggregates	12.5 mm
Slump/Target flow	180-220 mm
Concrete cube strength (fc^-)	35 MPa

3.3.6 Mixing Water

Normal drinkable water was used for mixing, and also curing concrete.

3.3.7 Mix Design

Based on the (ACI 211.1-R09) the job mix formula for manufacturing concrete was designed to meet concrete strength of 35 MPa, the proportions are listed in Table (3-8) below.

Table 3-8 Concrete mixture proportions.

	Cement	Coarse aggregates	Fine aggregates	Water	Admixture (superplasticizer)
Density (kg/m^3)	3150	2700	2620	1000	1195
Volume dm^{3*}	120.63	314	383.78	170	1.59
Ratio by weight	1	0.826	1.01	0.45	0.05

* dm^3: cubic decimeter.

3.3.8 Steel rebars test

All the tested beams featured an identical reinforcement design, specifically concerning the longitudinal reinforcement consisting of 2 Ø 12 bars, with 2 Ø 8 bars used for the bottom and top reinforcement respectively. Stirrups of Ø 8 at 85mm intervals were used. The stirrups of Ø8 and Ø10 steel bars were used with different schemes for reinforcing the openings. Table 3-9 lists the results of the tests conducted, while Fig. (3-5) displays the steel bar testing machine.

Table 3-9 Steel rebars test

no.	Weight (kg)	Length (mm)	D (mm)	L_0	L_1	L (Elongation) (L1-Lo/ Lo) %	F(yield) MPa	Ave. F(yield) MPa	Failure Load (kN)	F(ult) (Mpa)	Ave. F(ult) MPa
1	0.225	545	8	202	234	% 16.8	531	534.46	33.9	674.7	691.32
2	0.225	543	8	202	232	% 15.8	533		34.5	686.7	
3	0.222	541	8	202	236	% 17.8	539.4		35.8	712.57	
4	0.330	544	10	200	230	% 15	582.1	583.16	53.94	686.78	685.3
5	0.333	547	10	200	230	% 15	582		53.20	677.38	
6	0.328	549	10	200	231	% 15.5	585.4		54.33	691.75	
7	0.460	552	12	200	234	% 17	572.4	548.2	81.7	722.75	696.39
8	0.492	550	12	200	234	% 17	532.1		76.85	679.44	
9	0.467	552	12	200	233	% 16.5	540.1		77.70	687	

Fig. 3-5 The machine is used for testing the tensile strength of steel bars.

3.3.9 Epoxy paste

Polypoxy-NF is a two-part epoxy bonding and patching paste consisting of Part (A) resin and Part (B) hardener, as shown in Fig. (3-6). It has a mixing ratio of 60:40 (A: B) and is used for bonding NSM reinforcements the specifications of Polypoxy-NF have been described in Appendix-A. This epoxy product is suitable for the NSM technique as it can be used for patching repairs and bonding fresh to hardened concrete, as well as for dowel anchoring purposes. It is appropriate for use in aggressive weather conditions that the rebar may be exposed to. Table (3-10) provides the manufacturer's properties and other additional information about the epoxy paste.

Table 3-10 Technical specification of Epoxy paste

Properties	Values*	Test Standards
Color & appearance	Grey/off-white paste	-
Density, [g/cc]	1.85 ± 0.05	ASTM D 1475
Application life, [minutes]	45	-
Compressive strength @7days,[N/mm^2]	> 60	ASTM C 579
Flexural strength @7days, [N/mm^2]	> 30	ASTM C 580
Tensile strength @ 7 days, [N/mm^2]	> 12	ASTM C 307
Shear bond Strength @ 7 days, [N/mm^2]	> 40	ASTM C 882
Application thickness, [mm/layer]	0 to 5	-
Application temperature, [$^{\circ}C$]	5 to 35	-
Service temperature, [$^{\circ}C$]	-5 to 70	-
Initial cure, [hours]	Approx. 8	-
Final cure, [days]	7	-

*All values given are subject to a 5-10% tolerance.

Fig. 3-6 Epoxy paste (Polypoxy-NF)

3.4 Beam Mold

To prepare the tested RC beam mold, a wooden formwork 18mm thick mold was constructed according to the dimensions 2000 mm x 100 mm x 200 mm and placed on a leveled surface as shown in Fig. (3-7). The formwork was then coated with a layer of release agent to prevent the concrete from sticking to the formwork. Next, the reinforcement bars were placed in the mold according to the design requirements.

Fig. 3-7 Beam molds by (Author).

3.5 Cage and Placement

The tested RC beam cage was prepared by first cutting and bending the reinforcement bars according to the design requirements. The bars were then assembled into the required shape and tied together at their intersections with wire ties as shown in Fig. (3-8). The cage was then placed into the prepared mold and adjusted to ensure proper placement and alignment, then made a cover by putting a plastic spacer as illustrated in Fig. (3-9).

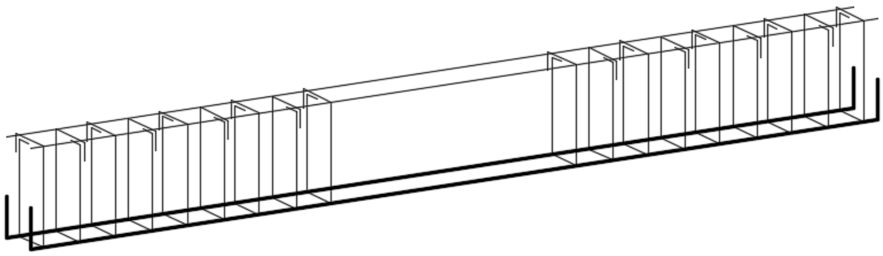

Group One-Reinforcement Cage

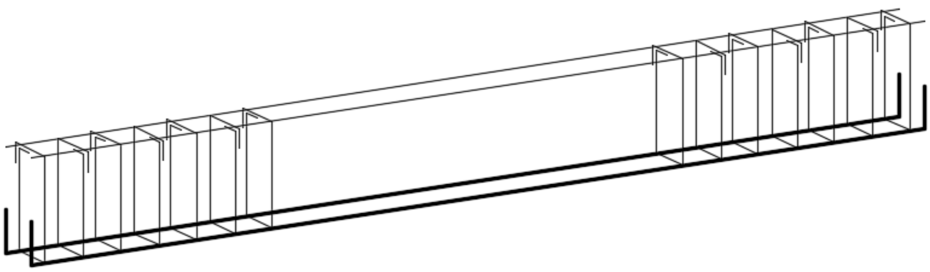

Group Two-Reinforcement Cage

Fig. 3-8 Reinforcement beam cages in Groups One and Two.

Fig. 3-9 Reinforcement beam cage inside the formwork by (Author).

3.6 Casting

After Fabricating the formwork and applying the oil to the surfaces in contact with the concrete. Mix the concrete using the design mix proportions of cement, sand, coarse aggregates, and water in a concrete mixer until a homogeneous mixture is obtained, then pour the mixed concrete into the formwork in layers and compact it using a vibrator to ensure there are no voids or air pockets as shown in Fig. (3-10). Following the pouring of concrete, employ a trowel to smooth and even out the concrete surface. After 24 hours of casting, the forms were removed and draped with wet cloth and burlap. To ensure proper curing over 28 days, the cloth and burlap were kept moist by sprinkling water every day as demonstrated in Fig. (3-11).

Fig. 3-10 Casting concrete by (Author).

Fig. 3-11 Removing formwork and curing the samples by (Author).

3.7 Drilling RC Beams by Core Machine

After 28 days of the curing beam samples, the opening of RC beams was conducted by the core machine. Drilling RC beams by core machine is a technique used to create holes or openings in reinforced concrete RC beams for various purposes, such as installing pipes, ducts, or electrical wiring. The process involves using a specialized machine called a core drill, which has a diamond-tipped drill bit that can penetrate through the concrete and steel reinforcement.

The core drilling process involves several steps:

1. Marking: Indicate the position and dimensions of the hole to be drilled on the beam's surface, as depicted in Fig. (3-12).

2. Setup: The core drilling machine is positioned and secured in place using clamps or other mounting devices.

3. Drilling: The diamond-tipped drill bit is inserted into the machine and the drilling process begins. The drill bit rotates at a high speed and cuts through the concrete and steel reinforcement to create the desired hole.

4. Extraction: Once the hole is complete, the core drill is removed and the cylindrical piece of concrete and steel, called a "core," is extracted from the hole as shown in Fig. (3-13).

Fig. 3-12 Marking the position of openings by (Author).

Fig. 3-13 A sample of the core by (Author).

3.8 NSM Steel Bar Installation Procedure

(NSM) reinforcement is a method used to enhance the shear strength and stiffness of concrete elements. This is achieved by affixing steel bars or fibers within the concrete in both the tension and shear zones. It is an alternative to externally bonded reinforcement (EBR) and has several advantages, including better durability and easier application.

Here are the steps for installing NSM steel bars for RC beams around an opening:

1) The reinforcement bars and adhesive material are selected: Based on the design requirements and properties of the existing concrete, the appropriate size and type of reinforcement bars and adhesive material are chosen.

2) The surface is prepared: The surface of the beam where the steel bars will be installed is cleaned and roughened to ensure good adhesion between the concrete and adhesive material. Any loose or deteriorated concrete is removed to create a clean surface, as shown in Fig. (3-14. a).

3) Create grooves or holes: Use a saw or drill to create grooves or holes in the surface of the beam with (1.5 db) depth according to the (Square, Diamond, and Parallelogram) design for the required strengthening capacity as illustrated in Fig (3-14. b).

4) Install the steel bars: Firmly press the steel bars into place within the grooves or holes created in the surface of the beam according to the design specifications for their positioning as demonstrated in Fig (3-15. a).

5) Inject the adhesive material: Using a caulking gun or similar equipment, inject the adhesive material into the grooves or holes until they are filled, and remove any excess adhesive as presented in Fig (3-15. b).

6) Allow the adhesive to cure: Allow the adhesive material to cure for several days while maintaining the temperature and humidity of the surrounding environment within the specified range.

7) Test the strengthened beam: After the adhesive has cured, conduct a load test on the beam to ensure that it meets the required load capacity.

a) Making groove to the surface the beam in (1.5db) depth.

b) Cleaning the groove by the of brush and water to be no dust.

Fig. 3-14 Cutting and grooving process by (Author).

a) installing the rebars into the grooves.

b) Filling the grooves with epoxy paste.

Fig. 3-15 Installing and epoxy process by (Author).

3.9 Instrumentation

Instrumentation for experimental reinforced concrete (RC) beams typically involves measuring various parameters related to the behavior of the beam during loading. The following are some common instrumentation techniques used in RC beam experiments to gain accurate experimental data:

1) **Load cells:** These are devices that measure the force or load applied to the beam that has been used for load measures.
2) **Strain gauges:** These are devices that measure the deformation or strain in a material such as concrete and steel which are used for both.
3) **Displacement transducers (Dial gauge):** These are devices that measure the displacement or movement of the beam during loading which is used for deflection measurements.
4) **Data logger:** A data logger is an electronic device employed to automatically record and store data from diverse sensors or instruments over a period, as exemplified by strain gauges.

3.9.1 Load Measurements

During the experimentation, a 600 kN capacity universal testing machine, as depicted in Fig. (3.16) was used to subject all beams to a two-point loading test. The loads applied on the beams were measured using a 600kN capacity load cell refer to Fig. (3.17), which was connected to the testing equipment.

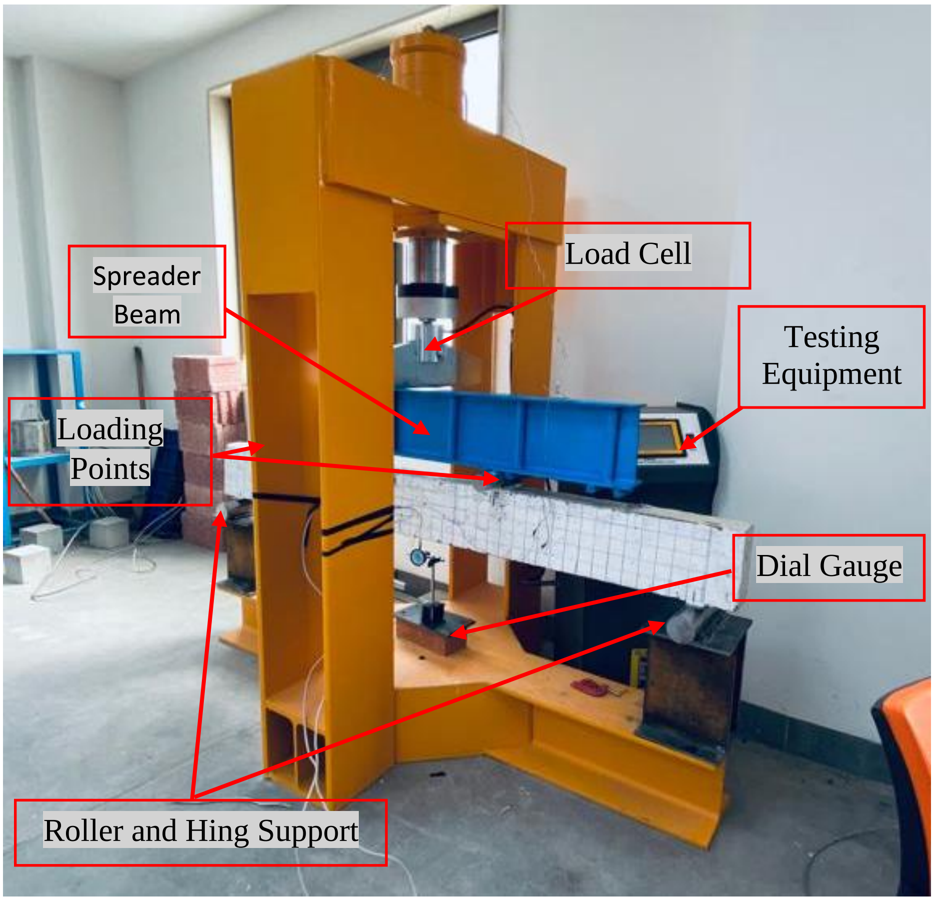

Fig. 3-16 Testing Machine Details by (Author).

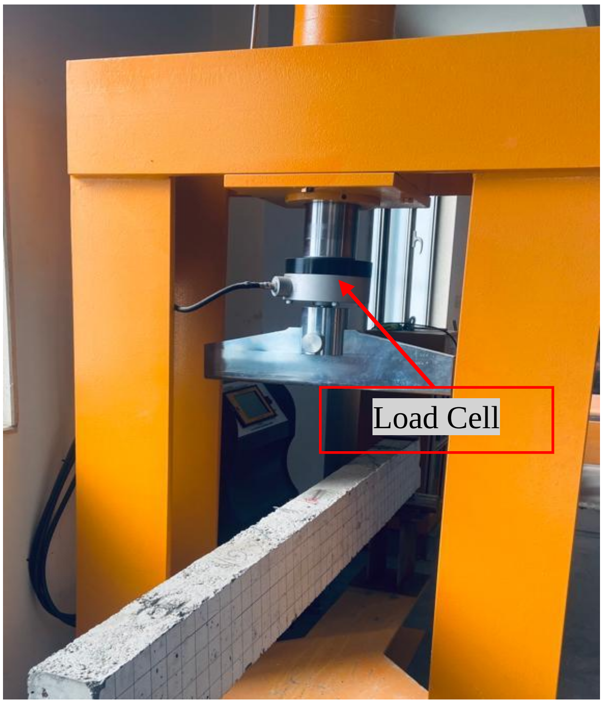

Fig. 3-17 Load Cell by (Author).

3.9.2 Deflection Measurements

The dial gauge is positioned at the mid-span of the beam, serving to measure the deflection in RC beams. It has a 100 mm maximum travel with 0.01mm accuracy, as depicted in Fig. (3-18).

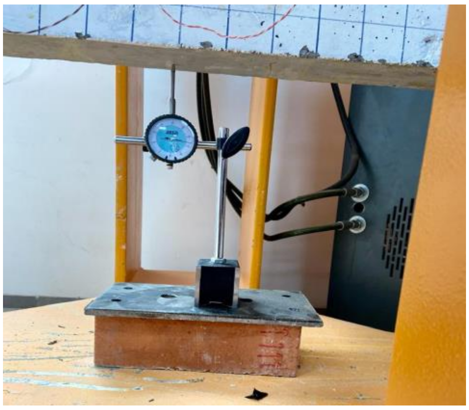

Fig. 3-18 Dial gauge used for deflection measurement by (Author).

3.9.3 Concrete Strain Measurements

A specific type of electronic strain gauge, namely the BF120-60AA model manufactured by Dongguang Souyh China Electronic Co., Ltd, was employed to measure the strain in the concrete. This was done to enhance the accuracy of the results obtained from the measurements. The strain gauge was positioned on the upper middle section of the compression zone of the concrete beam. Before placement, the surface was smoothed and cleaned using Carbon and Choke cleaner. The location of the concrete strain is illustrated in Fig. (3-19). To attach the gauges to the prepared concrete surface, the commonly used adhesive.

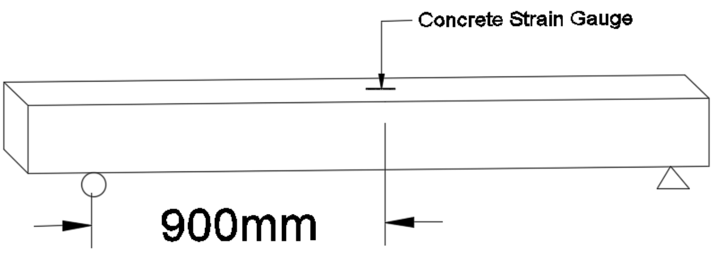

Fig. 3-19 Location of concrete strain gauge.

3.10 Testing Procedure

To detect cracks and the spread of cracks, a layer of white paint was applied to all the specimens before testing. Subsequently, adhesive material was utilized to affix concrete strain gauges onto the surface of the specimens. The specimens were allowed to sit for at least 24 hours to ensure the bonding epoxy adhesive material had been fully set. A self-supporting loading frame with a hydraulic jack of 600 kN capacity was used to test all the specimens. Fig. (3-20) illustrates the details of the specimens of the two groups being tested. A 600 kN load cell was employed to measure the applied loads.

The experiment involved testing beam specimens in a simply supported beam configuration. To prevent local bearing failure during testing, steel plates measuring 150x40x10 mm were placed at the load application and reaction points. To further safeguard against this failure, a thin layer of felt, specifically plaster of Paris, was inserted between the steel plates and the beam surface at the loading and supporting points. Dial gauges were used to instrument the beams at mid-span for monitoring deflection.

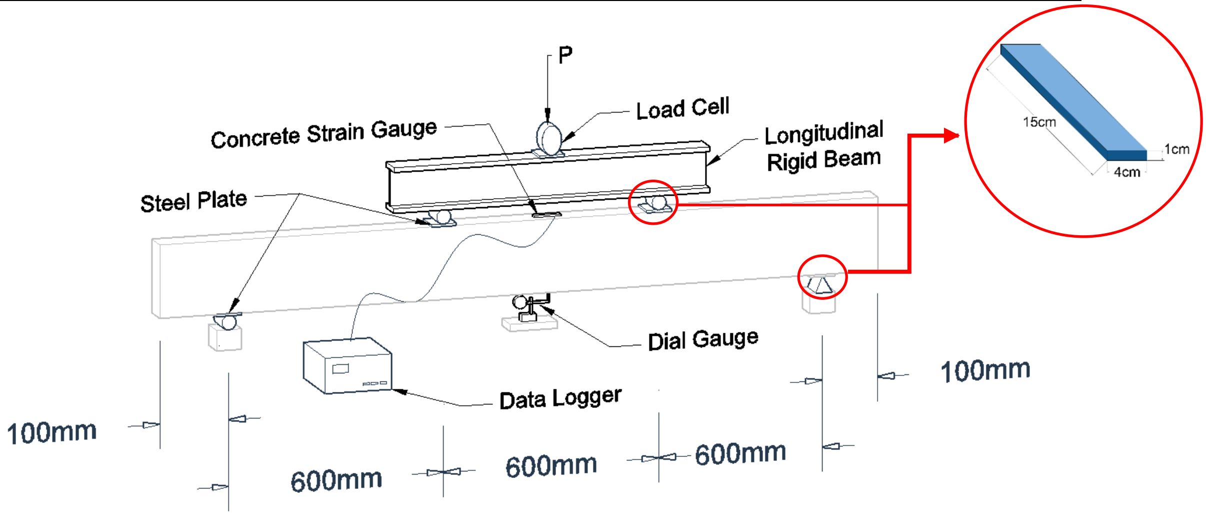

a) Load arrangement-Group one.

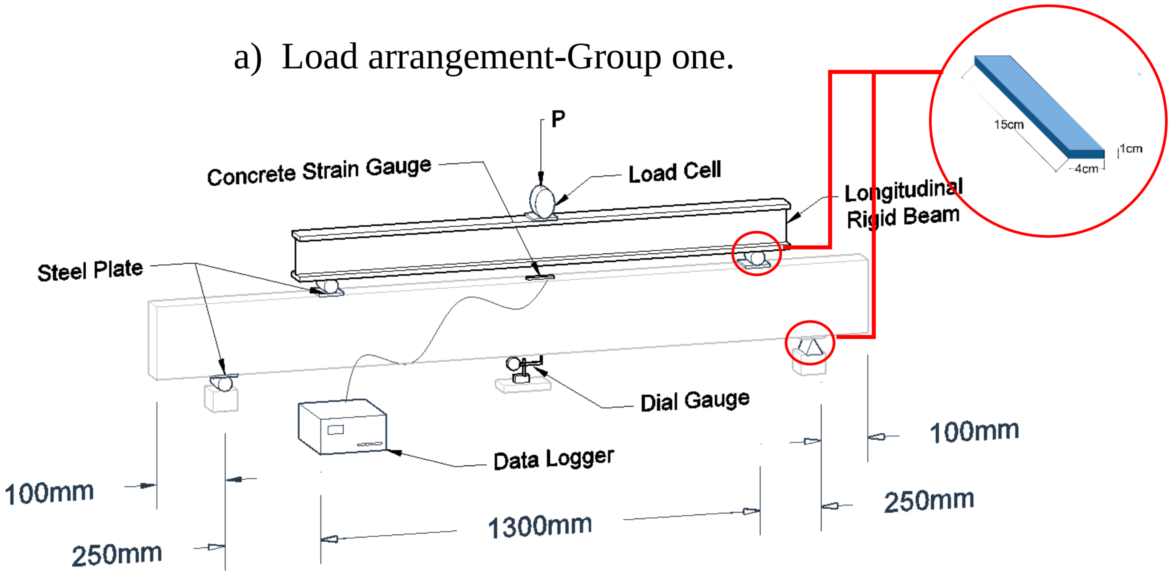

b) Load arrangement-Group two.

Fig. 3-20 Loading arrangement with measuring instrumentation

3.11 <u>Mechanical Properties of Concrete:</u>

3.11.1 <u>Compressive Strength of Concrete (fc')</u>

The compressive strength stands as a crucial mechanical property of concrete. Twelve cubes were manufactured for assessing the concrete's compressive strength, three cubes were tested for each of these days (7, 28) days, and six cubes were tested at the ages of the beams test by using the MATEST Hydraulic Compression Machine with a maximum capacity of 2400 kN, as shown in Fig. (3-21).

Fig. 3-21 Compressive strength machine by (Author).

3.11.2 Splitting Tensile Strength (fc_t)

The splitting tensile strength holds significance for concrete since it is a brittle material with lower tensile strength compared to its compressive strength. Therefore, knowing the splitting tensile strength is important for evaluating the ability of concrete to resist cracking as shown in Fig. (3-22). Three cylindrical concrete specimens (300mm length and 150mm diameter) were tested by using the MATEST Hydraulic Compression Machine with a maximum capacity of 2000 kN at the age of beam specimens test for splitting tensile strength.

Fig. 3-22 Compressive machine for splitting tensile strength test by (Author).

3.11.3 Flexure Strength (fr)

The prism test is a common method used to evaluate the flexural strength of concrete. The experiment involved testing three concrete prisms, each measuring 150 x 150 x 700 mm, per ASTM C78(02) standards. The testing was conducted using a Hydraulic Compression Machine, which has a maximum capacity of 2000 kN, as illustrated in Fig. (3-23).

Fig. 3-23 Compression machine for flexure strength (fr) by (Author).

CHAPTER FOUR

TEST RESULTS AND DISCUSSION

CHAPTER FOUR

TEST RESULTS AND DISCUSSION

4.1 Introduction

The present investigation entailed the analysis of fourteen specimens, consisting of two solid beams as control samples and twelve with openings. The twelve samples were divided into two groups, taking into account the size and location of the openings, as well as the shear span to effective depth ratio (a/d). The initial group included six samples, with one acting as a control beam without any opening, and the rest featuring large and small openings situated in the shear and flexure zones. The shear span to effective depth ratio (a/d) for this group was set at 3.61. The second group contained eight beams with a shear span to effective depth ratio of (a/d) (1.5) that were strengthened by NSM, with the adopted strengthening methods explained in chapter three. To explore the impact of reinforcement with NSM steel bars, six specimens were cast and subsequently reinforced using different methods, with their performance being compared to that of the unreinforced specimens.

4.2 <u>Mechanical Properties of Normal Strength Concrete (NSC):</u>

An examination was carried out on the mechanical properties of normal strength of reinforced concrete. The normal-strength concretes were evaluated for their mechanical attributes, incorporating parameters such as compressive strength, splitting tensile strength, and flexural strength.

4.2.1 Compressive Strength (fcu)

For the experiment, a complete set of twelve 150mm cubes was prepared, with three cubes subjected to testing at 7 days, another three at 28 days, and the remaining six cubes at testing specimens. The compressive strength outcomes for Normal Strength Concrete are detailed in Table (4-1).

4.2.2 Tensile Splitting Strength (fc_t)

By conducting tests on cylinders measuring 150 mm x 300 mm, as represented in Table (4-2), the splitting tensile strength is determined.

4.2.3 Flexure Strength (fr)

Evaluating the flexural strength of concrete involves conducting the prism test. In this experiment, three concrete prisms, each measuring 150 x 150 x 700 mm, were tested. The outcomes of this experiment are documented in Table (4-3).

Table 4-1 Compressive Strength of Cubes

Days	Cube No.1 (MPa)	Cube No.2 (MPa)	Cube No.3 (MPa)	Cube No.4 (MPa)	Cube No.5 (MPa)	Cube No.6 (MPa)	Average Compressive Strength (fc^{-}) (MPa)
7	33.83	34.66	35.44	-	-	-	34.31
28	44.8	42.8	43.84	-	-	-	43.81
Specimen Beams	47.28	45.2	42.84	45.61	41.2	43.52	44.27

Table 4-2 Splitting tensile result.

No.	Specimens	Tensile Splitting Strength (fct) MPa	Tensile Splitting Strength According to ACI-318 fr=k** $\sqrt{fc'}$ MPa
1	T1*	4.38	3.52
2	T2	4.14	
3	T3	5.44	
Average (MPa)		4.65	3.52

T1* Splitting Tensile Strength (sample one)

(k=0.53) ** Value of the constant coefficient, according to ACI-318, but in test (**k=0.698**).

Table 4-3 Flexure strength result

No.	Specimens	Flexure Strength (fr) MPa	Flexure Strength According to ACI-318 fr=n** $\sqrt{fc'}$ MPa
1	F1*	3.637	4.12
2	F2	4.807	
3	F3	4.713	
Average (MPa)		4.386	4.12

(F1) * Flexure Strength (sample one)

(n=0.62) ** Value of the constant coefficient, according to ACI-318, but in test (**n=0.66**).

4.3 The Behavior of Tested Beams:

Table (4-4) presents the experimental results and observed failure modes of two groups of simply supported beams, and Fig (4-1) illustrates the load-carrying capacities of the beams that underwent testing in this research study.

4.3.1 Specimen Behavior in Group One

In this group, a total of six beams were tested, all having an (a/d) ratio of (3.61). This includes one control specimen without any openings and five specimens that have openings.

This group designates it as the control beam SCB. The initial crack emerged close to the center of the beam's span within the tension zone when the load reached 12 kN. This crack is classified as a flexural crack. As the applied load increases, the crack progressively widens and extends until it reaches the compression strut zone.

The existence of a sizable aperture in a reinforced concrete (RC) beam. group one SBLS, SBLF, and SBLSF can significantly affect its behavior, particularly in terms of the occurrence of the first crack. When a large opening is present, the first crack tends to initiate near the opening or at the corners adjacent to the opening. The crack formation is influenced by factors such as the size and shape of the opening, the specimens of SBLS, and SBLSF openings closer to the supports may result in higher stress concentrations and earlier crack initiation.

In reinforced concrete RC beams with a small circular opening, the first crack typically initiates near the edges of the opening, similar to beams with larger circular openings. While the stress concentrations around a small opening are relatively lower compared to larger openings, they can still influence crack formation.

The onset of the initial crack may differ based on whether the opening is situated in the shear zone or the flexural zone of the beam.

In specimen SBSF, the first crack is more likely to initiate away from the small circular opening. The opening itself may not significantly affect the flexural behavior of the beam, and the crack formation is primarily influenced by the applied load and the distribution of stresses along the beam's span. Typically, the initial crack tends to form in proximity to the load application points or near the supports where the bending moment is at its peak.

Concerning small openings within both the shear and flexural zones of specimen SBSSF, the initial crack is likely to originate near the edges of the opening. This occurrence is attributed to stress concentrations resulting from the presence of the opening in the shear zone. Furthermore, cracks may also propagate away from the opening in the flexural zone due to the bending moment applied to the beam.

4.3.2 Specimen Behavior in Group Two

In this particular group, a series of tests were conducted on eight beams, each having a consistent aspect ratio (a/d) of (1.5). Among these beams, one served as a control specimen, free from any openings, while the remaining seven featured large openings. Out of the seven beams with large openings, six were strengthened using NSM (Near-Surface Mounted) techniques in various schemes.

The presence of a large circular opening in the shear zone of an RC beam can greatly diminish its shear capacity. This occurs because the opening causes a loss of concrete area that contributes to shear resistance, making the beam more prone to shear failure.

The crack formation, a large circular opening in an RC beam creates stress concentrations in the surrounding concrete, resulting in the formation of cracks near the edges of the opening. These cracks can propagate along the length of the beam, causing further structural weakening.

NSM Steel Rebars, strengthening the beam using NSM steel rebars can effectively enhance its shear capacity. NSM rebars are embedded into the beam's surface near the circular opening, typically using epoxy adhesive. These rebars serve as additional reinforcement, redistributing shear forces and reducing stress concentrations. The NSM steel rebars help to redistribute shear forces across a larger portion of the beam, effectively bypassing the weakened region around the circular opening. This redistribution of forces helps prevent localized shear failures and limits crack propagation.

Table 4-4 Summary of test results

Group No.	Specimen	Shear span ratio (a/d)	First cracking load (kN)		Failure load (kN)	Failure mode
			Shear Cracking (kN)	Flexure Cracking (kN)		
G1	SCB	3.61	-	12	61.5	F*
	SBLS		-	9	50	S**
	SBLF		-	8	58	F
	SBLSF		-	7	52.5	S
	SBSF		-	10	58.5	F
	SBSSF		-	7	49.5	S
G2	DCB	1.5	-	16	156.5	S
	DBLS		13.5 around opening	5.5	86	S
	DBLSS8		35.5 around opening	15	109.5	S
	DBLSS10		41 around opening	18.5	125.5	S
	DBLSD8		48 around opening	11	128.5	S
	DBLSD10		62 around opening	25.5	120	S
	DBLSP 8		90 around opening	18	117	S
	DBLSP 10		40.5 around opening	20.5	129	S

(F*) failure mode in Flexure

(S**) failure mode in Shear

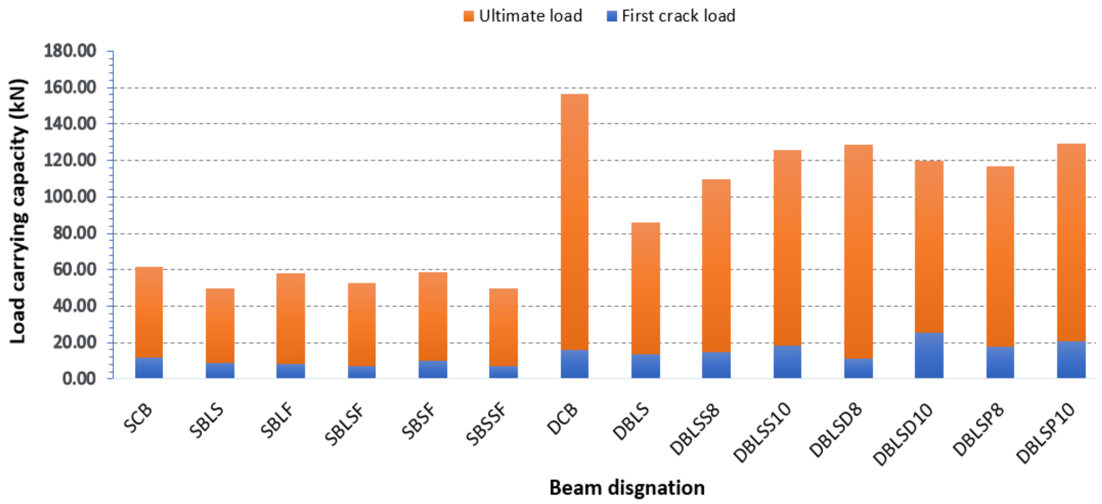

Fig. 4-1 First crack load and load carrying capacity of tested beams.

4.4 Load-Deflection Relationship

Fig. (4-2 and 4-4) illustrate the load-deflection curves observed at the mid-span of each beam sample. The load-deflection relationship of a beam is valuable in characterizing its response to applied loads.

4.4.1 Group One un-strengthened Specimens:

The load-deflection relationship of the solid specimen SCB provides valuable insights into how a beam responds to applied loads. It allows us to observe two distinct stages in the beam's behavior. Initially, there is an initial linear phase characterized by a steep slope, indicating an intact, uncracked beam. Once the cracking load reaches around 12 kN, a reduction in slope becomes evident due to the gradual development of cracks within the beam. Eventually, the cracking process stabilizes, and the beam exhibits an almost linear segment until it ultimately fails

The load-deflection behavior of the solid specimen SCB exhibits two distinct linear sections Fig. (4-2) which were before the first crack and after the first crack. The initial section displayed a steeper slope compared to the subsequent section, with a slope transition occurring around 12 kN.

For comparative analysis, Fig (4-3) illustrates the load-deflection behavior of specimens SBLS, SBLF, and SBLSF, along with the solid specimen. SBLS, SBLF, and SBLSF displayed a bilinear response in their load-deflection characteristics, with the change in slope occurring at approximately 10 kN. The flexural stiffness of SBLF matched that of the solid specimen, while SBLS and SBLSF exhibited slightly lower stiffness. The ultimate loads for SBLS and SBLSF were 50 kN and 52.5 kN, respectively, with corresponding deflections at peak loads measuring 9.62 mm and 9.8 mm. In contrast, for SBLF and the solid specimen SCB, the ultimate loads were recorded at 58 kN and 61.5 kN, with corresponding deflections at peak load measuring 11.38 mm and 16.5 mm, respectively.

Fig. (4-4) illustrates the load-deflection characteristics of specimens SBSF, SBSSF, and the solid specimen. All specimens displayed a bilinear behavior in their load-deflection relationship. Beams with small openings exhibited a marginal increase in deflection at the same applied load compared to a control beam. These findings suggest that compressive strength has a relatively less pronounced impact on the load-deflection curve.

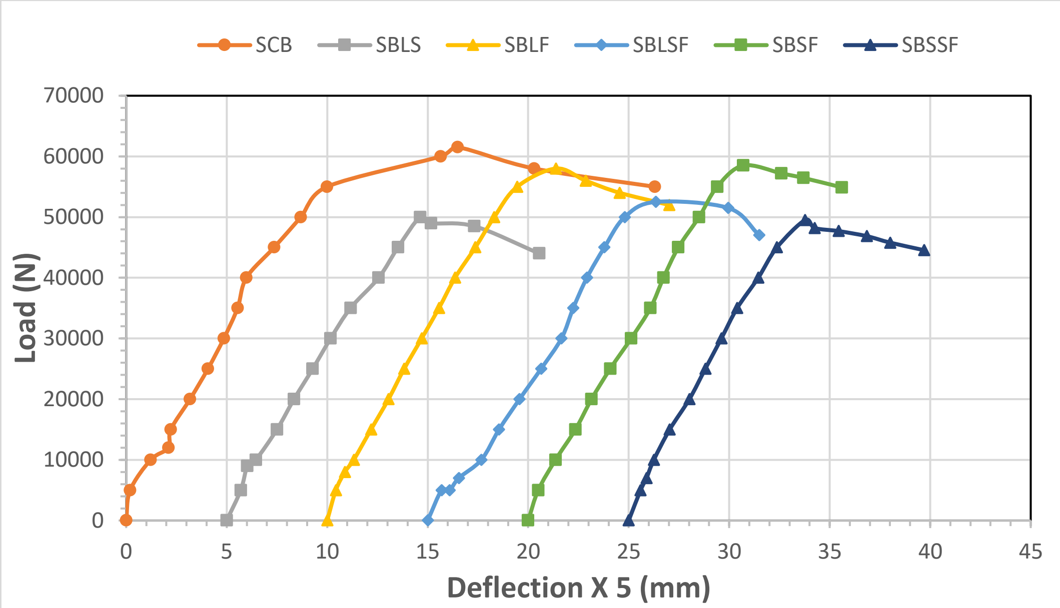

Fig. 4-2 Load deflection curves for group one

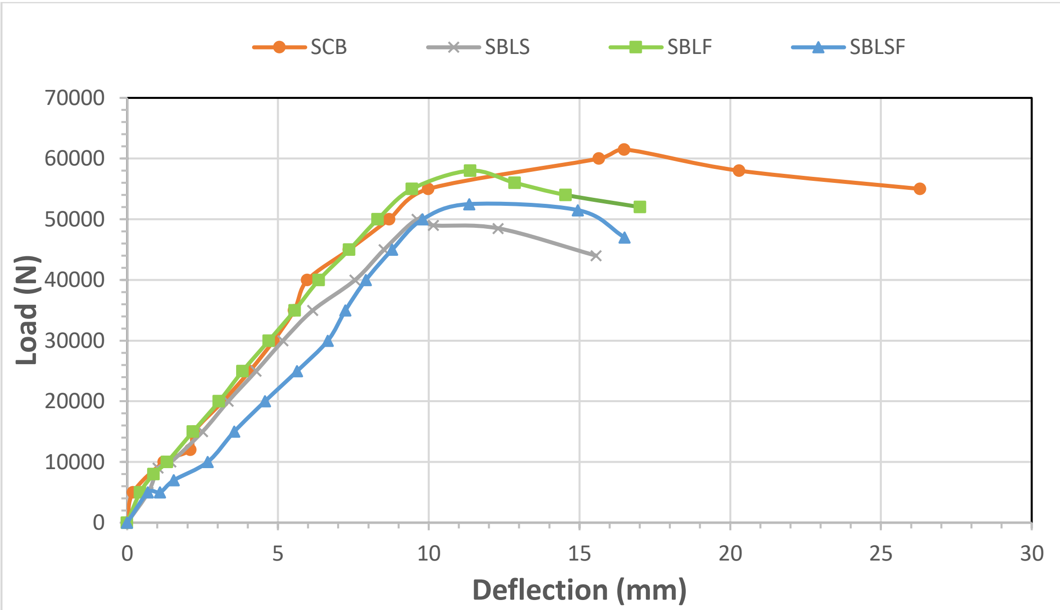

Fig. 4-3 Load-deflection response of control and large opening specimens in group one.

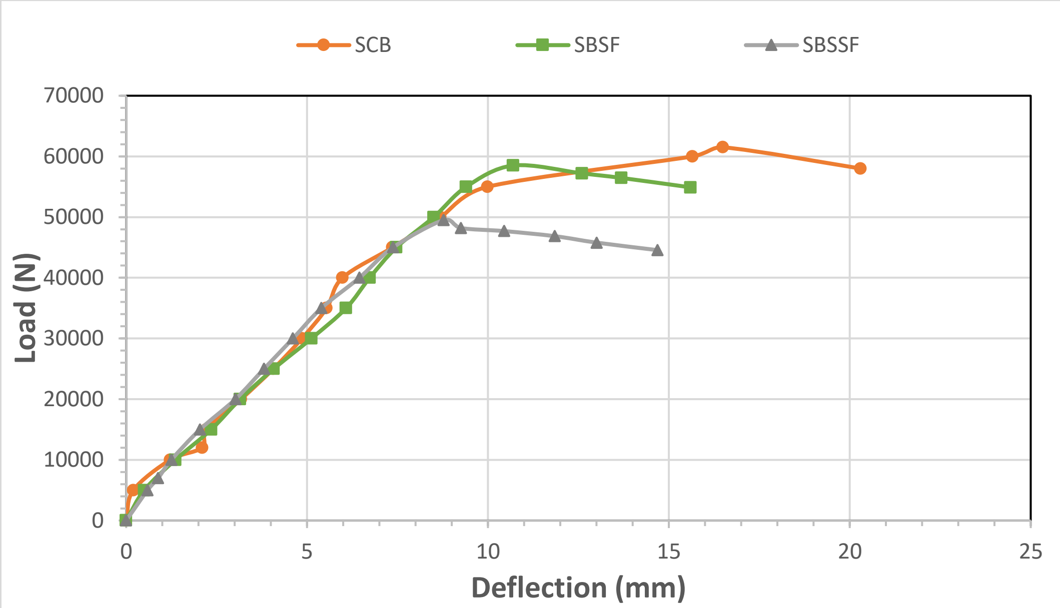

Fig. 4-4 Load-deflection response of control and small opening specimens.

4.4.2 Group Two Strengthened Specimens – Scheme Square Steel Bar:

Fig. (4-5) showcases the load-deflection behavior of specimens DBLSS8, DBLSS10, and the DBLS specimen. The load-deflection behavior of all specimens demonstrated a bilinear pattern. Initially, the reinforced specimens exhibited an almost identical response up to a load of around 20 kN, beyond which the deflection began to increase at a faster rate. The DBLS specimen exhibited reduced stiffness compared to DBLSS8 and DBLSS10, primarily due to the higher concentration of NSM steel bars, especially in DBLSS10. DBLSS8 and DBLSS10 specimens experienced failure at load values of 109.5 kN and 125.5 kN, respectively. The deflection at failure for both specimens was approximately 10.5 mm.

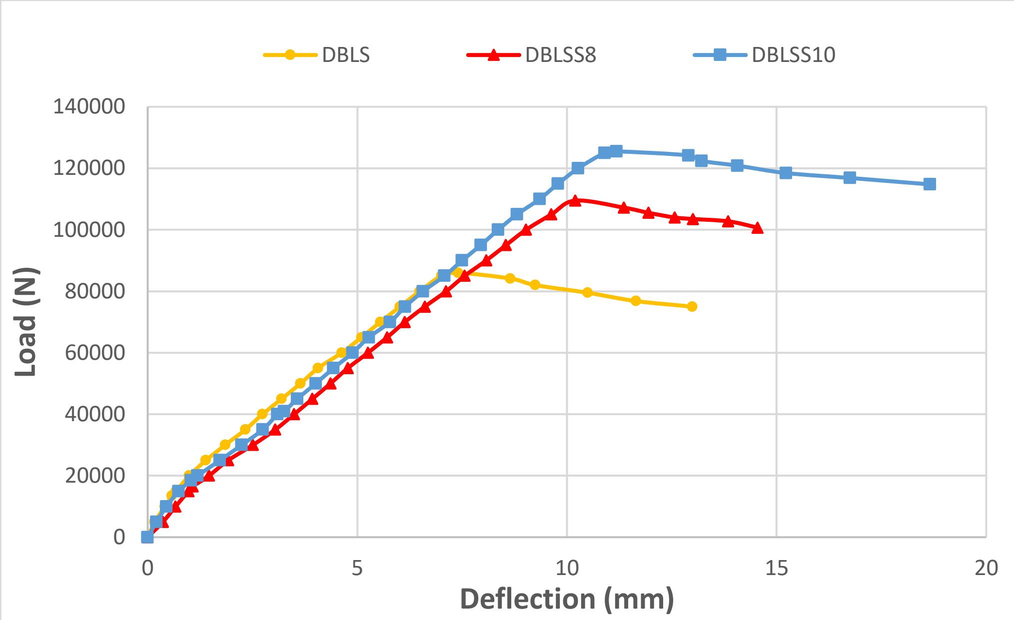

Fig. 4-5 Load-deflection behavior of the square strengthening scheme and DBLS specimens.

4.4.3 Group Two Strengthened Specimens – Scheme Diamond Steel Bar:

In (Fig. 4-6), the load-deflection responses of specimens DBLSD8, DBLSD10, and the DBLS specimen are presented. The load-deflection relationship for all specimens displayed a bilinear pattern. Notably, when comparing the load-deflection behavior at a load of 45 kN, the strengthened specimen DBLSD10, reinforced with diamond stirrup bars with DBLS, exhibited a lower deflection of 2.8 mm, whereas DBLSD8 had a deflection of 4 mm.

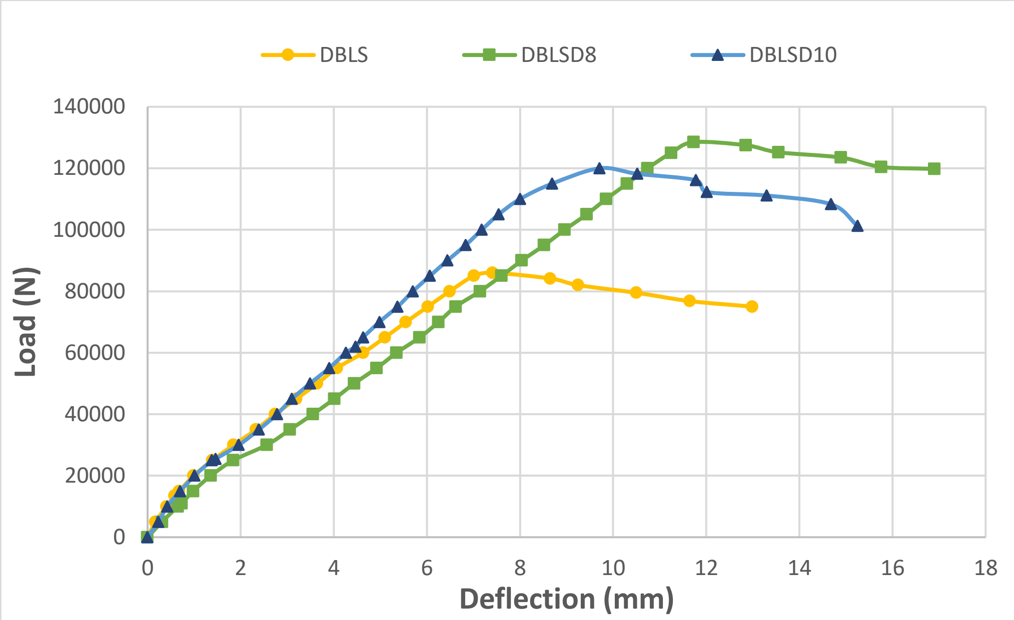

Fig. 4-6 Load-deflection behavior of the diamond strengthening scheme and DBLS specimens.

4.4.4 <u>Group Two Strengthened Specimens – Scheme parallelogram Steel Bar:</u>

Fig. (4-7) illustrates the load-deflection behavior of specimens DBLSP8, DBLSP10, and the DBLS specimen. The load-deflection relationship for all specimens exhibited a bilinear pattern. Significantly, when comparing the load-deflection behavior at a load of 45 kN, the strengthened specimen DBLSP8, which was reinforced with diamond stirrup bars in conjunction with DBLS, demonstrated a lower deflection of 2.8 mm, while DBLSP10 had a deflection of approximately 4.3 mm.

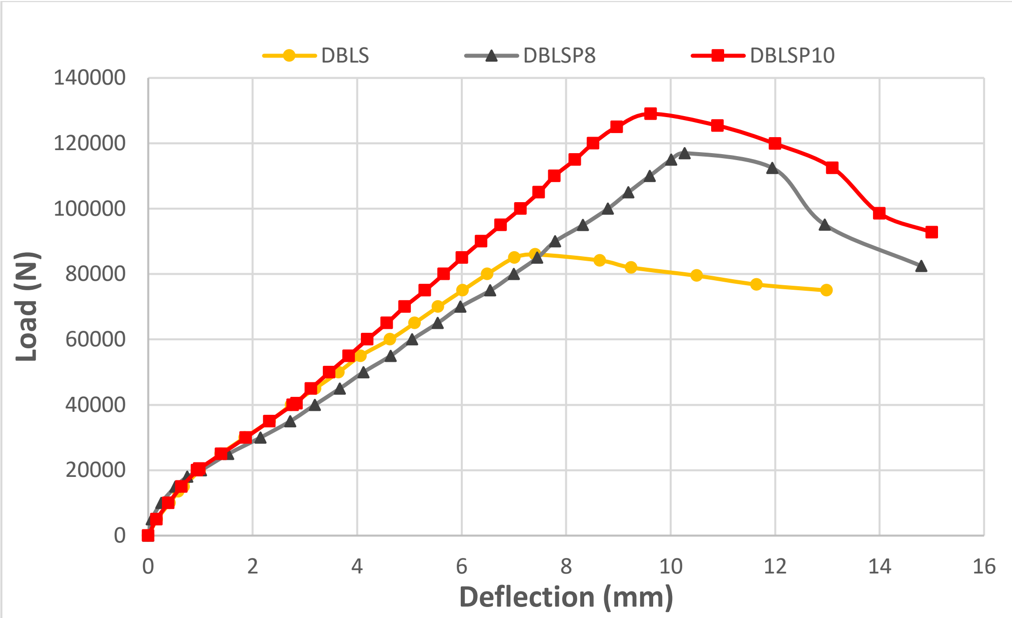

Fig. 4-7 Load-deflection behavior of the parallelogram strengthening scheme and DBLS specimens.

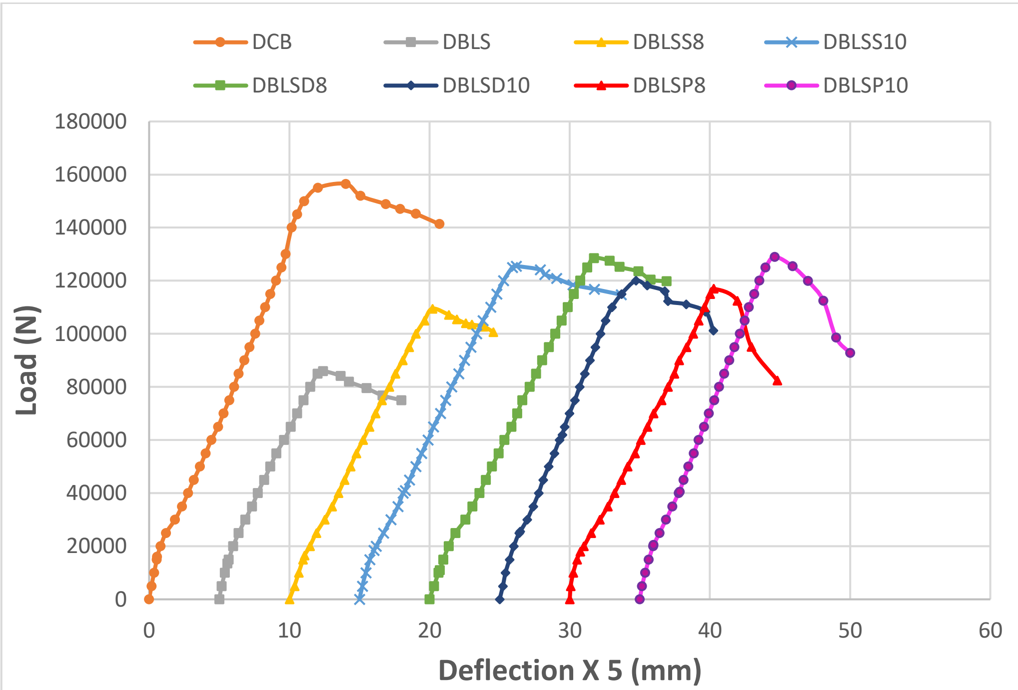

Fig. 4-8 Load deflection curves for group two.

4.5 Crack Pattern and Failure Mode:

4.5.1 Un-strengthened Specimens - Group One

Fig. (4-9 to 4.10) display the crack patterns observed at the point of failure for all beams. The crack patterns and modes of failure varied among the beams due to differences in the presence, position, and sizes of the openings.

Fig. (4-9. a) depicts the crack pattern displayed by the solid specimen SCB. Initially, the first flexural crack appeared near the midspan when the load reached 12 kN. Subsequent diagonal cracks developed in the shear spans near the support plates. As the load increased, the flexural cracks extended from the midspan towards the loading direction. Simultaneously, new flexural cracks developed while existing ones extended vertically upward. Ultimately, the beam experienced failure through flexural compression, resulting in concrete crushing.

Fig. (4-9. b, 4-9. d, and 4-9. f) provide a visual representation of the crack pattern observed in opening specimens SBLS, SBLSF, and SBSSF. Initially, when the openings are positioned in the shear zone or a combination of shear and flexural zones, a diagonal shear crack originates at the bottom of the openings near the support. At a load of around 10 kN, an initial diagonal crack forms, crossing the center of the opening in the left shear span of the specimens. Simultaneously, multiple flexural cracks emerge in the middle span of the beams. The failure of SBLS, SBLSF, and SBSSF occurs abruptly in the right shear span, representing a shear-compression failure. This is due to the shear resistance sections proving to be more effective than the flexural sections for failure when the load reaches 50 kN, 52.5 kN, and 49.5 kN, respectively.

Beams SBLF and SBSF experienced failure due to concrete cracking on the bottom surface within the pure bending zone. Additionally, during the early stages of the post-cracking phase, the beams exhibited the initial flexural cracks primarily at the bottom of the opening. These cracks were observed throughout the mid-span at loads of 8 kN and 10 kN for SBLF and SBSF, respectively.

As the load increased, cracking occurred outside the constant moment zone, following a similar pattern of flexural cracking. However, the cracking in this region happened at a higher load level. Furthermore, in beam SBLF, there were instances of diagonal shear cracks initiating near the support, whereas no diagonal cracks were observed in beam SBSF.

a) The crack patterns observed and the mode of failure for specimen SCB.

b) The crack patterns observed and the mode of failure for specimen SBLS.

c) The crack patterns observed and the mode of failure for specimen SBLF.

d) The crack patterns observed and the mode of failure for specimen SBLSF

e) The crack patterns observed and the mode of failure for specimen SBSF

f) The crack patterns observed and the mode of failure for specimen SBSSF

Fig. 4-9 Crack patterns and failure mode for group one specimens by (Author).

4.5.2 Strengthened Specimens - Group Two

Fig. (4-10) displays the crack pattern observed in the specimens of group two strengthened beams following testing. The dashed lines indicate the placement of NSM-steel stirrup rebars, which were embedded around the openings to reinforce the shear zones. Initially, prominent flexural cracks emerged in the middle span of the strengthened beams. Subsequently, diagonal cracks were observed around the openings in the strengthened beams.

Fig. (4-10. a) depicts the crack pattern observed in the solid specimen DCB. At an applied load of 16 kN, the initial flexural crack became evident near the midspan. Subsequently, diagonal cracks developed within the shear spans adjacent to the support plates. With the ongoing increase in load, these diagonal cracks extended from the supports towards the loading direction. Simultaneously, the commencement of flexural cracks within the constant moment region was observed. As the applied load advanced, these pre-existing cracks underwent extension while additional shear cracks emerged. Ultimately, at a load of 156.5 kN, the occurrence of two distinct splitting cracks within the right and left shear spans precipitated the sudden failure of the beam.

Fig. (4-10. b) illustrates the crack pattern observed in specimen DBLS. In the early stages, at a load of 13.5 kN, a diagonal shear crack was initiated at the lower corner of the opening near the support. Following a slight increase in the load, another shear crack developed on the opposite side of the beam. Moreover, a total of fifteen flexural cracks appeared within the constant moment region at the mid-span of the beam. Ultimately, the beam underwent failure at a load of 86 kN, characterized by a diagonal compression mode of failure.

The beams depicted in Figs. (4-10. c to 4-10. h), wherein the openings were reinforced using square, diamond, and parallelogram steel stirrup rebars, exhibited a notable increase in deflection when compared to the un-strengthened specimen. The implementation of these strengthening strategies played a significant role in enhancing the beam's overall stiffness. Notably, the introduction of strengthening bars in the form of square, diamond, and parallelogram stirrups resulted in an obstruction of the load path, as indicated by the red hidden line. This obstruction consequently led to the formation of multiple cracks surrounding the openings. Furthermore, it is noteworthy that all of the strengthened beams ultimately experienced failure in a shear compression mode.

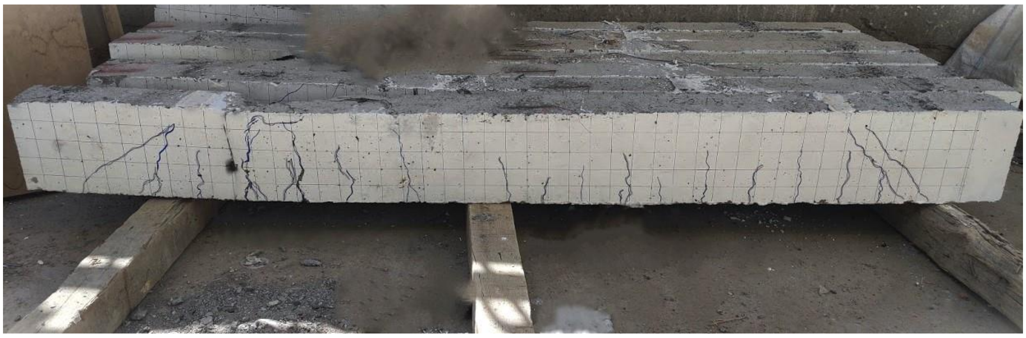

a) The crack patterns observed and the mode of failure for specimen DCB.

b) The crack patterns observed and the mode of failure for specimen DBLS.

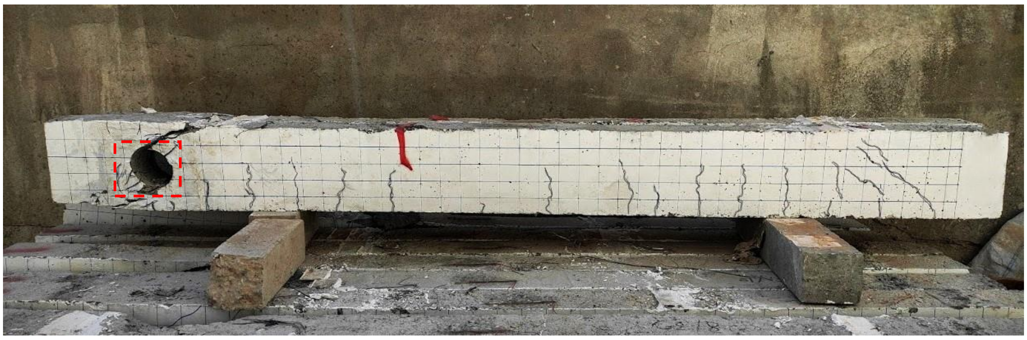

c) The crack patterns observed and the mode of failure for specimen DBLSS8.

d) The crack patterns observed and the mode of failure for specimen DBLSS10.

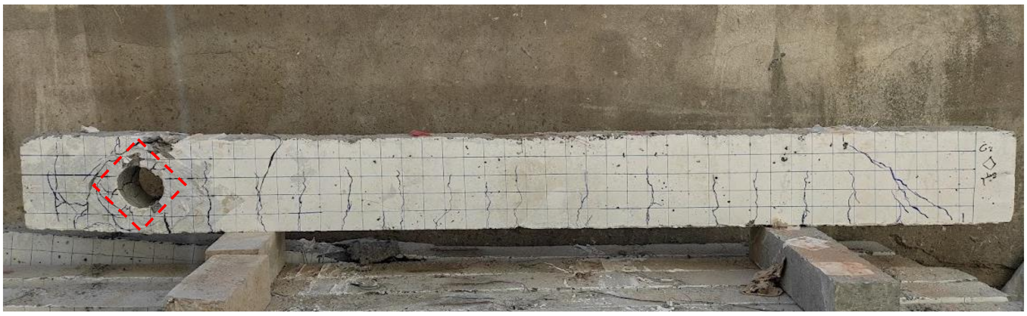

e) The crack patterns observed and the mode of failure for specimen DBLSD8.

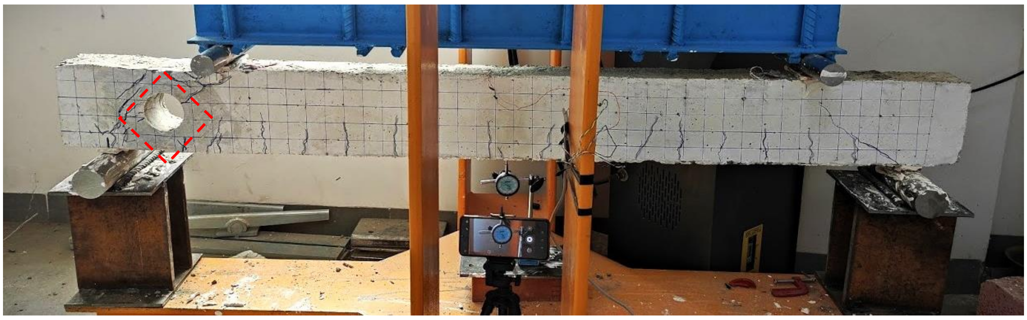

f) The crack patterns observed and the mode of failure for specimen DBLSD10.

g) The crack patterns observed and the mode of failure for specimen DBLSP8.

h) The crack patterns observed and the mode of failure for specimen DBLSP10.

Fig. 4-10 Crack patterns and failure mode for group two specimens by (Author).

4.6 Strain Measurements:

4.6.1 Concrete strain

(Figs. 4-11 and 4-12) show the concrete strain distribution in all the tested beams in group one and group two at the mid-span flexural compression section.

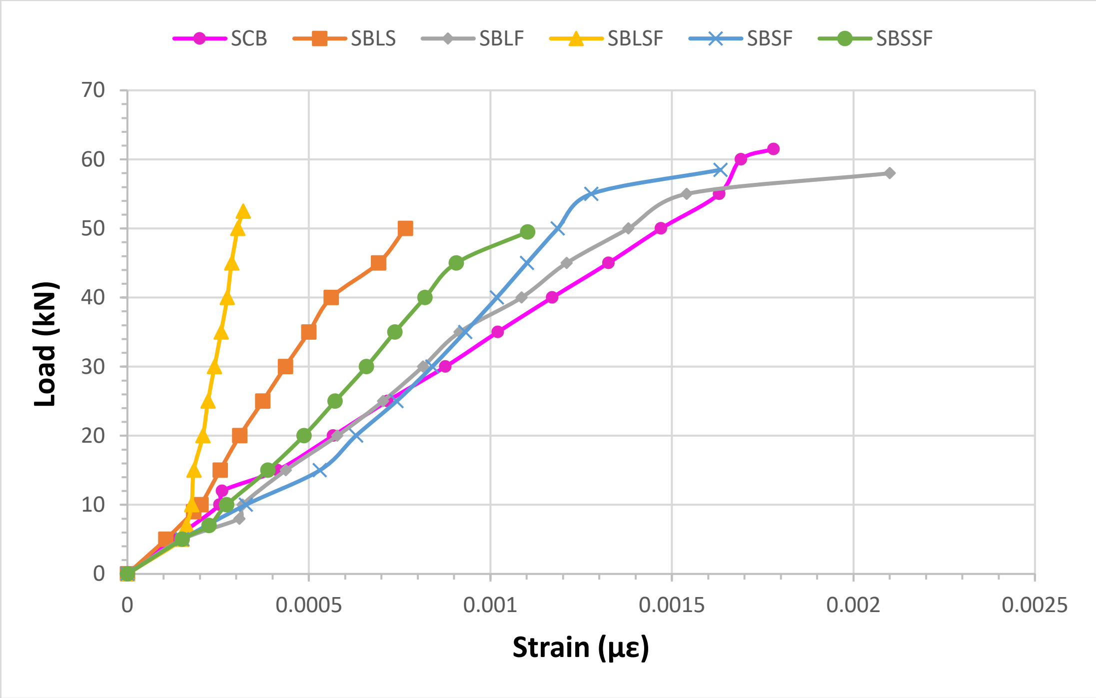

Fig. 4-11 Load-compression strain relationship for specimens in group one.

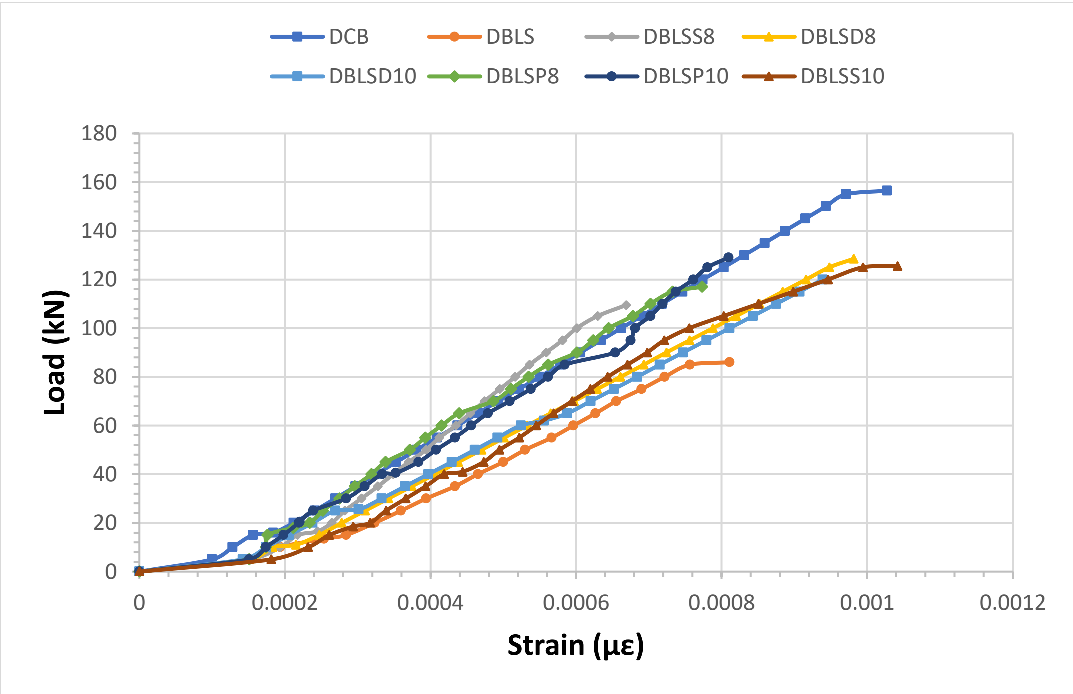

Fig. 4-12 Load-compression strain relationship for specimens in group two.

4.7 Ultimate Loads and Failure Mode

Table (4-5) contains ultimate stages, decrease in ultimate load, and strength gain results for all groups. The flexural and shear cracking load for the solid specimens in groups one and two was around 19.51% and 10.22% of the ultimate load, respectively. These cracking loads were reached at midspan deflections of 2.1 mm and 0.57 mm, respectively. Ultimately, the solid specimens failed under flexural compression modes of failure. This occurred at an ultimate load of 61.5 kN and 156.5 kN, with corresponding deflections of 16.5 mm and 16 mm, respectively.

In group one, all specimens with openings, specifically those subjected to shear (SBLS), flexural and shear (SBLSF), and shear and flexural combined (SBSSF) failures, experienced failure in the shear zone (shear compression). This failure mode occurred due to separation along planes located above and below the openings. Ineffective reinforcement in the chord above and below the openings, along with the cracking load of the specimens (9 kN, 7 kN, and 7 kN, respectively), corresponded to 18%, 13.5%, and 14.15% of the peak loads, respectively.

In the case of specimens SBLF and SBSF, which have openings in the flexural zone, the failure mode was observed in the flexural zone (flexural compression). The flexural cracking failure mode in reinforced concrete beams can arise from various factors, such as excessive bending moments, high tensile stresses in the bottom fibers, inadequate reinforcement, insufficient concrete cover, or excessive loading. These factors can contribute to the development of cracks and eventual failure in the flexural zone of the beams. The cracking load of specimens SBLF and SBSF was recorded as 8 kN and 10 kN, respectively, with a corresponding decrease in ultimate loads of 5.7% and 4.8%.

In group two, when openings or cracks appear in the shear zone of a reinforced concrete deep beam, it can result in shear failure. Shear failure occurs when the applied shear forces exceed the beam's capacity to withstand them. Comparing the ultimate and shear cracking loads of the DBLS specimens with the solid specimens in group two (DCB), the DBLS specimens exhibited cracking loads that were approximately 15.7% and 10.22% of the ultimate load, respectively. These cracking loads were observed at midspan deflections of 0.57 mm and 0.58 mm, respectively. Ultimately, both the solid specimens and DBLS specimens failed due to shear diagonal compression modes of failure.

The presence of diagonal compression failure in an RC deep beam with openings can have detrimental effects on its load-carrying capacity and structural integrity. The openings weaken the beam's ability to effectively transfer and distribute shear forces. Consequently, the beam may develop diagonal cracking or shear deformations that can propagate and lead to failure.

From the test results of strengthened specimens, the diamond and parallelogram DBLSD8, and DBLSP10 gave a good improvement in the ultimate load, compared with the other strengthened specimens (square) which were 128.5 kN and 129 kN they improved with DBLS about 33.1% and 33.33% respectively.

Table 4-5 Ultimate loads and Failure mode results.

Group no.	Specimens	First Cracking stage		Ultimate stage		Decrease in ultimate load*%	Strength gain** %	Failure mode
		Pcr (kN)	*Δcr* (mm)	*Pmax* (kN)	*Δpeak* (mm)			
Group one	SCB	12	2.1	61.5	16.5	-	-	Flexure compression
	SBLS	9	1.03	50	9.62	18.7	-	Shear compression
	SBLF	8	0.88	58	11.38	5.7	-	Flexure compression
	SBLSF	7	1.09	52.5	9.8	14.6	-	Shear compression
	SBSF	10	1.36	58.5	10.7	4.8	-	Flexure compression
	SBSSF	7	0.89	49.5	8.77	19.5	-	Shear compression
Group two	DCB	16	0.57	156.5	16	-	-	Diagonal compression
	DBLS	13.5	0.58	86	7.41	45	-	Diagonal compression
	DBLSS8	15	0.98	109.5	10.2	30	21.5	Shear compression
	DBLSS10	18.5	1.04	125.5	11.18	19.8	31.5	Shear compression
	DBLSD8	11	0.73	128.5	11.73	17.9	33.1	Shear compression
	DBLSD10	25.5	1.46	120	9.71	23.3	28.3	Shear compression
	DBLSP 8	18	0.75	117	10.27	25.2	26.5	Shear compression
	DBLSP 10	20.5	0.98	129	9.62	17.6	33.3	Shear compression

* With respect to the SCB specimen in group one and DCB in group two.
**With respect to the DBLS specimen.

Pcr= Cracking Load**; Δcr=** Midspan Deflection at the first cracking stage**; Pmax=** Ultimate Load**; Δpeak=** Midspan Deflection at the Peak Load**.**

CHAPTER FIVE

THEORETICAL ANALYSIS

CHAPTER FIVE

THEORETICAL ANALYSIS

5.1 Introduction

In this chapter, numerical modeling was employed to investigate reinforced concrete beams strengthened by NSM (Near Surface Mounted) techniques using the finite element method, utilizing ABAQUS software. The primary objective of this investigation is to assess the performance of these beams and to scrutinize the factors that impact the role of transverse openings in enhancing their flexural strength. The parameters under examination encompass:

1. The performance of RC beams featuring transverse openings of varying sizes (large and small).
2. Impact of the shear span ratio.
3. Strengthening the performance of RC deep beams by near-surface-mounted steel bars.

5.2 Finite Element Method

The Finite Element Method (FEM) is a numerical technique used for solving partial differential equations (PDEs) and simulating physical systems in engineering and scientific applications. It's a powerful and versatile numerical method employed to approximate solutions to problems involving the behavior of materials, structures, fluids, and other physical phenomena. The Finite Element Method is widely used in various engineering disciplines, including structural analysis, heat transfer, fluid dynamics, electromagnetics, and more. Its flexibility allows engineers and scientists to model complex geometries and study the behavior of materials and structures under various conditions.

5.2.1 ABAQUS Software

ABAQUS is a widely used finite element analysis (FEA) software suite developed and marketed by Dassault Systèmes' SIMULIA brand. It is specifically designed for simulating and analyzing complex mechanical and Multiphysics problems encountered in various engineering and scientific fields. ABAQUS provides a range of tools and capabilities for performing finite element simulations and is known for its versatility, robustness, and extensive user community.

Key features and capabilities of ABAQUS include:

1. Finite Element Analysis (FEA): ABAQUS allows users to model and analyze a wide range of physical phenomena, including structural mechanics, thermal analysis, fluid dynamics, electromagnetics, and coupled multiphysics simulations.
2. Geometry Modeling: It provides tools for creating and importing complex 3D geometries, allowing users to represent real-world structures and components accurately.
3. Mesh Generation: ABAQUS includes meshing capabilities to discretize the geometry into finite elements, enabling the numerical solution of partial differential equations governing the behavior of the system.
4. Material Models: It offers a library of material models that can be customized to simulate a variety of materials, from metals and composites to elastomers and biological tissues.
5. Boundary Conditions: Users can define boundary conditions and constraints to represent how a structure interacts with its environment, such as applying loads, constraints, and thermal conditions.

6. Analysis Types: ABAQUS supports a wide range of analysis types, including linear and nonlinear static analysis, dynamic analysis, heat transfer analysis, and more.
7. Contact Analysis: It includes robust contact algorithms for simulating interactions between multiple parts or components, which is crucial for modeling assemblies and complex mechanical systems.
8. Post-processing: ABAQUS provides post-processing tools for visualizing simulation results, creating plots and animations, and extracting engineering data such as stress, strain, temperature, and displacement.
9. User-Friendly Interface: It offers a user-friendly graphical interface for setting up simulations, defining parameters, and monitoring results. Additionally, it supports scripting through Python for automation and customization.
10. Parallel Processing: ABAQUS supports parallel computing, enabling users to perform simulations faster by distributing the workload across multiple processors or cores.
11. Versatility: It is widely used in various industries, including aerospace, automotive, civil engineering, biomechanics, and more, for simulating and solving complex engineering problems.
12. Solver Options: ABAQUS offers different solvers to handle linear and nonlinear problems efficiently, including the Standard Solver, Explicit Dynamics Solver, and others.

Abaqus software simulated RC beams, strengthened with NSM steel bars. Abaqus/explicit was used for modeling due to its efficiency in pre-processing and seamless integration of areal elements or bars with solid concrete elements.

5.2.1.1 Abaqus/explicit

Abaqus/Explicit is a specific module or solver within the Abaqus software suite developed by Dassault Systèmes' SIMULIA brand. Unlike Abaqus/Standard, which primarily focuses on implicit or quasi-static analysis, Abaqus/Explicit is designed specifically for explicit dynamic analysis. Here are some key points about Abaqus/Explicit:

1. Explicit Dynamics: Abaqus/Explicit is tailored for solving dynamic problems, particularly those involving high-speed impact, transient events, and short-duration simulations. It's well-suited for scenarios where inertia and wave propagation effects are significant.
2. Time Integration: It uses explicit time integration techniques, such as the central difference method, to advance the simulation through time increments. This approach is more suitable for problems with sudden changes and dynamic loading conditions.
3. Inertia Effects: Abaqus/Explicit accounts for the effects of inertia, making it suitable for simulating fast-moving objects or systems subjected to impulsive loads.
4. Transient Events: It is commonly used for simulating crash tests, impact analyses, explosion dynamics, drop tests, and other situations where the response of the system changes rapidly over time.
5. Nonlinear Material and Contact Behavior: Abaqus/Explicit handles nonlinearities in material behavior and contact interactions efficiently, allowing for realistic modeling of complex materials and contact conditions.
6. Explicit Element Technology: It uses explicit element formulations that are tailored for dynamic problems, making it capable of handling large deformations and significant strain rates.

7. Parallel Computing: Abaqus/Explicit can take advantage of parallel processing to accelerate simulations, which is crucial for solving large-scale, computationally intensive dynamic problems.

8. Applications: Typical applications of Abaqus/Explicit include automotive crash simulations, structural impact analysis, metal forming processes, and any scenario where rapid and violent deformations need to be accurately modeled.

In summary, Abaqus/Explicit is a powerful tool for engineers and researchers dealing with dynamic and highly nonlinear simulations. It excels in scenarios where traditional static analysis techniques are not suitable due to the rapid and transient nature of the events being studied.

5.3 Materials:

5.3.1 Concrete

The Concrete Damage Plasticity Model (CDP) is utilized to describe the response of concrete. This model posits the existence of two primary types of concrete failure: tension-induced cracking and compression-induced crushing. Table (5-1) provides the experimental findings related to concrete properties.

Table 5-1 Concrete Properties.

Group	Compressive Strength (MPa)	Tensile Strength (MPa)
1 and 2	44.27	4.65

The CDP model used in Abaqus is a variant of the Drucker-Prager hypothesis. It defines the flow surface (F) according to the flow function presented by Lubliner et al. (1989), which is defined by two constraint invariants. The geometry is established within the deviation plane and is controlled by an input parameter denoted as Kc as depicted in (Fig. 5-1). ABAQUS recommends a default value of Kc = 2/3, which is known to yield dependable results Chen, (2007). The parameter fb0/fc0, which influences the configuration of the surface (F), signifies the ratio of resistance under biaxial compression to the resistance under uniaxial compression. In this study, the value of fb_0/fc_0 is set at 1.16, following the recommendation by (Kupfer, Hilsdorf, and Rusch 1969).

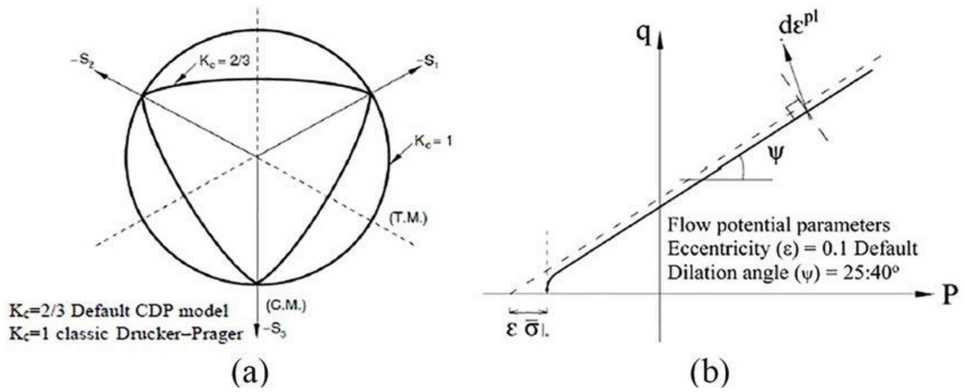

a) Deformation surface within A deviation.

b) Potential surface region within a meridian plane.

Fig. 5-1 Modeling Plastic Damage of Reinforced Concrete in Finite-Element Applications.

The stress-strain correlation of concrete in the CDP model is illustrated in Fig. 5-2.

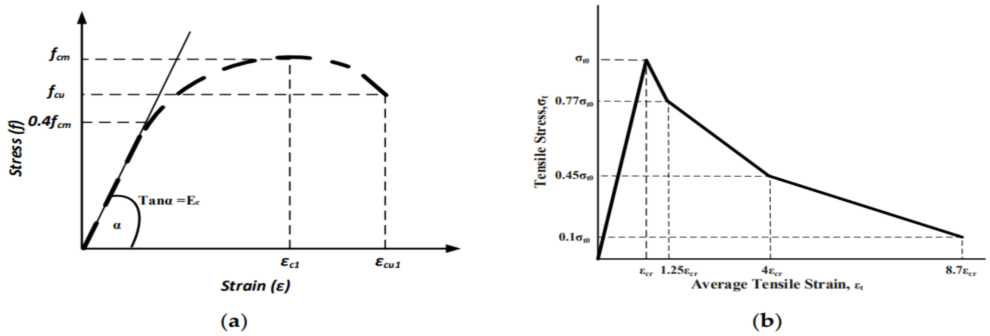

a) Compressive stress-strain relationship. b) Tensile stress-strain relationship

Fig. 5-2 displays the stress-strain relationship for compression and tension according to Eurocode.

The concrete's stress-strain characteristics under compression were defined using the model specified by Eurocode, as outlined in the equations.

$$\varepsilon_{c1} = 0.0014\left[2 - e^{-0.024 f_{cm}} - e^{-0.140 f_{cm}}\right] \quad (5\text{-}1)$$

$$\sigma_c = f_{cm}\frac{k\eta - \eta^2}{1 + (k-2)\eta} \quad (5\text{-}2)$$

Where,

$$k = 1.05 E_{cm}\frac{\varepsilon_{c1}}{f_{cm}} \quad (5\text{-}3)$$

$$\eta = \frac{\varepsilon_c}{\varepsilon_{c1}} \quad (5\text{-}4)$$

$$E_{cm} = 4500\sqrt{\hat{f}_c} \quad (5\text{-}5)$$

σ_c : Compressive stress in the concrete.

f_{cm} : Mean value of concrete cylinder compressive strength.

K: Coefficient Factor.

E_{cm} : Secant modulus of elasticity of concrete.

By employing the equations mentioned earlier, the Hognestad parabola was formulated to supply ABAQUS with a stress-strain curve depicting compressive behavior during compression, as depicted in Fig. (5-3).

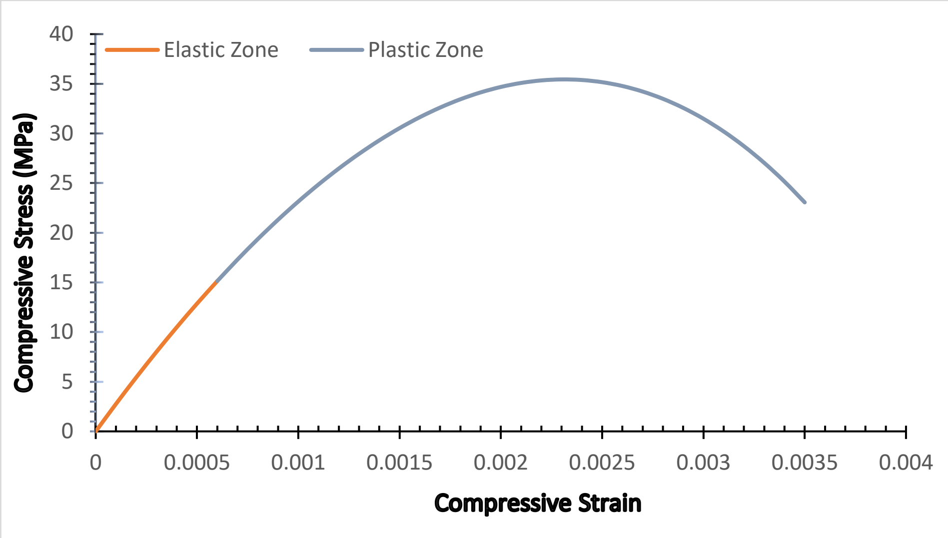

Figure 5-3 Compression behavior of concrete.

The following parameters, which are listed in Table (5-2), are essential in this context: The parameters include the dilation angle (ψ), flow potential ratio, eccentricity, the ratio of the initial equi-biaxial compressive yield stress (fb_0) to the initial uniaxial compressive yield stress (fco), the ratio of the second stress invariant on the tensile meridian to that on the compressive meridian (K), and the viscosity parameter employed for visco-plastic regularization. (Qiao et al. 2011).

Table 5-2 Parameters of plastic damage

Dilation angle **ψ**	30
Eccentricity **ϵ**	0.1
Biaxial and uniaxial resistance ratio in compression	f_{bo}/f_{co}=1.16
Kc	0.667
Viscosity Parameter **μ**	0.01

After concrete cracks, it can still carry tensile loads, a phenomenon known as (tension stiffening). ABAQUS provides three approaches for simulating tension stiffening, allowing for the definition of tensile stress based on cracking strain, displacement, or fracture energy.

In this model, the cracking method is employed for its efficiency in terms of time. Tensile stress is defined as a function of cracking strain in this approach and the model is illustrated in Fig. (5-4).

$$\sigma_t^1 = E_O \varepsilon_t \tag{5-6}$$

Where $\varepsilon_t < \varepsilon_{cr}$

$$\sigma_t^2 = f_t' \left(\frac{\varepsilon_{cr}}{\varepsilon_t}\right)^{0.4} \tag{5-7}$$

Where $\varepsilon_t > \varepsilon_{cr}$

$$\varepsilon_{cr} = \frac{\dot{f}_c}{E_o} \tag{5-8}$$

$$E_o = 4500\sqrt{\dot{f}_c} \tag{5-9}$$

$$f_t = 0.33\sqrt{\dot{f}_c} \tag{5-10}$$

Where:

σ_t^1: Concrete tensile stress which is the end of the elastic zone.
σ_t^2 : Concrete stress after the elastic zone and corresponding to a given concrete strain.
ε_{cr}: Concrete tensile strain which is the end of the elastic zone.
ε_t: Concrete strain corresponding to a given concrete stress (σ_t^2).

E_o: Young's modulus of concrete.

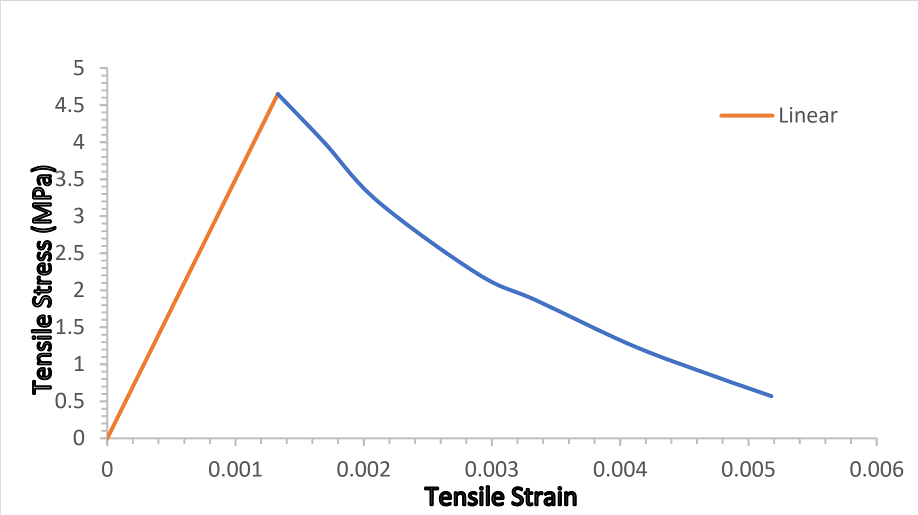

Fig. 5-4 Tensile behavior of concrete.

5.3.2 Steel rebars

Different yield stress steel reinforcement bars were utilized in this study. Specifically, two 12 mm diameter steel rebars were employed for tensile reinforcement, while two 8 mm diameter steel rebars were used for compressive reinforcement. Additionally, Ø8 mm stirrups were placed at 85 mm intervals for shear reinforcement, and also (8mm and 10 mm) were utilized for strengthening around the openings. Table (5-3) provides the material properties of these steel reinforcement elements. The model assumes the reinforcement elements to be elastic and perfectly plastic, as illustrated in Fig. (5-5). Notably, steel hardening was not considered in the analysis, as it made no discernible difference when applied. The stress-strain curve equation is presented in this context.

$$f_s = \varepsilon_s E_s \tag{5-11}$$

Where:

f_s : Yield stress; ε_s: Yield Strain; E_s: Modulus of elasticity.

Table 5-3 Steel rebars material properties

Properties of materials	Values		
	Ø8	Ø10	Ø12
(f_s)	534.5 MPa	583 MPa	548.2 MPa
(E_s)	200 GPa		
Poisson's ratio (v)	0.33		

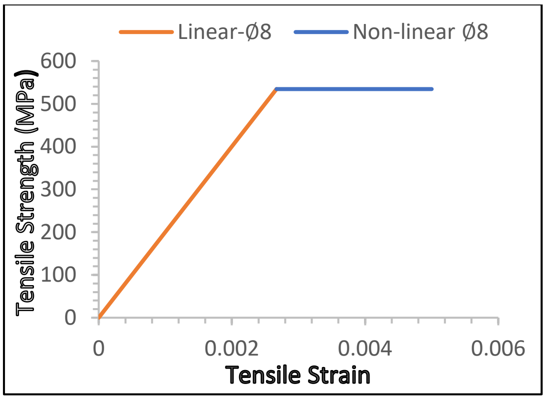

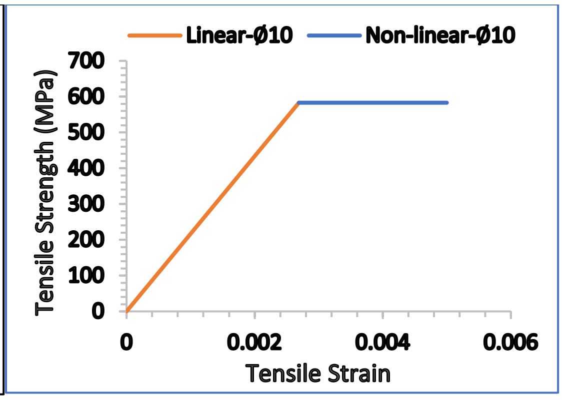

a) (Ø8) Steel reinforcement tensile behavior.

b) (Ø10) Steel reinforcement tensile behavior.

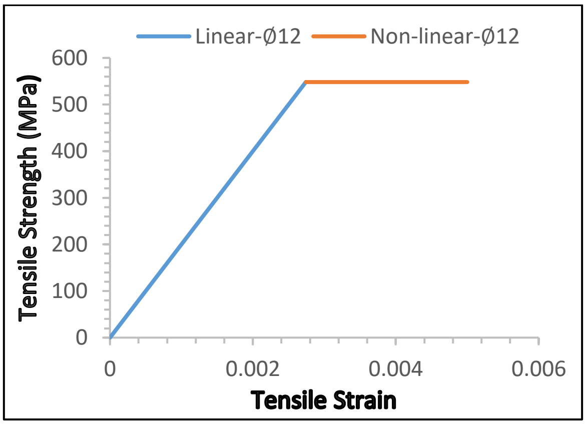

c) (Ø12) Steel reinforcement tensile behavior.

Fig. 5-5 Steel reinforcements tensile behavior.

5.4 Element types

The Finite Element Method (FEM) offers a variety of elements to precisely replicate the behavior of each component during modeling. Choosing the appropriate element is crucial and should be based on experimental assessments for accurate results. In this model, solid elements for the concrete model, truss elements for the stirrups, and beam elements for the main rebars top and bottom main rebars were predominantly utilized, as illustrated in Fig. (5-6).

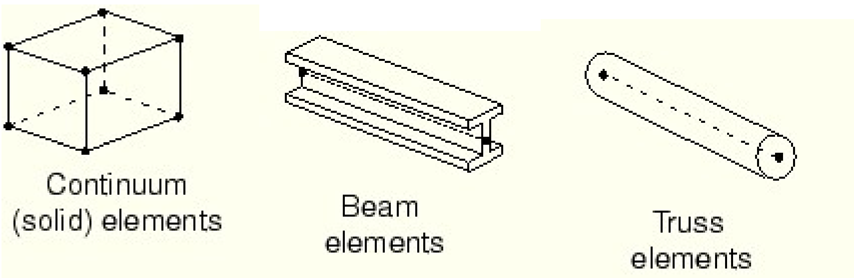

Figure 5-6 Components within the Finite Element Method as described in the ABAQUS Documentation from 2010.

5.5 Element interactions:

In this model, two contact surfaces were employed. The initial surface represents the embedded area of internal steel reinforcement inside the concrete, while the second surface simulates the external contact between concrete and support loading plates. Both these contact types are elaborated upon in sections 5.5.1 and 5.5.2 and the interaction between concrete and reinforcement and concrete with supports and loading used for modeling RC beam models are shown in Fig. (5-7).

5.5.1 Interaction between Concrete and Internal Reinforcement

Establishing contact between concrete and internal steel reinforcements is pivotal for the precise simulation of reinforced concrete sections. In this scenario, bonding between concrete and internal reinforcements can be achieved using three distinct techniques in ABAQUS:

1. Discrete technique: This approach is suitable when a bond is formed by sharing nodes between steel reinforcements and concrete elements. However, it restricts the concrete mesh to the positions of the reinforcement nodes.
2. Smeared element method: In this method, the connection between steel reinforcements and concrete elements is established by incorporating composite layers.
3. Embedded element method: This method entails directly situating the embedded nodes onto the host nodes during implementation.

The embedded elements method was utilized to model the interaction between concrete and steel reinforcement. In this technique, it is crucial to distinguish between host and embedded elements. For instance, concrete is recognized as the host region, while internal steel reinforcements are labeled as the embedded region. In this approach, the nodes of embedded elements are aligned with the nodes of the host region to constrain the translation degree of freedom for embedded nodes.

5.5.2 Interaction between Concrete and support loading plates

Tie interaction in Abaqus is a method used to define a kinematic connection between nodes on different surfaces or edges of separate parts. This connection allows these surfaces or edges to move together without merging the nodes, simulating interaction without a physical connection.

In tie interactions, the nodes on the surfaces or edges are "tied" together, meaning they move together but retain their identities. This approach is often used when modeling interactions like bonding, adhesion, or friction between components without actually merging their geometry.

5.6 Boundary Conditions and Loading

The beams were tested under four-point loading. Boundary conditions and loading used for modeling both RC beams are shown in Fig. (5-8). For boundary conditions, in the experimental test, a simply supported beam was tested for two groups. To replicate the support conditions positioned 100 mm from the beam ends, as illustrated in Fig. (5-8), displacement in both X and Y directions was limited. This restriction was denoted by $U2 = U3 = 0$. Conversely, the other support was constrained only in the Y direction, specified as $U3 = 0$. For loading, a displacement-controlled loading approach was employed. To elaborate, a designated displacement value of 50 mm was applied at two points on the beam, simulating four bending tests. To represent these loadings, permissible displacements were set to 50 mm in the vertical axis direction (Y), $U2 = -50$ mm, and were positioned 900 mm away from each support, as depicted in Fig. (5-8).

5.7 Meshing

Meshing, in the context of Abaqus, refers to the process of discretizing a three-dimensional model into smaller elements, creating a mesh. Each element represents a portion of the physical structure and helps in approximating the behavior of the entire structure under different conditions. To mesh elements effectively, several steps must be taken, including specifying the number of seeds used in elements and determining the mesh order. (20) mm mesh element size has been used for all specimens. The meshing for a concrete beam is depicted in Fig. (5-9). All specimens' models have been illustrated in Appendix B.

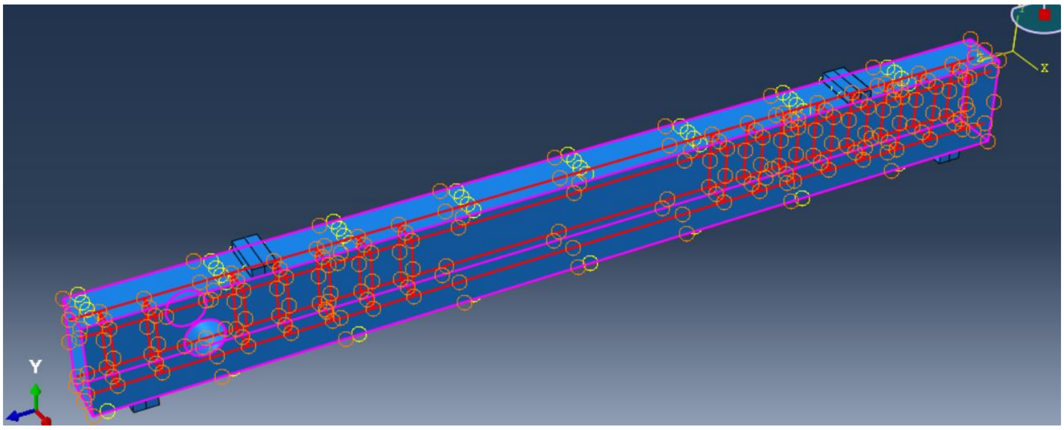

Fig. 5-7 Interaction of the models.

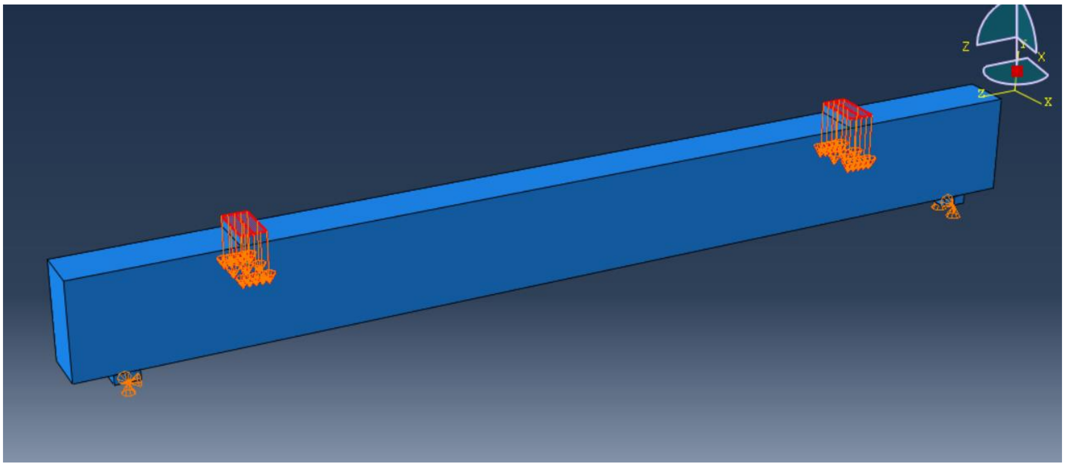

Fig. 5-8 Loading and boundary conditions.

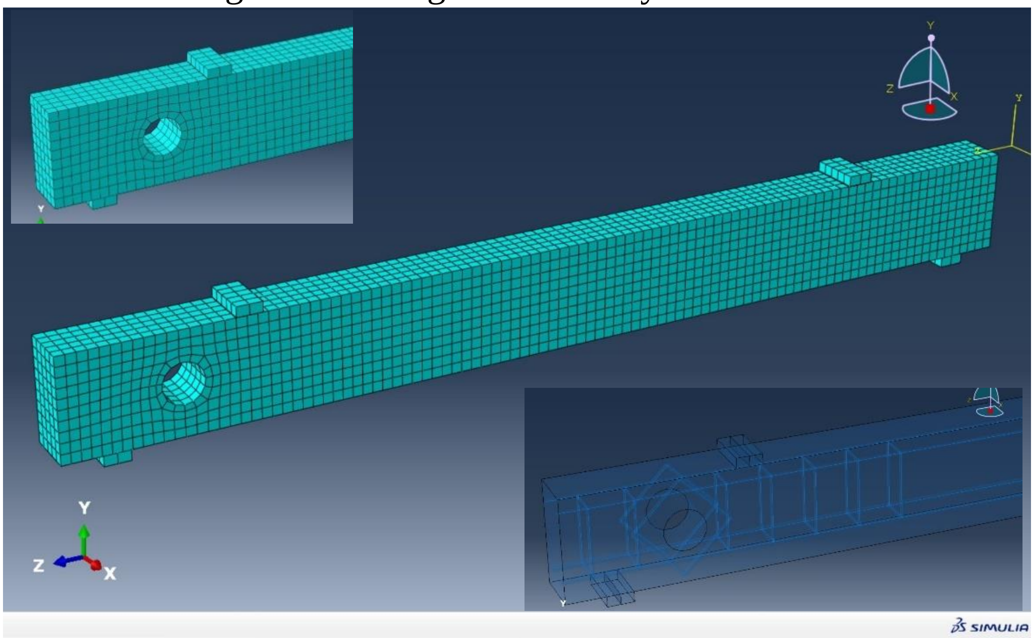

Fig. 5-9 Meshing of RC models.

5.8 Results and Discussion:

5.8.1 Load and Deflection

A precise estimation of the complete load-deflection curves over the entire loading history is essential to establish confidence in the accuracy of the Finite Element (FE) simulation. Figs. (5-10 and 5-11) illustrate the comparison between the load-deflection curves derived from numerical analysis and those obtained from experimental tests for two groups. These figures demonstrate a strong alignment between the FE results and the experimental findings. However, there is a slightly more rigid behavior observed in the Finite Element Model FEM compared to the experimental tests. This disparity could be attributed to the formation of micro-cracks in the experimental beam due to the drilling process, transportation, handling, and drying shrinkage, which led to a reduction in beam stiffness. These micro-cracks were not accounted for in the numerical analysis. Additionally, the ABAQUS program assumes material homogeneity, which is challenging to achieve perfectly during the mixing process in experimental work. Furthermore, the assumption of complete bonding between steel reinforcement and concrete in the finite element method does not hold in experimental conditions. Despite these differences, the overall agreement between the numerical and experimental results supports the use of ABAQUS for studying various cases, offering a more efficient alternative to time-consuming and costly experimental work.

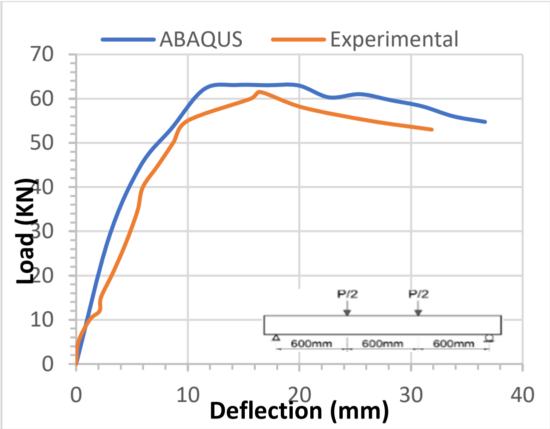

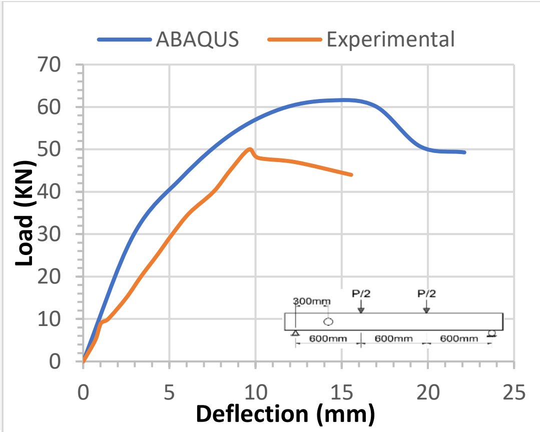

a) Load-Deflection curve of specimen SCB.

b) Load-Deflection curve of specimen SBLS.

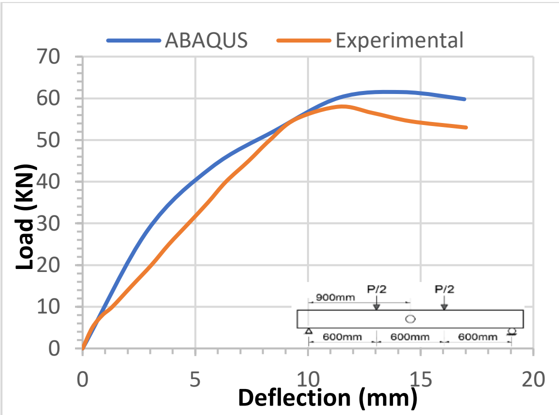

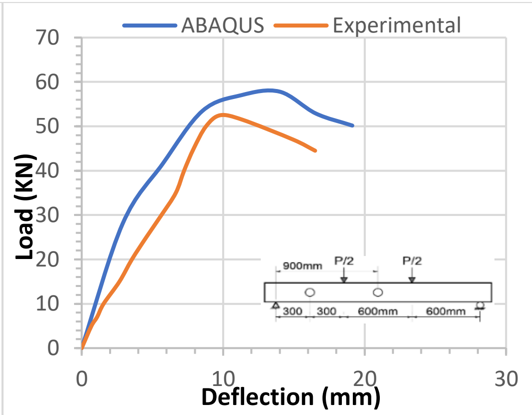

c) Load-Deflection curve of specimen SBLF.

d) Load-Deflection curve of specimen SBLSF.

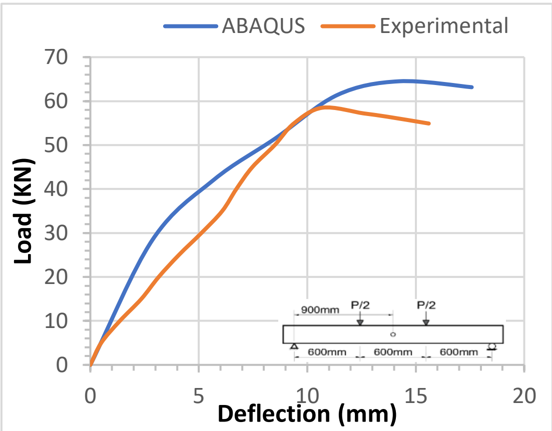

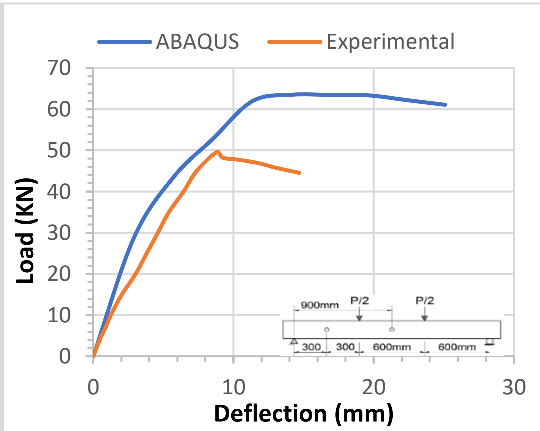

e) Load-Deflection curve of specimen SBSF.

f) Load-Deflection curve of specimen SBSSF.

Fig. 5-10 Group one Numerical and Experimental load-deflection curves.

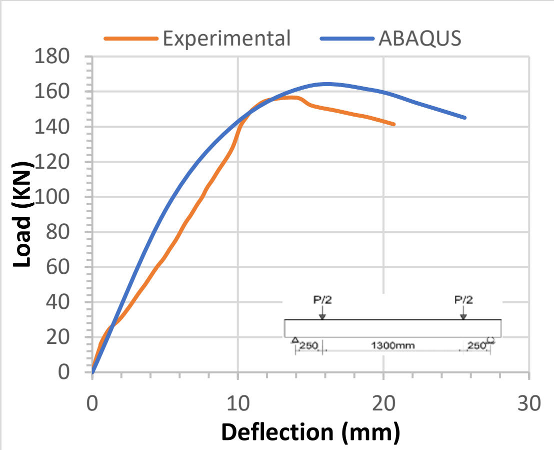

a) Load-Deflection curve of specimen DCB.

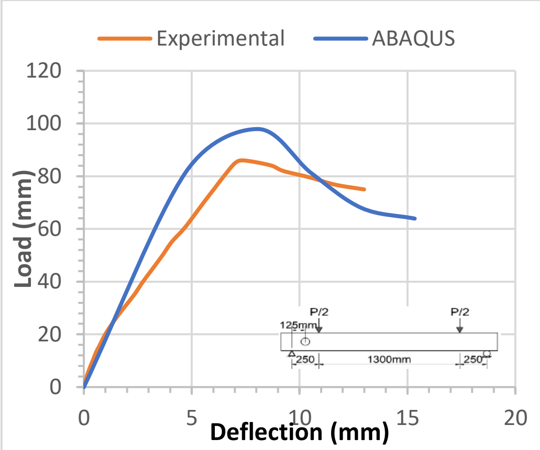

b) Load-Deflection curve of specimen DBLS.

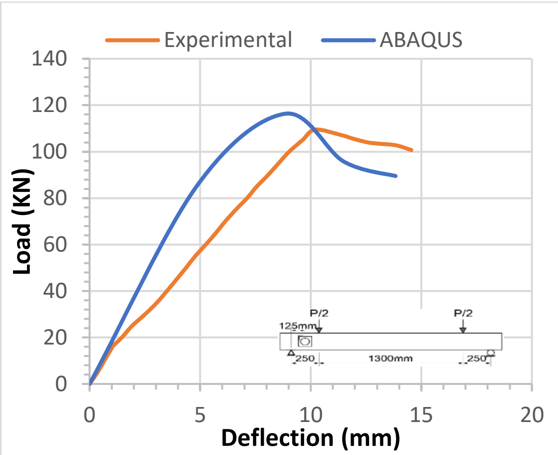

c) Load-Deflection curve of specimen DBLSS8.

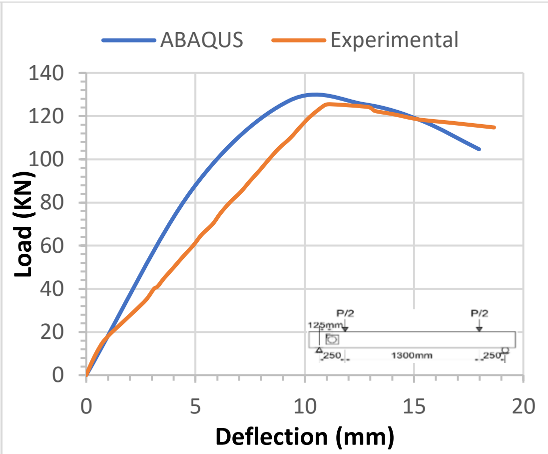

d) Load-Deflection curve of specimen DBLSS10.

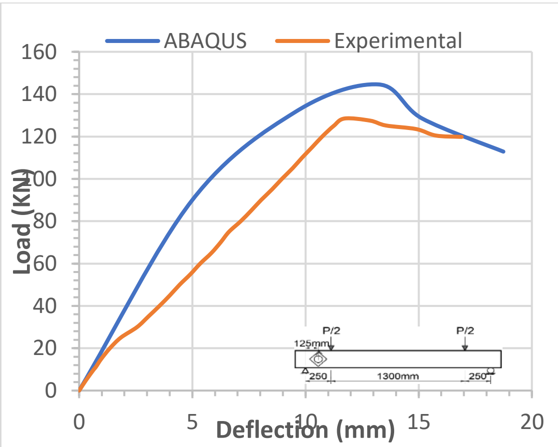

e) Load-Deflection curve of specimen DBLSD8.

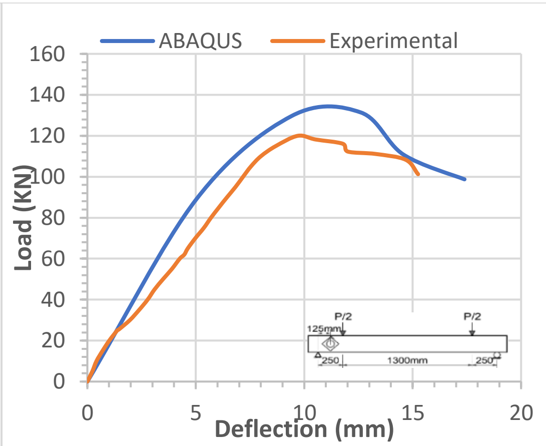

f) Load-Deflection curve of specimen DBLSD10.

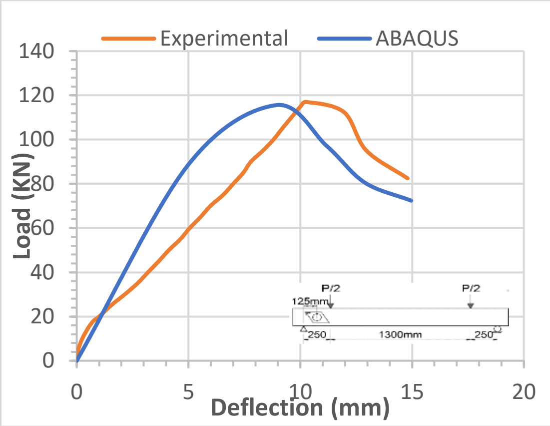

g) Load-Deflection curve of specimen DBLSP8.

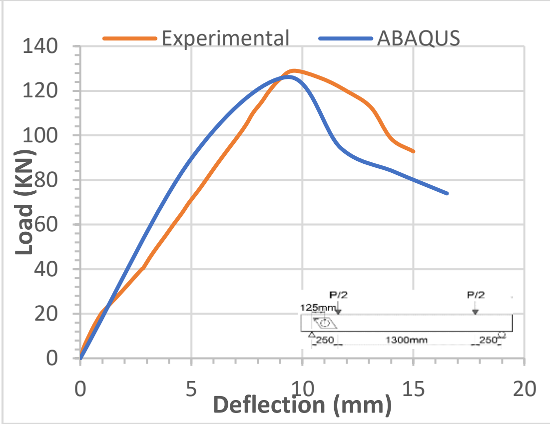

h) Load-Deflection curve of specimen DBLSP10.

Fig. 5-11 Group two Numerical and Experimental load-deflection curves.

5.8.2 Comparison of Failure Load Between ABAQUS Simulation and Experimental Results

The investigation of flexural shear response in reinforced concrete (RC) members often involves analyzing the ultimate load-carrying capacity, a parameter significantly influenced by various failure modes. In this study, failure load values were compared with those obtained from ABAQUS models, as shown in Table (5-4). The comparison revealed that the ABAQUS models accurately estimated the ultimate loads.

Table 5-4 Experimental and ABAQUS failure load results.

Group name	Specimen	Failure Load (kN)		Failure load Experimental/ ABAQUS
		Experimental (kN)	ABAQUS (kN)	
Group 1	SCB	61.5	63.08	0.975
	SBLS	50	61.52	0.813
	SBLF	58	61.5	0.943
	SBLSF	52.5	57.81	0.908
	SBSF	58.5	64.5	0.907
	SBSSF	49.5	63.52	0.779
Group 2	DCB	156.5	163.06	0.960
	DBLS	86	97.91	0.878
	DBLSS 8	109.5	116.31	0.941
	DBLSS 10	125.5	127.14	0.987
	DBLSD 8	128.5	144.6	0.889
	DBLSD 10	120	131.4	0.913
	DBLSP 8	117	115.56	1.012
	DBLSP 10	129	126.16	1.023

5.8.3 <u>Crack Pattern</u>

The numerical representations of crack patterns observed at the point of failure are contrasted with those documented in Figs. (5-12 and 5-13). The images in these figures illustrate the complete side of the beam where the failure occurred, showcasing the corresponding crack pattern. It is noticeable that there is a notable concurrence between the crack patterns predicted by FEM and those documented in the experimental tests, albeit with a slight variance. This discrepancy might be attributed to the presence of initial hairline cracks that emerged before the application of loading.

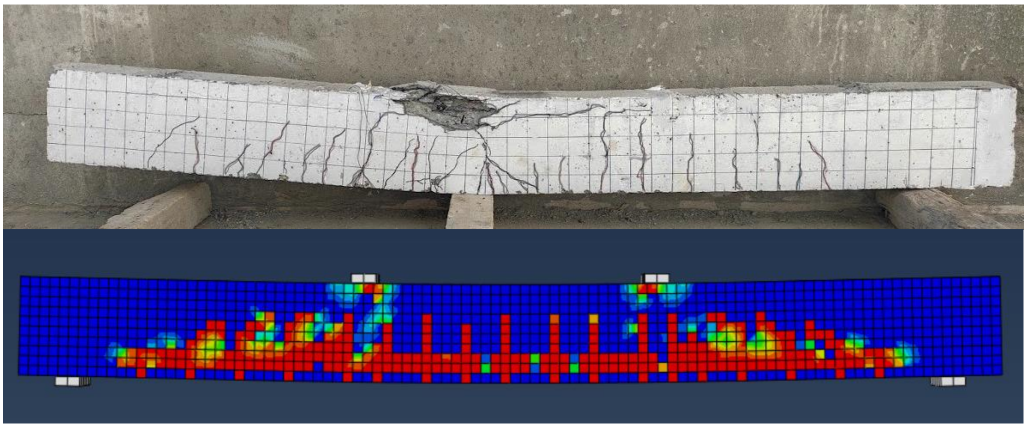

a) SCB

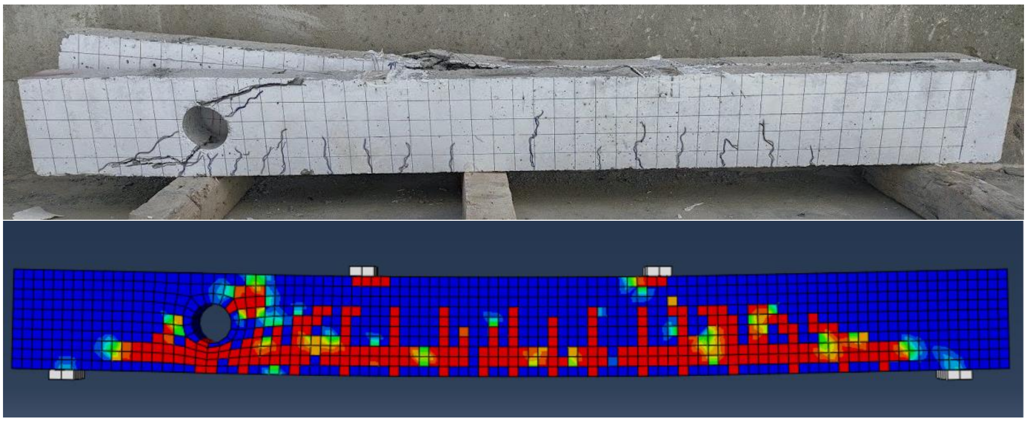

b) **SBLS**

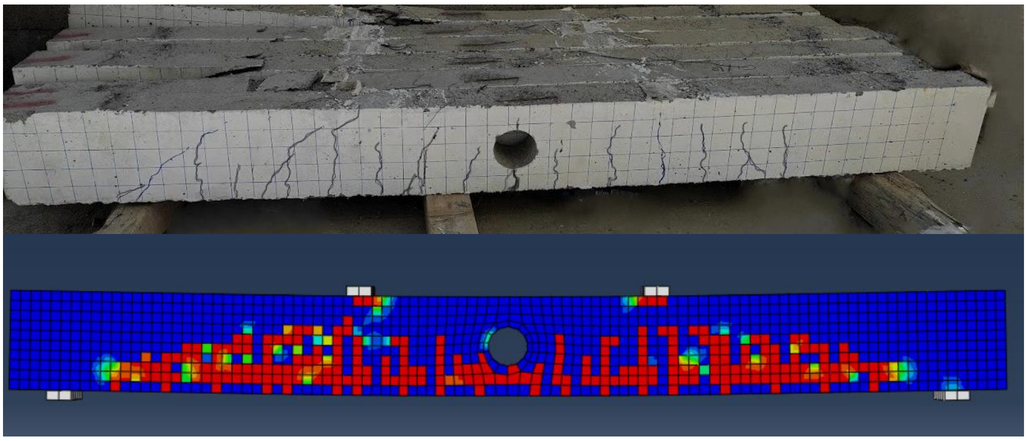

c) **SBLF**

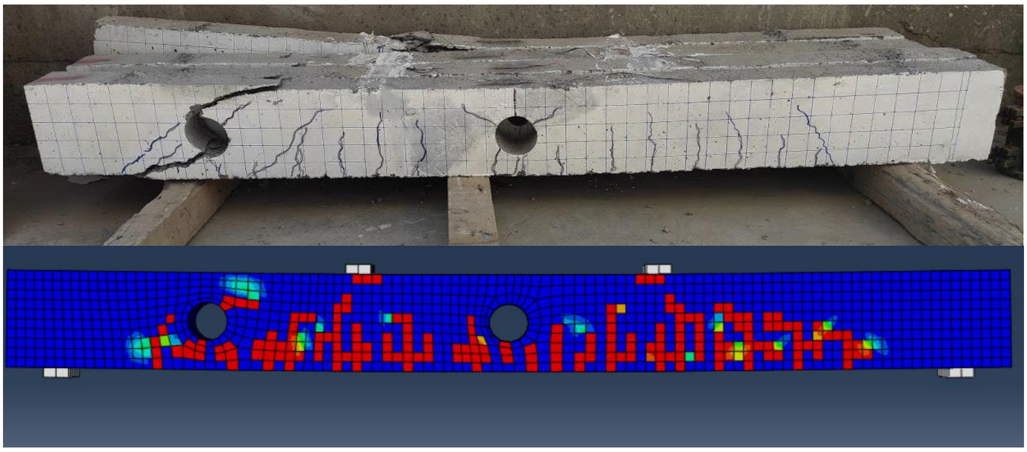

d) **SBLSF**

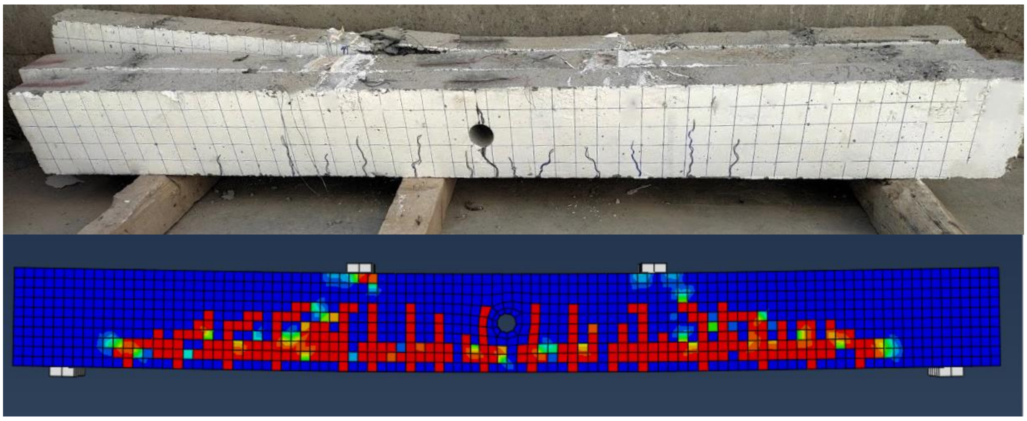

e) **SBSF**

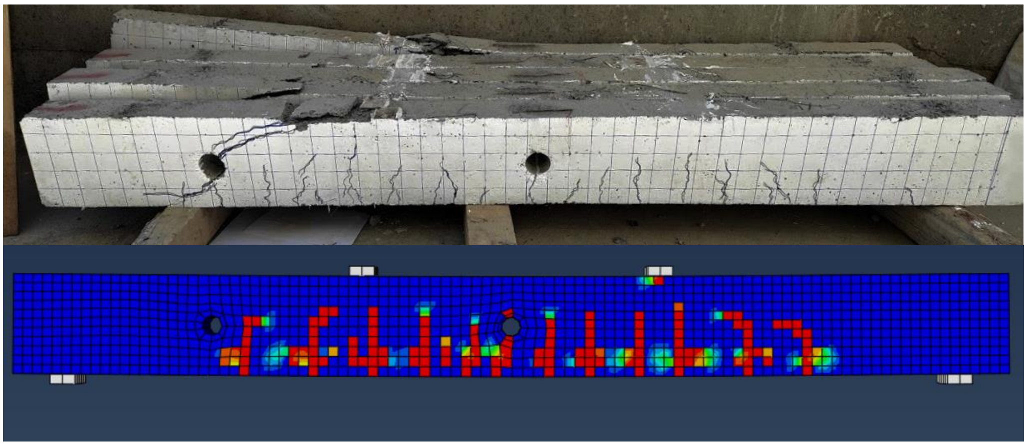

f) **SBSSF**

Fig. 5-12 Crack patterns of Numerical and Experimental group one specimens by (Author).

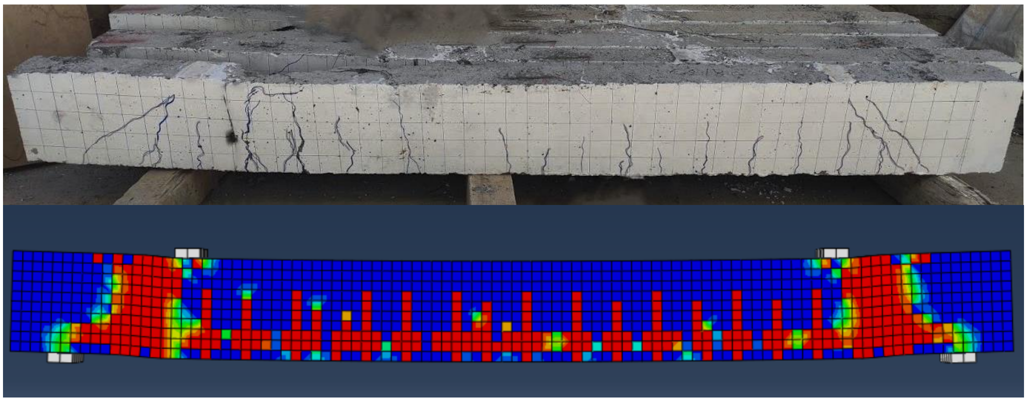

a) **DCB**

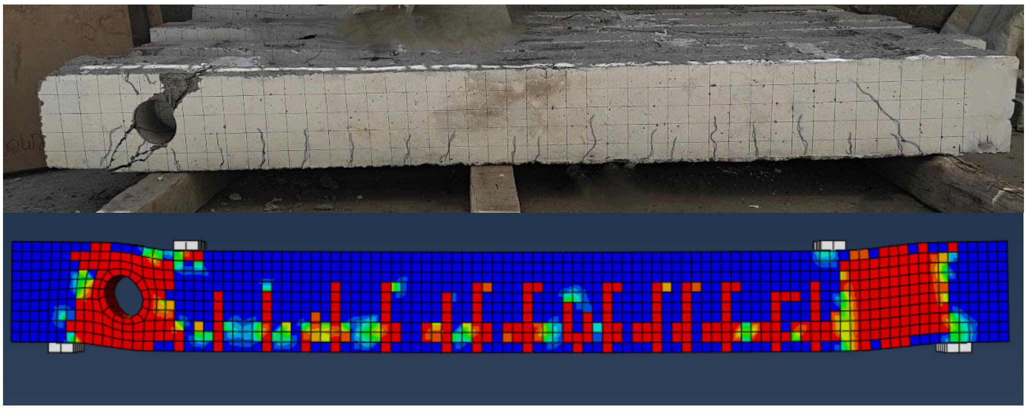

b) **DBLS**

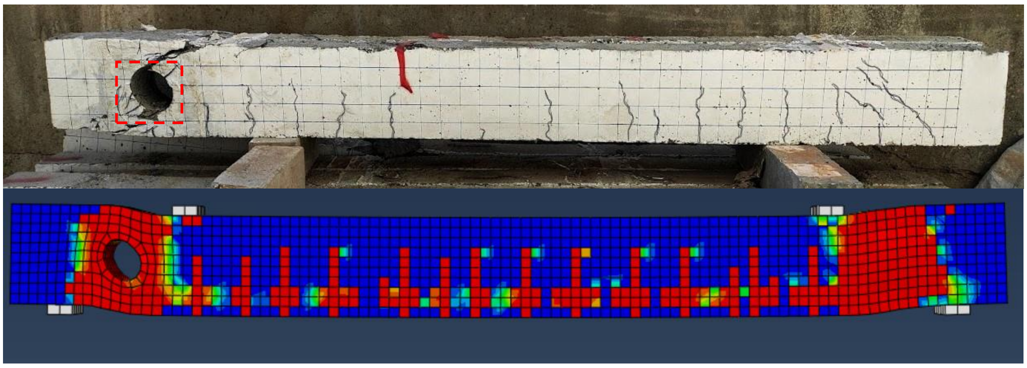

c) **DBLSS8**

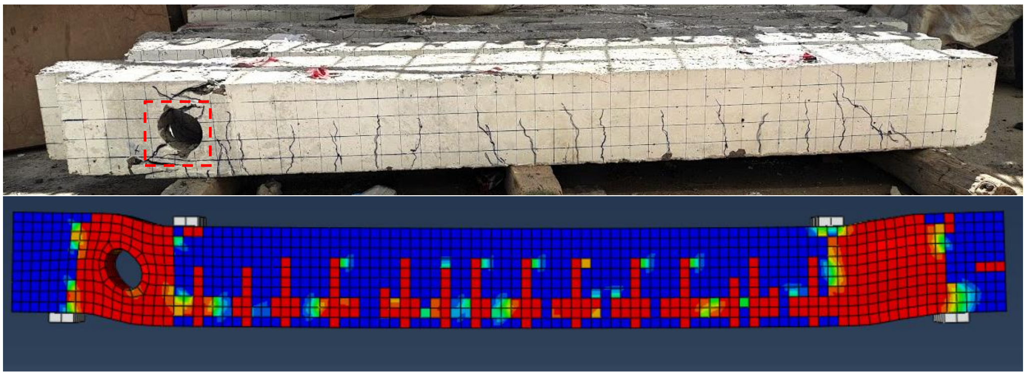

d) **DBLSS10**

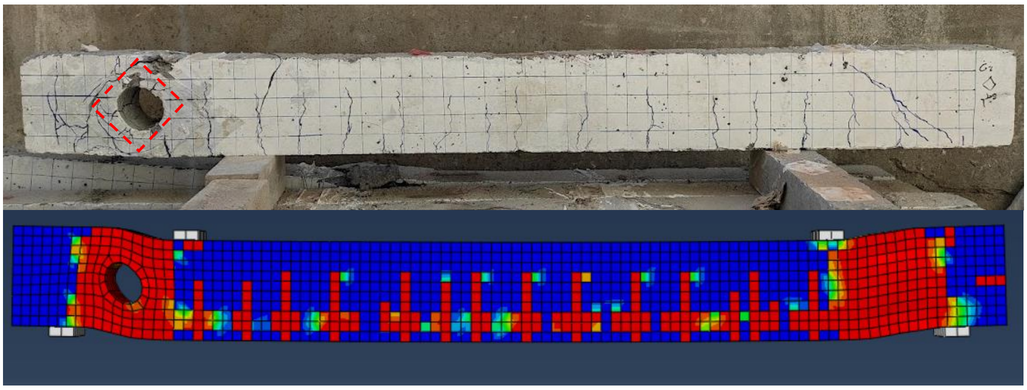

e) **DBLSD8**

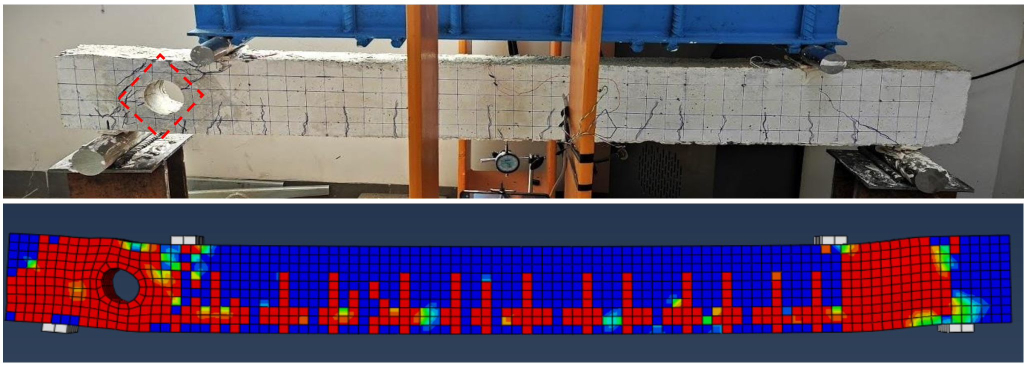

f) **DBLSD10**

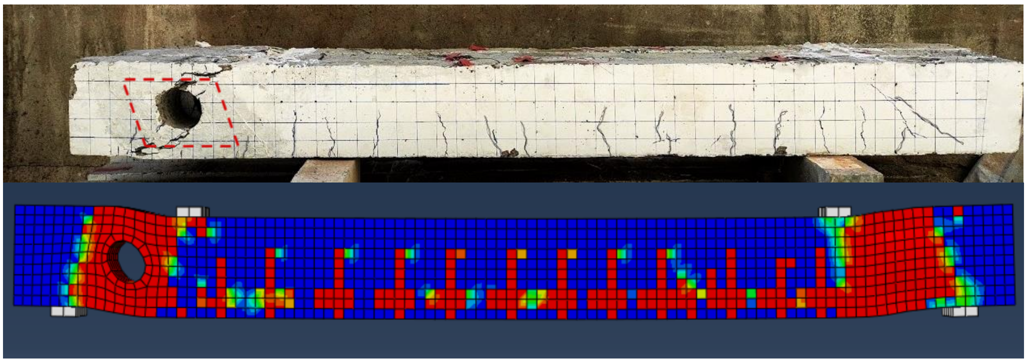

g) **DBLSP8**

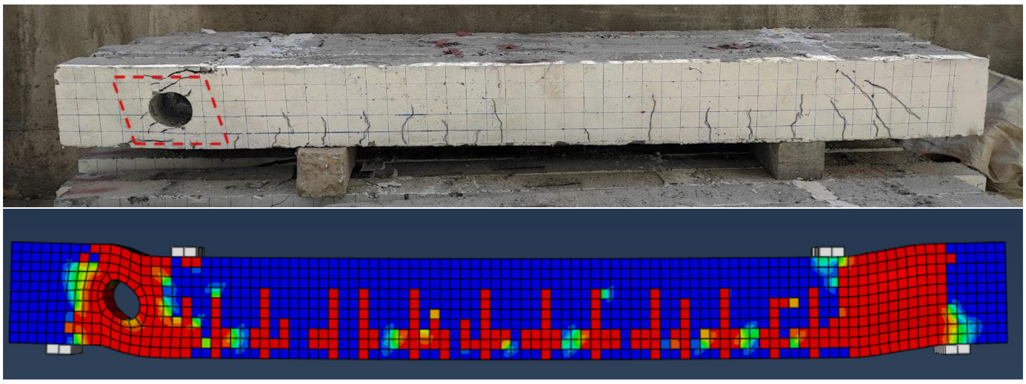

h) **DBLSP10**

Fig. 5-13 Crack patterns of Numerical and Experimental group two specimens by (Author).

CHAPTER SIX

CONCLUSION AND RECOMMENDATION

CHAPTER SIX

CONCLUSIONS AND RECOMMENDATIONS

6.1 Conclusions

In this study, an experiment was conducted to investigate the behavior of RC beams with strengthened openings using NSM steel bars refer to the shear zone. Based on the findings of the study, the following conclusions can be derived.

6.1.1 Experimental work

1) The introduction of openings in the beam led to reductions in the ultimate load by 18.7%, 14.6%, and 5.7% for the beam with large openings located in the shear, shear with flexure, and flexure zones, respectively.

2) By incorporating small-sized openings in the flexure and shear with flexure zones, the ultimate load of the beam experienced a reduction of 4.8% and 19.8%, respectively.

3) The utilization of 8 mm steel stirrups in various configurations (square, diamond, and parallelogram) to reinforce the openings did not increase the first cracking load. Nonetheless, it significantly enhanced the ultimate load by approximately 21.5%, 33.1%, and 26.5% for the beam with large openings located in the shear zone, respectively.

4) The addition of 10 mm stirrup bars in square, diamond, and parallelogram configurations resulted in an improvement in the beam capacity, with percentage increases of approximately 31.5%, 28.3%, and 33.3% observed for the samples where significant openings are situated close to the load, respectively.

6.1.2 Numerical Study

1) The numerical findings demonstrated strong concordance with experimental outcomes regarding failure loads, load-deflection curves, and crack patterns, showing a maximum deviation in ultimate load of approximately 1.023%. Thus, the precision of the numerical results affirms the effectiveness of employing (FEM) for predicting the behavior of reinforced concrete beams with openings.

2) The specimen with large openings located in the flexure and shear zone showed the decrease ultimate load compared with the specimen where have small openings in the flexure and shear zone about 9% .

3) A decrease in the ultimate load of about 1.05% was achieved when increasing the size of the openings from D=80mm to D=40mm in flexural zone.

4) A significant decrease in the ultimate load of about 39.95% was achieved when creating the large opening in deep beam without strengthening size compared with control beam.

5) Changing the steel bars from 8mm to 10mm in square and parallelogram stirrups led to give an additional increase in the ultimate load in 8.52% and 9.17%, respectively.

6) Strengthening the specimen by diamond stirrup bars led to give decrease in the ultimate load by changing bar diameters 10mm to 8mm about 9.13%.

6.2 Recommendation

Contemporary investigations have yielded innovative perspectives on the performance of RC beams, particularly in the context of augmenting the structural integrity of RC deep beams through the implementation of (NSM) reinforcement utilizing composite materials involving steel rebars in the vicinity of structural openings. In light of these findings, the ensuing recommendations are put forth for prospective research endeavors within this specific domain:

1) Examine the structural performance of RC beams reinforced with carbon fiber-reinforced polymer (CFRP) rebars near structural openings.

2) Utilize high-performance concrete to investigate the impact of compressive strength on RC beams strengthened with Near-Surface Mounted (NSM) steel rebars.

3) Evaluate the effectiveness of precast concrete reinforced with Near-Surface Mounted (NSM) steel rebars using diverse reinforcement strategies.

4) Investigate the efficacy of a circular stirrup arrangement in the proximity of openings for RC beams.

5) Examining the behavior of a reinforced concrete beams featuring irregularly shaped openings reinforced with NSM steel bars.

6) Investigate the structural performance of a T-shaped beam featuring openings strengthened with NSM steel bars.

7) Study the structural response of a continuous RC T-beam with openings, reinforced using either NSM (Near Surface Mounted) method steel bars or FRP (Fiber-Reinforced Polymer) bars.

REFERENCE

Asplund, S.O., 1949, January. Strengthening bridge slabs with grouted reinforcement. In Journal Proceedings (Vol. 45, No. 1, pp. 397-406).

Amiri, J.V. and Alibygie, M.H., 2004, August. Effect of small circular opening on the shear and flexural behavior and ultimate strength of reinforced concrete beams using normal and high strength concrete. In Proceedings of the 13th World Conference on Earthquake Engineering, Vancouver, BC, Canada (Vol. 18).

Al-Mahmoud, Firas, Arnaud Castel, Raoul François, and Christian Tourneur. 2009. "Strengthening of RC Members with Near-Surface Mounted CFRP Rods." Composite Structures 91 (2): 138–47.

Amiri, Soroush, Reza Masoudnia, and Ali Akbar Pabarja. 2011. "The Study of the Effects of Web Openings on the Concrete Beams." Australian Journal of Basic and Applied Sciences 5 (7): 547–56.

Blaschko, M, and K Zilch. 1999. "Rehabilitation of Concrete Structures with CFRP Strips Glued into Slits." In Proceedings of the Twelfth International Conference of Composite Materials, ICCM. Vol. 12. Citeseer.

Chin, S.C., Shafiq, N. and Nuruddin, M.F., 2011. Strengthening of RC beams containing large opening at flexure with CFRP Laminates. Int. J. Civ. Environ. Eng, 5, pp.743-749.

Chin, Siew Choo, Fadzil Mat Yahaya, DOHS Ing, Andri Kusbiantoro, and Wen Khai Chong. 2015. "Experimental Study on Shear Strengthening of Rc Deep Beams with Large Openings Using CFRP." In Proceedings of the International Conference on Architecture, Structure and Civil Engineering (ICASCE'15), Antalya, Turkey, 7–8.

De Lorenzis, L., Nanni, A. and La Tegola, A., 2000, May. Strengthening of reinforced concrete structures with near surface mounted FRP rods. In International meeting on composite materials, PLAST (pp. 9-11).

De Lorenzis, L. and Nanni, A., 2001. Shear strengthening of reinforced concrete beams with near-surface mounted fiber-reinforced polymer rods. Structural Journal, 98(1), pp.60-68.

De Lorenzis, L. and Nanni, A., 2002. Bond between near-surface mounted fiber-reinforced polymer rods and concrete in structural strengthening. Structural Journal, 99(2), pp.123-132.

Deepra, R A J S, and R S Surumi. 2012. "Shear Strengthening of Reinforced Concrete Beams Using Near Surface Mounted Glass Fibre Reinforced Polymer."

Diab, H.M., Abdelaleem, T. and Rashwan, M.M., 2020, December. Moment redistribution and flexural performance of RC continuous T-beams strengthened with NSM FRP or steel bars. In Structures (Vol. 28, pp. 1516-1538). Elsevier.

Hassanien, K.F.K., 2015. Strengthening of reinforced concrete beams using near-surface mounted FRP. International Journal of Engineering Science and Innovative Technology (IJESI.

Hawileh , W., Nawaz, R.A., Saqan, E.I. and Abdalla, J.A., 2016. Effect of longitudinal carbon fiber-reinforced polymer plates on shear strength of reinforced concrete beams. ACI Structural Journal, 113(3).

Hamid, N A A, N Salleh, N Ali, S R Abdullah, S H Adnan, and Z Jamellodin. 2022. "Strengthening of Reinforced Concrete Beams with Circular Opening at Flexure Zone by Various Types of Fiber Reinforced Polymer." In IOP Conference Series: Earth and Environmental Science, 1022:12053. IOP Publishing.

Kupfer, Helmut, Hubert K Hilsdorf, and Hubert Rusch. 1969. "Behavior of Concrete under Biaxial Stresses." In Journal Proceedings, 66:656–66.

Khalil, A.A., 2004. Strengthening of Reinforced Concrete Continuous Beams in Sagging and Hogging Moment Regions using CFRP. Scientific Bulletin of Ain Shams University, 39(1), pp.75-98.

KAMONNA, HAYDER H, and LUBNA R ALKHATEEB. 2020. "STRENGTHENING OF REINFORCED CONCRETE DEEP BEAMS WITH OPENINGS BY NEAR SURFACE MOUNTED STEEL BAR." Journal of Engineering Science and Technology 15 (4): 2559–79.

Kartal, Saruhan, Ilker Kalkan, Ahmet Beycioglu, and Magdalena Dobiszewska. 2021. "Load-Deflection Behavior of Over-and Under-Reinforced Concrete Beams with Hybrid FRP-Steel Reinforcements." Materials 14 (18): 5341.

Lorenzis, Laura De, Brian Miller, and Antonio Nanni. 2001. "Bond of FRP Laminates to Concrete." ACI Materials Journal 98 (3): 256–64.

Lorenzis, Laura De, and Antonio Nanni. 2002. "Bond between Near-Surface Mounted Fiber-Reinforced Polymer Rods and Concrete in Structural Strengthening." Structural Journal 99 (2): 123–32.

Lorenzis, Laura De, Antonio Nanni, and Antonio La Tegola. 2000. "Strengthening of Reinforced Concrete Structures with Near Surface Mounted FRP Rods." In International Meeting on Composite Materials, PLAST, 9–11.

Lubliner, Jacob, Javier Oliver, Sand Oller, and EJIJos Onate. 1989. "A Plastic-Damage Model for Concrete." International Journal of Solids and Structures 25 (3): 299–326.

Mansur, M.A. and Tan, K.H., 1999. Concrete beams with openings: analysis and design (Vol. 20). CRC Press.

Mansour, Moustafa Seifeddin. 2019. Strengthening of Concrete Deep Beams with Extreme Discontinuities Using Near-Surface-Mounted Composites. United Arab Emirates University (United Arab Emirates).

Mansur, Webe João. 1983. "A Time-Stepping Technique to Solve Wave Propagation Problems Using the Boundary Element Method." University of Southampton.

Morsya, A, and Amr M Barima. 2019. "Behavior of RC Beams with Openings Using Different Strengthening Techniques." International Journal of Sciences: Basic and Applied Research (IJSBAR) 46 (1): 195–219.

Novidis, Dimitris G, and Stavroula J Pantazopoulou. 2008. “Bond Tests of Short NSM-FRP and Steel Bar Anchorages.” Journal of Composites for Construction 12 (3): 323–33.

Özkılıç, Y.O., Aksoylu, C., Gemi, L. and Arslan, M.H., 2022, July. Behavior of CFRP-strengthened RC beams with circular web openings in shear zones: Numerical study. In Structures (Vol. 41, pp. 1369-1389). Elsevier.

Prentzas, E.G., 1968. Behaviour and reinforcement of concrete beams with large rectangular apertures (Doctoral dissertation, University of Sheffield, Civil & Structural Engineering).

Pimanmas, Amorn. 2010. “Strengthening R/C Beams with Opening by Externally Installed FRP Rods: Behavior and Analysis.” Composite Structures 92 (8): 1957–76.

Qiao, H, Q D Yang, W Q Chen, and C Z Zhang. 2011. “Implementation of the Arlequin Method into ABAQUS: Basic Formulations and Applications.” Advances in Engineering Software 42 (4): 197–207.

Salam, S A. 1977. “Beams with Openings under Different Stress Conditions.” In Conference on Our World in Concrete and Structures, Singapore, 25–26.

Somes, N F, and W G Corley. 1974. “Circular Openings in Webs of Continuous Beams.” Special Publication 42: 359–98.

Schlaich, J. and Schafer, K., 1991. Design and detailing of structural concrete using strut-and-tie models. Structural Engineer, 69(6), pp.113-125.

Schäfer, K. and Schlaich, J., 1993. On the Consistent Design of Structural Concrete with Strut-and-Tie Models. In Proceedings of the Int. Conf. Analytical Models and New Concepts in Mechanics of Structural Concrete, Białystok University of Technology.

Shubbar, A.A.F., Alwan, H., Phur, E.Y., McLoughlin, J. and Al-khaykan, A., 2017. Studying the structural behaviour of RC beams with circular openings of different sizes and locations using FE method. International Journal of Civil, Environmental, Structural, Construction and Architectural Engineering, 11(7), pp.849-852.

Tan, C.M., 2003. Nonlinear vibrations of cracked reinforced concrete beams (Doctoral dissertation, University of Nottingham).

Teng, J.G., De Lorenzis, L., Wang, B., Li, R., Wong, T.N. and Lam, L., 2006. Debonding failures of RC beams strengthened with near surface mounted CFRP strips. Journal of composites for construction, 10(2), pp.92-105.

Appendix A

Polybit

Polypoxy NF

Epoxy repair putty and bedding mortar

Used for bedding, gap filling, repair and adhesive applications.

CHARACTERISTICS

- Easy to use, non slumping
- Good impact resistance
- Resistant to acids, alkalis, oil, grease, hydrocarbon fuels and saline water
- No primer or bonding agent required
- High compressive strength
- Can be trowelled to smooth finish
- Does not Contain Asbestos, Chromated copper arsenate and Lead

DESCRIPTION

Polypoxy NF is an easy to use non-flowing, sand filled two component epoxy compound which can be used for bedding, gap filling, repair and adhesive applications.

FIELDS OF APPLICATION

- as concrete repair: repairing damaged concrete, filling of cracks.
- as a skim coat/filler on prepared floors prior to application of floor coatings and screeds
- as jointing compound: can be used to join pre cast concrete / GRC structures.
- as a bedding material: can be used for fixing tiles on heavy duty areas, bedding bridge beams or bridge bearing.
- excellent for anchoring bolts or replacement rebar and filling bolt pockets.
- as a bonding agent: it bonds to almost all rigid surfaces.
- as a mould: it can be molded to any shape.

ENVIRONMENTAL INFORMATION

Contributes toward satisfying LEED® v4 requirements of the EQ Credit- Low-emitting Materials (for the VOC content)

APPLICATION INSTRUCTIONS

Surface preparation

Clean all the surfaces and remove any loose particles, laitance, dust, oil, grease, paint etc. Abrade the bond area to improve mechanical bond.

TDS_Polypoxy NF_GCC_0322

1

Mixing

Polypoxy NF part A and part B shall be mixed thoroughly using a trowel or gloved hand until a uniform color and consistency is achieved. For small mixes, ensure that both the parts are mixed as per the ratio of 60:40 (A:B).

Application

Application can be carried out by putty knife, trowel or wooden float. Press firmly to ensure proper adhesion and full contact. Additional build up can be done by multiple layer application. Thickness can be from 0mm - 5mm. The application of additional layers should follow between 8 - 24 hours after the first application.

CLEANING

Clean all the tools with Polysolvent immediately after use. Hardened materials can be removed mechanically only.

STORAGE & SHELF LIFE

Store in a cool, dry place and keep away from all sources of heat and sunlight. In tropical climates, store in air condition rooms. The shelf life is up to 12 months in un-opened conditions and if stored as per recommendations. Excessive exposure to sunlight, humidity and UV will result in the deterioration of the quality of the product and reduce its shelf life.

Quality for Professionals

HEALTH & SAFETY

As with all construction chemical products caution should always be exercised. Protective clothing such as gloves and goggles shall be worn. Treat any splashes to the skin or eyes with fresh water immediately. Should any of the products be accidentally swallowed, do not induce vomiting, but call for medical assistance immediately.

COVERAGE

3 kg kit will cover 1.67 m² at 1mm thickness.

SUPPLY

Polypoxy NF	3kg kit

Apart from the information given here it is also important to observe the relevant guidelines and regulations of various organizations and trade associations as well as the respective standards. The aforementioned characteristics are based on practical experience and applied testing. Warranted properties and possible uses which go beyond those warranted in this information sheet require our written confirmation. All data given was obtained at an ambient and material temperature of +23°C and 50 % relative air humidity at laboratory conditions unless specified otherwise. Please note that under other climatic conditions hardening can be accelerated or delayed.
The information contained herein, particularly recommendations for the handling and use of our products, is based on our professional experience. As materials and conditions may vary with each intended application, and thus are beyond our sphere of influence, we strongly recommend that in each case sufficient tests are conducted to check the suitability of our products for their intended use. Legal liability cannot be accepted on the basis of the contents of this data sheet or any verbal advice given, unless there is a case of wilful misconduct or gross negligence on our part. This technical data sheet supersedes all previous editions relevant to this product.

TECHNICAL SPECIFICATION

PROPERTIES	VALUES	TEST STANDARDS
Color & appearance	Grey/off white paste	-
Density, [g/cc]	1.85±0.05	ASTM D 1475
Application life, [minutes]	45	-
Compressive strength @7days, [N/mm²]	>60	ASTM C 579
Flexural strength @7days, [N/mm²]	>30	ASTM C 580
Tensile strength @7 days, [N/mm²]	>12	ASTM C 307
Shear bond strength @7 days, [N/mm²]	>40	ASTM C 882
Application thickness, [mm/layer]	0 to 5	-
Application temperature, [°C]	5 to 35	-
Service temperature, [°C]	-5 to 70	-
Initial cure, [hours]	Approx. 8	-
Final cure, [days]	7	-

All values given are subject to 5-10% tolerance

TDS_Polypoxy NF_GCC_0322

2

Henkel Polybit Industries Ltd.; PO Box: 293, Umm Al Quwain, UAE
Tel:+971(6)7670777; Fax:+971(6)7670197; henkelpolybit@henkel.com
Henkel Polybit Industries Ltd.; PO Box: 5911, Dammam-31432, KSA
Tel:+96613808 4061 / 62, Fax: +966 13 812 1164; polybitdammam@henkel.com
www.henkelpolybit.com

Quality for Professionals

Appendix B

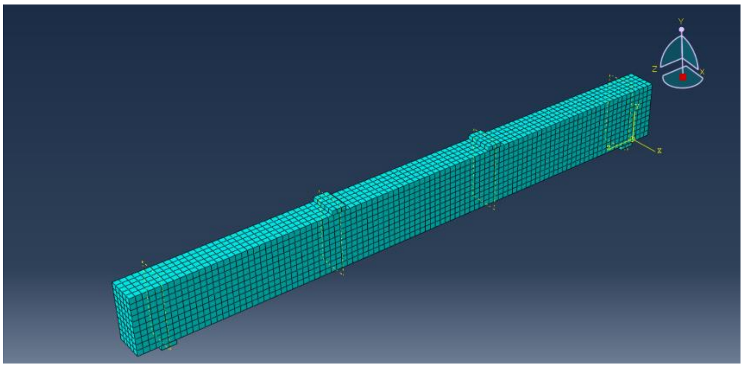

SCB

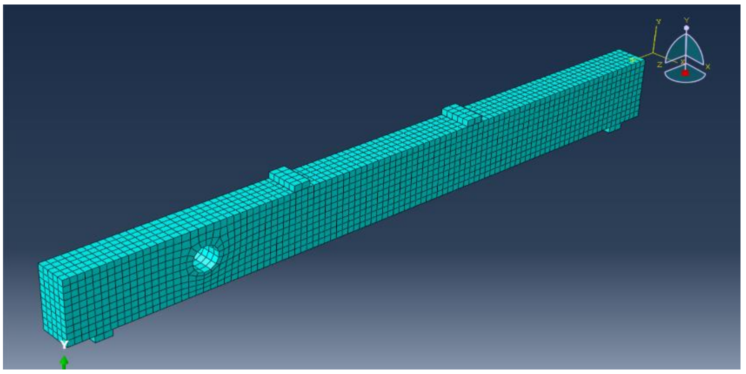

SBLS

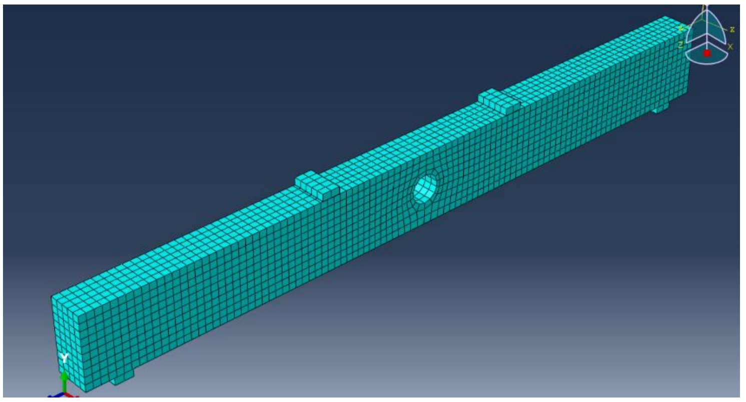

SBLF

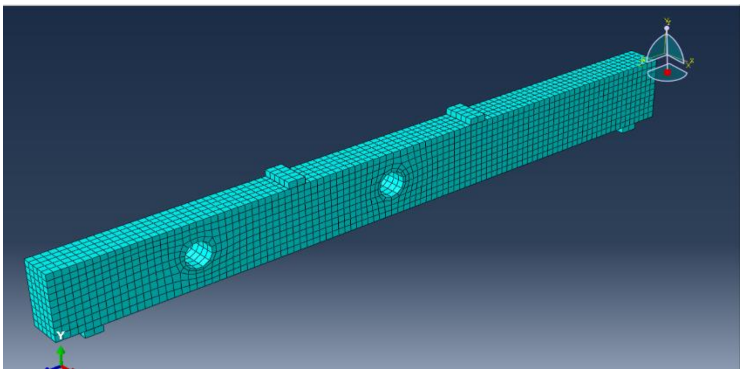

SBLSF

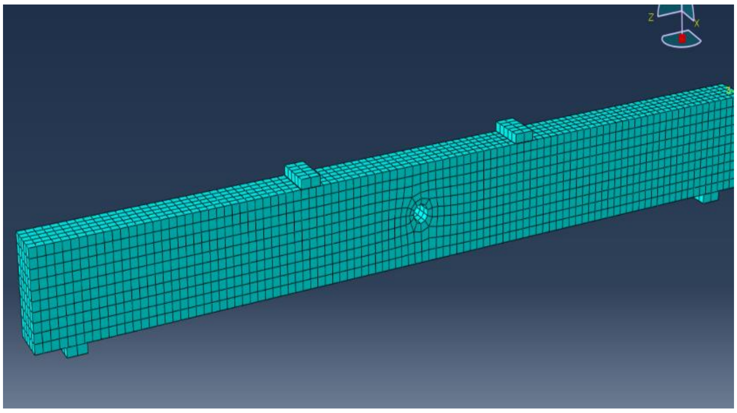

SBSF

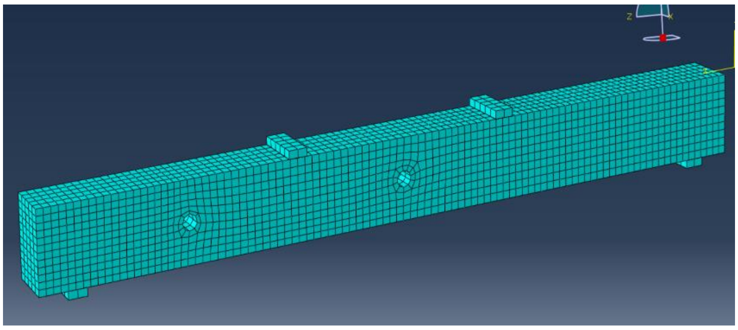

SBSSF

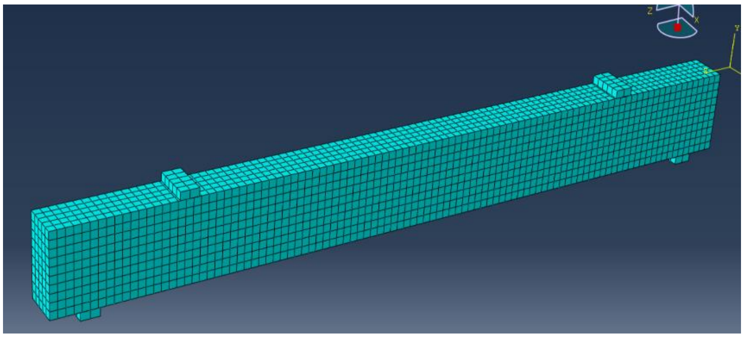

DCB

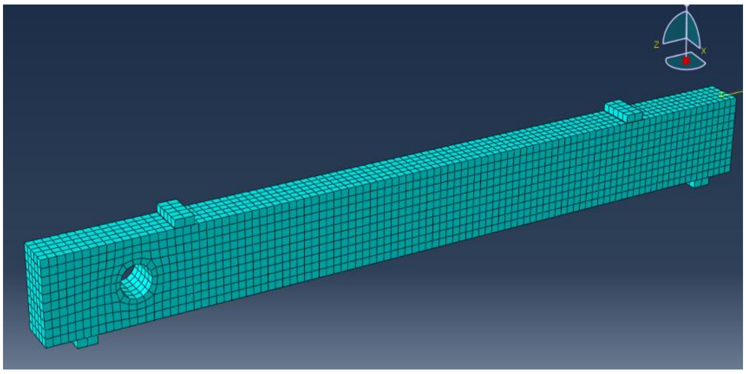

DBLS

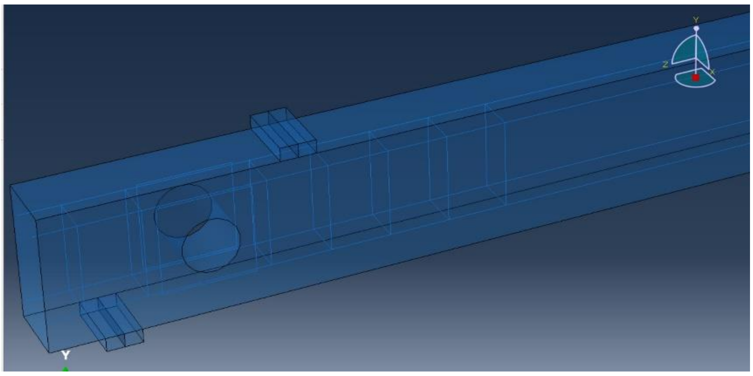

DBLSS8

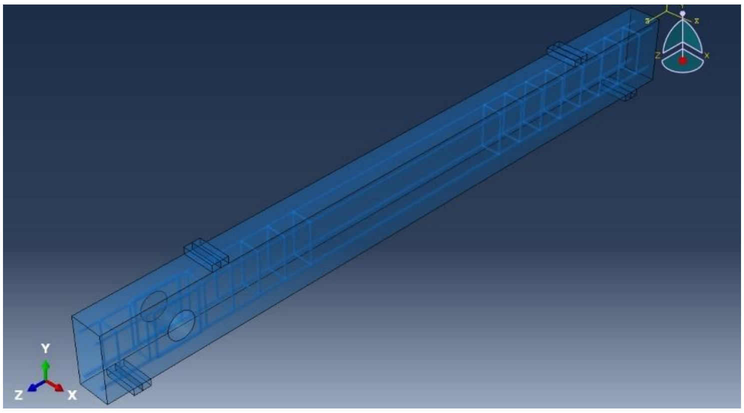

DBLSS10

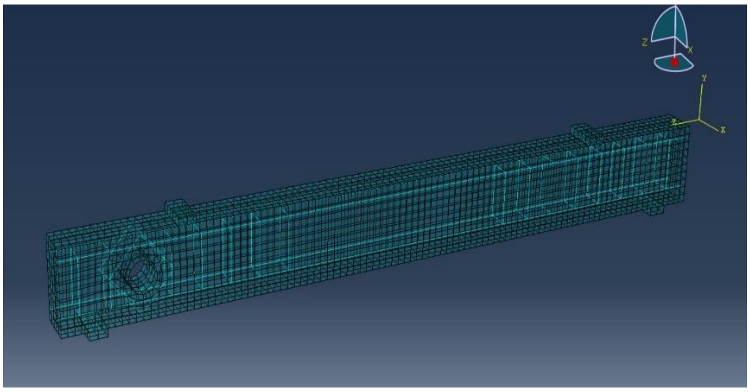

DBLSD8

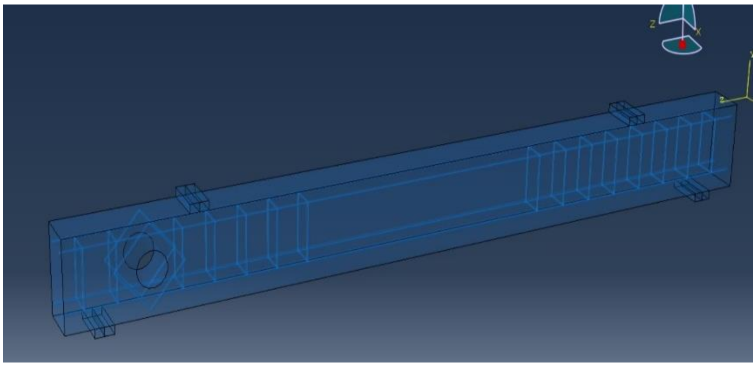

DBLSD10

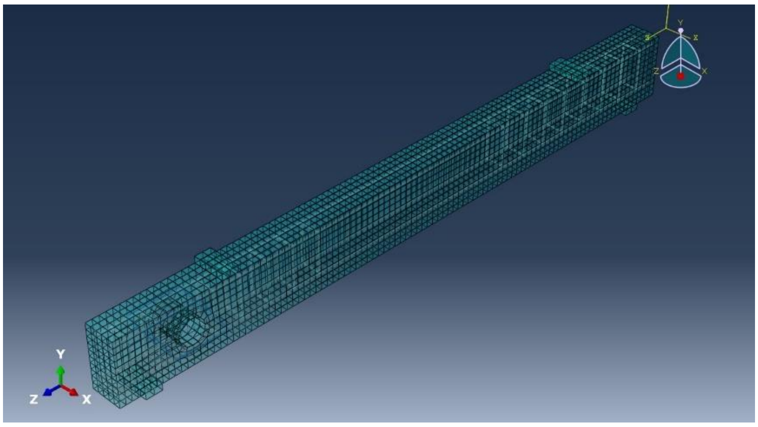

DBLSP8

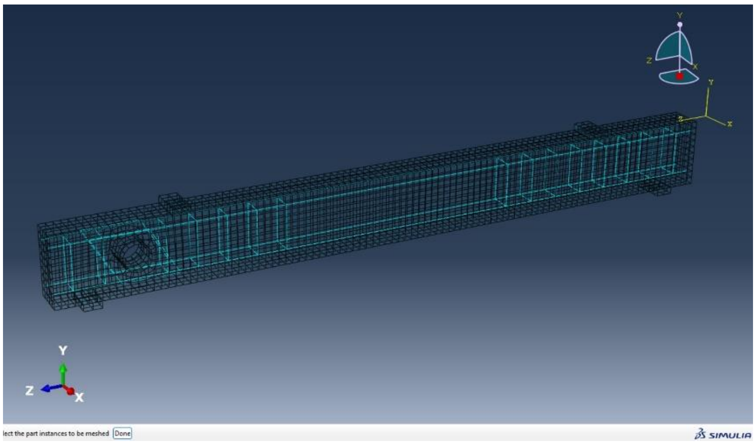

DBLSP10

POLYTECHNIC JOURNAL

Polytechnic Journal
Polytechnic Journal

Volume 13 | Issue 2 Article 7

November 2023

Strengthening of Reinforced Concrete Beams with Circular Openings Using Near Surface Mounting Steel Bars

Hoshang Hayder Anwer
Erbil Technical Engineering College, Erbil Polytechnic University, Erbil-Iraq., hoshang.anwer@epu.edu.iq

Bahman Omar Taha
Erbil Technical Engineering College, Erbil Polytechnic University, Erbil-Iraq.

How to Cite This Article
Anwer, Hoshang Hayder and Taha, Bahman Omar (2023) "Strengthening of Reinforced Concrete Beams with Circular Openings Using Near Surface Mounting Steel Bars," *Polytechnic Journal*: Vol. 13: Iss. 2, Article 7.
DOI: https://doi.org/10.59341/2707-7799.1721

زانکۆی پۆلیتەکنیکی هەولێر
ERBIL POLYTECHNIC UNIVERSITY

بەهێزکردنی (بیمی) کۆنکرێتی شیشدار کە دەرچەی بازنەییان تێیدایە بە بەکارهێنانی شیش لەدەوری دەرچەکان

نامەیەکە

پێشکەشی ئەنجومەنی کۆلێژی تەکنیکی ئەندازیاری کراوە لەزانکۆی پۆلیتەکنیکی هەولێر

وەکو بەشێك لە پێداویستیەکانی بەدەست هێنانی ماستەر لە (ئەندازیاری شارستانی-سترەکچەر)

لەلایەن

هۆشەنگ حەیدەر ئەنوەر

بەکالۆریۆس لە ئەندازیاری شارستانی - زانکۆی پۆلیتەکنیکی هەولێر (2015)

بەسەرپەرشتی

پ.ی. د. بەهمەن عمر طه

کوردستان -هەولێر

2024 - ڕێبەندان

پوختە

بیمی کۆنکرێتی شیشدار (RC) کە دەرچەی بازنەیی تێدایە ئاڵنگاریی پێکهاتەیی دروست دەکات، سەرەنجام کەمبوونەوە لەسەر توانای هەڵگرتنی بار و یەکپارچەیی پێکهاتەیی گشتییان لێدەکەوێتەوە. ئەم تێزە هەوڵدەدات بۆ قوڵبوونەوە و چارەسەرکردنی ئەم کێشەیە لە ڕێگەی جێبەجێکردنی ڕێبازێکی داهێنەرانە کە بریتییە لە جێگیرکردنی شیش لە ڕووی نزیک رووکار (NSM). دەرچەی بازنەیی کە بەشێکی دانبڕاوە لە دیزاینە تەلارسازییەکان، زۆرجار دەبێتە هۆی کەمبوونەوەی هێزی بیمەکان. ئەم توێژینەوەیە لێکۆڵینەوەی لە کاریگەری بەکارهێنانی شیش لە ڕووی نزیک رووکار (NSM) کردووە بۆ گەڕاندنەوەی هێزی بڕینی بیمی قووڵ و بوونی دەرچە لە بیمی باریکدا. کارە تاقیکارییەکە بریتی بوو لە تاقیکردنەوەی چواردە بیمی کۆنکرێتی شیشدار کە بەراگری جۆری سادە راگیرابوو. ئەم بیمانە دابەشکرابوون بەسەر دوو گرووپدا، هەریەکێک لە بیمەکان پێکهاتبوون لە ڕێژەی جیاوازی بڕین بۆ قووڵیی ($a/h = 1.5$ و 3.65). دوو دانەیان وەک نمونەی کۆنترۆڵ بەکارهێنرا، لە کاتێکدا کە بیمەکانی دیکە دەرچەیان تێدا دانرا لە شوێنی جیاجیادا. دەرچەکان بۆ دوو جۆر پۆلێن کران گەورە یان بچووک، بە ڕێژەی بەرزی کرانەوە (h_o/h) بە 0.4 و 0.2 یەک لە دوای یەکدا. لە گرووپی دووەمدا، شەش نمونە بەهێزکران بە بەکارهێنانی شیش لە ڕووی نزیک رووکار (NSM) کە بە سێ پێکهاتەی جیاوازی ئەڵقە ڕێکخراون: (چوارگۆشە، شێوە ئەڵماس و لاتەریب). هەموو بیمەکان بە قەبارەی 100 ملم × 200 ملم و درێژی 2000 ملم بووە. ئەو گۆڕاوانەی لە تاقیکردنەوەکاندا پشکنینیان بۆ کرا بریتی بوون لە قەبارە و شوێنی دەرچەکان، تیرەی شیشەکان و ڕێکخستنی شیشی بەهێزکەر لە دەوری دەرچەکان. لە ئەنجامی تاقیکردنەوەکاندا دەرکەوت کە بوونی دەرچە لە بیمەکاندا دەبێتە هۆی کەمبوونەوەی توانای راگرتن. بۆ ئەو نمونانەی کە دەرچەی بازنەیی گەورەیان لە ناوچەی بڕینی بیمە قووڵەکاندا هەیە، دەرچەی بازنەیی گەورە لە بیمی باریکدا کە تووشی بڕین بووە، هەروەها دەرچەی بازنەیی گەورە کە تووشی باری بڕین و چەمانەوە بووە، و دەرچەی بچووک لە بیمی باریکدا کە تووشی باری بڕین و چەمانەوە بووە، باری کۆتایی بە ڕێژەی نزیکەی 45%، 18.7%، 14.6% و 19.5% کەمیکردووە. سەرەڕای ئەوەش، ئەنجامی تاقیکردنەوەکە دەریخست کە ئەو نمونانەی کە بە ئەڵقەی شێوە ئەڵماس بەهێزکراون، باشتربوونیان لە باری کۆتاییدا تا 33.1% نیشانداوە. لە هەمان کاتدا، ئەو نمونانەی کە بە ئەڵقەی چوارگۆشە و لاتەریب بەهێزکراون، پێشکەوتنیان تا 21.5% و 26.5% یەک لە دوای یەک نیشانداوە. گۆڕینی تیرەی شیشەکە کاریگەرییەکی کەمی هەبووە لەسەر زیادکردنی باری

کۆتایی، بە تایبەتی بۆ ئەڵقەی شێوە لاتەریب و چوارگۆشە، لە ئەنجامدا زیادبوونی نزیکەی 10% و 7%، یەک لە دوای یەک